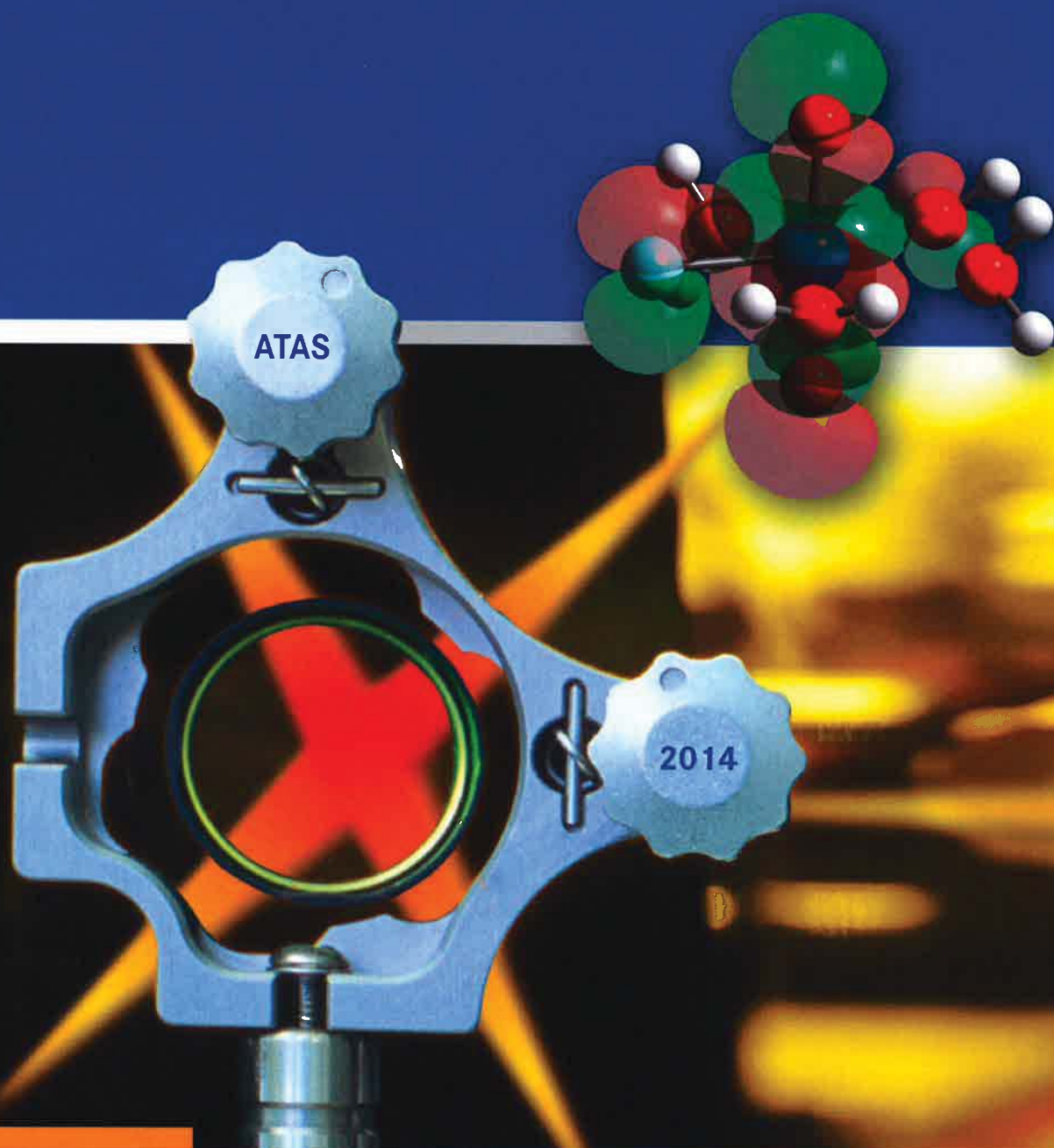


HZDR-054

Wissenschaftlich-Technische Berichte
HZDR-054 2014 · ISSN 2191-8708



2nd International Workshop on

ADVANCED TECHNIQUES IN ACTINIDE SPECTROSCOPY (ATAS 2014)

ABSTRACT BOOK

hZDR



HELMHOLTZ
ZENTRUM DRESDEN
ROSSENDORF

Wissenschaftlich-Technische Berichte
HZDR-054

2nd International Workshop on Advanced Techniques for Actinide Spectroscopy (ATAS 2014)

Abstract Book

November 03–07, 2014
HZDR – Helmholtz-Zentrum Dresden-Rossendorf
Dresden, Germany

Organized by
Institute of Resource Ecology
Helmholtz-Zentrum Dresden-Rossendorf e.V.

Editors:
H. Foerstendorf, K. Müller, R. Steudtner

HZDR

 **HELMHOLTZ**
ZENTRUM DRESDEN
ROSSENDORF

Print edition: ISSN 2191-8708

Electronic edition: ISSN 2191-8716

The electronic edition is published under Creative Commons License (CC BY-NC-ND):

Qucosa: <http://fzd.qucosa.de/startseite/>

Published by Helmholtz-Zentrum Dresden-Rossendorf e.V.

This abstract book is also available at <http://www.hzdr.de/FWO>

Contact

Helmholtz-Zentrum Dresden-Rossendorf e.V.
Institute of Resource Ecology

Postal Address

P.O. Box 51 01 19
D-01314 Dresden
Germany

Address for visitors

Bautzner Landstraße 400
D-01328 Dresden
Germany

Phone: ++49 (0) 351 260 3210

Fax: ++49 (0) 351 260 3553

e-mail: contact.resourceecology@hzdr.de

ATAS@hzdr.de

<http://www.hzdr.de/ATAS>

Contents

Preface.....	4
Scientific Committee	5
Local Committee.....	5
Sponsors.....	5
Information	7
Scientific Program	8
ABSTRACTS	
Oral Presentations.....	13
Poster Presentations.....	53
Round-Robin test in actinide spectroscopy	85
Index of Authors	91

Preface

IN 2012, THE INSTITUTE OF RESOURCE Ecology at the Helmholtz-Zentrum Dresden Rossendorf organized the first international workshop of Advanced Techniques in Actinide Spectroscopy (ATAS). A very positive feedback and the wish for a continuation of the workshop were communicated from several participants to the scientific committee during the workshop and beyond.

Today, the ATAS workshop has been obviously established as an international forum for the exchange of progress and new experiences on advanced spectroscopic techniques for international actinide and lanthanide research. In comparison to already established workshops and conferences on the field of radioecology, one main focus of ATAS is to generate synergistic effects and to improve the scientific discussion between spectroscopic experimentalists and theoreticians.

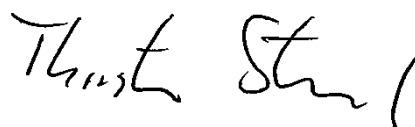
The exchange of ideas in particular between experimental and theoretical applications in spectroscopy and the presentation of new analytical techniques are of special interest for many research institutions working on the improvement of transport models of toxic elements in the environment and the food chain as well as on reprocessing technologies of nuclear and non-nuclear waste.

Spectroscopic studies in combination with theoretical modelling comprise the exploration of molecular mechanisms of complexation processes in aqueous or organic phases and of sorption reactions of the contaminants on mineral surfaces to obtain better process understanding on a molecular level. As a consequence, predictions of contaminant's migration behaviour will become more reliable and precise. This can improve the monitoring and removal of hazardous elements from the environment and hence, will assist strategies for remediation technologies and risk assessment.

Particular emphasis is placed on the results of the first inter-laboratory Round-Robin test on actinide spectroscopy (RRT). The main goal of RRT is the comprehensive molecular analysis of the actinide complex system U(VI)/acetate in aqueous solution independently investigated by different spectroscopic and quantum chemical methods applied by leading laboratories in geochemical research. Conformities as well as sources of discrepancies between the results of the different methods are to be evaluated, illuminating the potentials and limitations of coupling different spectroscopic and theoretical approaches as tools for the comprehensive study of actinide molecule complexes. The test is understood to stimulate scientific discussions, but not as a competitive exercise between the labs of the community.

Hopefully, the second ATAS workshop will continue to bundle and strengthen respective research activities and ideally act as a nucleus for an international network, closely collaborating with international partners. I am confident that the workshop will deliver many exciting ideas, promote scientific discussions, stimulate new developments and collaborations and in such a way be prosperous.

This workshop would not take place without the kind support of the HZDR administration which is gratefully acknowledged. Finally, the organizers cordially thank all public and private sponsors for generous funding which makes this meeting come true for scientists working on the heavy metal research field.



Thorsten Stumpf
Director of the
Institute of Resource Ecology

Scientific Committee

Christophe Den Auwer
Nice Sophia Antipolis University (France)

Isabelle Billard
LEPMI CNRS (France)

Katharina Müller
Helmholtz-Zentrum Dresden-Rossendorf (Germany)

Jörg Rothe
Karlsruhe Institute of Technology (Germany)

Georg Schreckenbach
University of Manitoba (Canada)

Robin Stedtner
Helmholtz-Zentrum Dresden-Rossendorf (Germany)

Satoru Tsushima
Helmholtz-Zentrum Dresden-Rossendorf (Germany)

Zoltán Szabó
Royal Institute of Technology (Sweden)

Local Committee

Katharina Müller

Satoru Tsushima

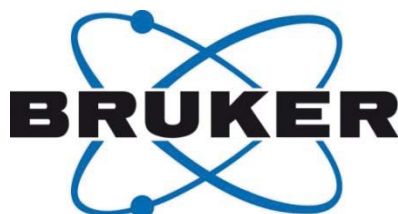
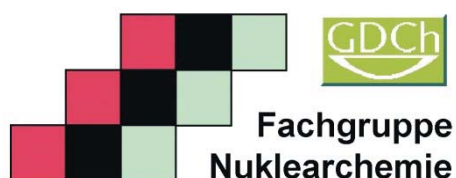
Frank Bok

Robin Stedtner

Harald Foerstendorf

Thorsten Stumpf

Sponsors





VERTEX Series

Research FT-IR Spectrometers

Bruker's VERTEX series FT-IR spectrometers are built on a fully upgradeable platform and share a variety of features for ease of use and ultimate performance. Vacuum models eliminate atmospheric moisture absorptions from the sample and the instrument for ultimate sensitivity and stability.

- VERTEX 70 and VERTEX 70v utilizes RockSolid™ permanently aligned interferometer.
- VERTEX 80 and VERTEX 80v utilizes UltraScan™ interferometer with precise linear air bearing scanner and TrueAlignment™ technology.
- Fully automated beamsplitter exchange for vacuum spectrometer VERTEX 80v
- **NEW** Wide range MIR-FIR DTGS detector

Contact us for more details: www.bruker.com/optics

Bruker Optics GmbH
Rudolf-Plank-Str. 27
76275 Ettlingen
Tel. +49 7243 504 2000
Fax. +49 7243 504 2050
E-Mail: info@brukeroptics.de

Information

– Registration

Registration desk will be open as follows:

Nov. 3rd: 9.30 a.m. – 2.00 p.m.

Nov. 4th: 8.30 a.m. – 2.00 p.m.

Nov. 5th: 8.30 a.m. – 11.00 p.m.

– Instructions of Presentations

All speakers are asked to upload their presentations at the lecture room before their session starts. Time allotted for oral presentations is 25 min including 5 min period for discussion. The plenary lectures are 45 min. The organizers kindly ask to keep these time standards.

Poster dimensions should not exceed A0 size, that is ~124 x 87 cm (~48 x 35 inch) and should be in portrait format. All posters can be presented throughout the workshop. Adhesives will be provided. All presenters are kindly asked to remove their posters before departure.

– Lunch & Refreshments

Lunch buffets will be provided for the participants of the workshop from Monday to Friday. Refreshments will be served during the breaks and poster session on Tuesday evening.

– HZDR Tours

If you are interested in the research facilities at HZDR, you are invited to participate in one of the guided tours on Monday, 10 a.m.

Guided tours are offered for:

- Dresden High Magnetic Field Laboratory
- ELBE - Center for High-Power Radiation Sources
- Ion Beam Center
- Radiochemical Laboratories
- TOPFLOW - Transient Two Phase Flow Test Facility

The HZDR tours are for free for workshop participants. However, for organization reasons, we kindly ask you to register for these events.

More information on HZDR tours are available from the ATAS website (<http://www.hzdr.de/atas>).

– Ice Breaker

On Monday evening (7.30 p.m.) an ice breaker party will take place at the restaurant “Wenzel Prager Bierstuben”, (Königsstr. 1, Dresden) located in the *Innere Neustadt* of Dresden (about 20 min walk from “Holiday Inn Express” hotel). Participants of this event will be picked up at the hotel’s reception at 7 p.m.

– Social Event

(Visit of “*Mathematisch-Physikalischer Salon*” & Banquet)

The visit of the museum of historical scientific instruments and the workshop banquet will take place on Wednesday afternoon and evening. Buses will pick up all attendees at 3 p.m. at HZDR. The visit of the museum ends at 6 p.m. The banquet will take place at the restaurant “*Henricus*” at *Neumarkt* close to the famous town’s landmark *Frauenkirche* at 7 p.m.

– ATAS Shuttle Service

For your convenience, shuttle buses will be arranged between Hotel „*Holiday Inn Express*“ (inner city) and HZDR. Departure of the buses as follows:

Date	Departure	
	at H. Inn Express	at HZDR
Nov. 3 rd	9.00 a.m./11.45 a.m.	5.15 p.m.
Nov. 4 th	8.00 a.m.	7.00 p.m.
Nov. 5 th	8.00 a.m.	3.00 p.m. ¹
Nov. 6 th	8.00 a.m.	5.45 p.m.
Nov. 7 th	8.00 a.m.	1.15 p.m. ²

¹: Transfer to social event (inner city).

²: Dest. Dresden main station; transport to Dresden airport will be organized if needed.

– Public Transport

Beside the shuttle service, there is an hourly public bus connection to HZDR (no. 261, dest. “*Sebnitz*”) passing bus stops “*Walpurgisstrasse*” or “*Pirnaischer Platz*” ~600 and 750 m from Hotel „*Holiday Inn Express*“, respectively. Departure time (a.m.): 7.15, 8.15, 9.15, 10.15... (a detailed map of the bus stops is recommended and available from ATAS website & registration desk). Get off at bus stop “*Forschungszentrum Rossendorf*” (travel time: ~35 min)*.

From HZDR to Dresden city take bus no. 261, (dest. “*Dresden Hbf*”, main station). Alternatively, take bus no. 229 (dest. “*Bühlau*”) with interchange to tram. no. 11 (destination: “*Zschertnitz*”) for Dresden city. Departure of the buses from HZDR’s main gate as follows:

Bus No. 261 (Dest.: <i>Dresden Hbf</i>)*	Bus No. 229 (Dest.: <i>Bühlau</i>)*
3.13 p.m.	3.41 p.m.
4.13 p.m.	4.41 p.m.
5.13 p.m.	5.41 p.m.
6.13 p.m.	6.41 p.m.
7.19 p.m.	

*: One-way fare: 2.20 €.

Scientific Program

Monday, Nov. 3rd

10:00 a.m. *HZDR tours*

12:00 p.m. *Lunch*

01:30 p.m. *Welcome & opening words*

Session 1: **BIOGEOCHEMISTRY**

(Chair: T. Stumpf)

	Page
01:45 p.m. Mechanism and products of U(VI) reduction in the subsurface (<i>INVITED</i>) <i>R. Bernier-Latmani, J. R. Bargar, D. S. Alessi, P. S. Shao, M. Stylo, N. Neubert, S. Weyer</i>	15
02:30 p.m. Importance of actinides-organic complexes in biodegradation and bioreduction <i>T. Ohnuki, Y. Suzuki, T. Nankawa, K. Tanaka</i>	22
02:55 p.m. TRLFS studies on biosorption of uranium on halophilic archaea at high ionic strength (3 M NaCl) <i>M. Bader, A. Cherkouk, B. Drobot, T. Stumpf</i>	23
03:20 p.m. <i>Coffee break</i>	
03:45 p.m. Uranium redox processes – initiated by plant cells <i>G. Geipel, K. Viehweger</i>	24
04:10 p.m. Mechanisms of uranium and thorium accumulation in the bone matrix <i>G. Creff, S. Safi, P. Lorenzo Solari, C. Vidaud, C. Den Auwer</i>	25
04:35 p.m. Chelation of uranyl by variants of the calmodulin EF-hand motif <i>R. Pardoux, S. Sauge-Merle, D. Lemaire, M. R. Beccia, N. Bremond, C. Battesti, M. L. Merroun, P. L. Solari, P. Delangle, P. Guilbaud, C. Berthomieu</i>	26
05:00 p.m. <i>End of session</i>	
<hr/>	
07:00 p.m. Ice Breaker Location: <i>Wenzel Prager Bierstuben, Königstrasse 1, Dresden</i>	7

Tuesday, Nov. 4th

Session 2: DISSOLVED ACTINIDE & LANTHANIDE SPECIES I

(Chair: L. Natrajan)

	Page
09:00 a.m. Theoretical actinide molecular science: aqueous species, macrocycles, mineral surfaces (<i>INVITED</i>) <i>G. Schreckenbach</i>	16
09:45 a.m. Study of paramagnetic actinide complexes with dipicolinate ligands <i>M. Autillo, C. Berthon, P. Moisy</i>	27
10:10 a.m. Plutonium oxidation state speciation in aqueous solution studied by Pu L and M edge high energy resolution XANES technique <i>I. Pidchenko, D. Fellhauer, T. Prüßmann, K. Dardenne, J. Rothe, E. Bohnert, B. Schimmelpfennig, T. Vitova</i>	28
10:35 a.m. <i>Coffee break</i>	
11:00 a.m. Coordination of actinyl ions to nitrogenous heterocyclic ligands: a joint theoretical and experimental study <i>P. Yang, Z. Wang, D. Pan, Y. Gong, J. Gibson</i>	29
11:25 a.m. Nuclear magnetic resonance spectroscopy in Ln/An research <i>J. Kretzschmar, J. Schott, S. Tsushima, A. Barkleit, S. Paasch, E. Brunner, G. Scholz, V. Brendler</i>	30
11:50 a.m. A joint photoelectron spectroscopy and theoretical study on uranium halide complexes <i>J. Su, P. D. Dau, H.-T. Liu, L.-S. Wang, J. Li</i>	48

12:15 p.m. *Lunch*

Session 3: ENVIRONMENTAL APPLICATIONS

(Chair: P. Reiller)

01:45 p.m. Uptake, reduction, and reoxidation mechanisms of uranium in biogeochemical systems studied by X-ray absorption spectroscopy (<i>INVITED</i>) <i>M. I. Boyanov, D. E. Latta, B. Mishra, E. J. O'Loughlin, K. M. Kemner</i>	17
02:30 p.m. Uranyl minerals as models for the long term storage of spent nuclear fuels <i>A. Walshe, E. D. Spain, T. A. Keys, R. A. Forster, T. Prüßmann, T. Vitova, R. J. Baker</i>	32
02:55 p.m. Molecular insights into actinide speciation at interfaces and nanoparticles <i>A. Campbell, N. Hess</i>	42
03:20 p.m. <i>Coffee break</i>	34
03:45 p.m. Eu³⁺ binding to deep groundwater humic substances studied by time resolved laser fluorescence spectroscopy and factor analysis <i>T. Saito</i>	
04:10 p.m. Elemental analysis of simulated debris of nuclear fuel in water by fiber-coupled Laser Induced Breakdown Spectroscopy <i>M. Saeki, C. Ito, I. Wakaida, B. Thornton, T. Sakka, H. Ohba</i>	35
04:35 p.m. Structure and inclusions in bulk and dispersed samples of Chernobyl "lava": data from vibrational spectroscopy, XAFS and X-ray tomography <i>A. A. Shiryaev, I. E. Vlasova, Y. V. Zubavichus, R. A. Senin, A. A. Averin, A. Pakhnevich, B. I. Ogorodnikov, B. E. Burakov</i>	36
05:00 p.m. AMS of actinides in ground- and sea-water: a new procedure for simultaneous trace analysis of U, Np, Pu, Am and Cm isotopes <i>F. Quinto, M. Lagos, M. Plaschke, T. Schäfer, P. Steier, R. Golser, H. Geckeis</i>	37

05:25 p.m. **POSTER SESSION** 55–84

Wednesday, Nov. 5th

ROUND ROBIN TEST

Page

09:00 a.m.	Introduction to RRT <i>K. Müller, R. Steudtner, S. Tsushima</i>	87–89
09:20 a.m.	Reports of cluster speakers 1–3 & panel discussion (Chairs: C. Den Auwer, R. Polly) Cluster: NMR (Speaker: Z. Szabó) IR (Speaker: G. Lefèvre) XAS (Speaker: J. Rothe)	
10:35 a.m.	<i>Coffee break</i>	
11:00 a.m.	Reports of cluster speakers 4–6 & panel discussion (Chairs: J.-F. Boily, M. I. Boyanov) Cluster: QC (Speaker: P. Yang) TRLFS (Speaker: M. U. Kumke) ESI-MS (Speaker: C. Walther)	
12:15 p.m.	<i>Lunch</i>	
01:45 p.m.	Panel discussion: evaluation of RRT (Chair: I. Billard) <i>M. U. Kumke, G. Lefèvre, J. Rothe, Z. Szabó, C. Walther, P. Yang.</i>	
03:00 p.m.	<i>End of session</i>	
04:00 p.m.	Social Event Location: <i>Staatliche Kunstsammlungen Dresden – Mathematisch physikalischer Salon</i>	7
07:00 p.m.	Banquet Location: <i>Henricus, An der Frauenkirche</i>	7

Thursday, Nov. 6th

Session 4: **SOLID STATE/PHASES & NANOPARTICLES**

(Chair: Z. Szabó)

	Page
09:00 a.m. Bose-Einstein-Hubbard condensate-type behavior via a novel mechanism in the f electron Mott insulator $\text{UO}_{2(+x)}$ (INVITED) <i>S. D. Conradson, D. A. Andersson, T. Durakiewicz, S. M. Gilbertson, G. Rodriguez, M. L. Neidig, S. Daifuku, J. Kehl</i>	18
09:45 a.m. Site-selective TRLFS of Eu(III) doped rare earth phosphates for conditioning of radioactive wastes <i>N. Huittinen, Y. Arinicheva, J. Holthausen, S. Neumeier, T. Stumpf</i>	38
10:10 a.m. Spectroscopic and microscopic characterization of U bearing multicomponent borosilicate glass <i>S. Bahl, V. Koldeisz, K. Kvashnina, T. Yokosawa, I. Pidchenko, H. Geckeis, T. Vitova</i>	39
10:35 a.m. <i>Coffee break</i>	
11:00 a.m. Hydrolysis of tetravalent cerium (Ce(IV)) – A multi-spectroscopic study on nanocrystalline CeO_2 formation <i>A. Ikeda-Ohno, S. Weiss, S. Tsushima, C. Hennig</i>	40
11:25 a.m. XPS and UPS study on the electronic structure of ThO_x ($x \leq 2$) and $(\text{U,Th})\text{O}_x$ ($x \leq 2$) thin films <i>P. Çakir, R. Eloirdi, F. Huber, R. J. M. Konings, T. Gouder</i>	41
11:50 a.m. Cryogenic Laser-Induced Time-Resolved Luminescence Spectroscopy of U(VI) in mineral mixtures and natural sediments <i>Z. Wang, J. M. Zachara, C. T. Resch, D. Pan, W. Wu, J.-F. Boily, C. Liu</i>	33

12:15 p.m. *Lunch*

Session 5: **SURFACE PROCESSES & REACTIVITY**

(Chair: S. Krüger)

01:45 p.m. Mineral surface hydroxo group identity and reactivity (INVITED) <i>J.-F. Boily</i>	19
02:30 p.m. Mechanistic understanding of mineral reactivity toward trace metals through density functional theory <i>K. D. Kwon</i>	43
02:55 p.m. Surface interaction of actinide oxides and mixed oxides with ice under UV light: an UPS, XPS investigation <i>P. Çakir, R. Eloirdi, F. Huber, R. J. M. Konings, T. Gouder</i>	44
03:20 p.m. <i>Coffee break</i>	
03:45 p.m. Computational modeling of actinide adsorption on edge surfaces of 2 : 1 clay minerals <i>A. Kremleva, S. Krüger</i>	45
04:10 p.m. Interaction of U(VI) with aluminium(hydr)oxides: structural analysis combining EXAFS and artificial intelligence <i>A. Rossberg, A. C. Scheinost</i>	46
04:35 p.m. Using CLSM and TRLFS analysis to describe spatial distributions of Eu surface complexes – Future perspectives <i>S. Britz, A. Schulze, R. Steudtner, K. Großmann</i>	47
05:00 p.m. <i>End of session</i>	

Friday, Nov. 7th

Session 6: DISSOLVED ACTINIDE & LANTHANIDE SPECIES II

(Chair: S. D. Conradson)

	Page
09:00 a.m. Monitoring redox and separation behavior of actinide ions by a combination of NMR and Emission Spectroscopy (<i>INVITED</i>) <i>L. S. Natrajan, S. D. Woodall, A. N. Swinburne, S. Randall, A. Geist, P. J. Panak, B. B. Beele, N. Banik, C. Adam, P. Kaden, A. Kerridge</i>	20
09:45 a.m. ATR-FTIR and UV-Vis spectroscopic studies of aqueous U(IV)-oxalate complexes <i>W. Cha, E. C. Jung, Y.-S. Park, H.-R. Cho, Y.-K. Ha</i>	49
10:10 a.m. Luminescence of lanthanides in aqueous solutions in the presence of small organic molecules <i>K. Burek, S. Eidner, K. Brennenstuhl, M. U. Kumke</i>	50
10:35 a.m. <i>Coffee break</i>	
11:00 a.m. Synthesis and laser spectroscopy of uranium(IV, VI) complexes in ionic liquids <i>N. Aoyagi, M. Watanabe, T. Kimura, A. Kirishima, N. Sato</i>	51
11:25 a.m. Development of accurate force field parameters for An(III)/Ln(III) ions in aqueous solution <i>B. Schimmelpfennig, M. Trumm, P. J. Panak, A. Geist</i>	52
11:50 a.m. <i>Closing words</i>	
<hr/>	
12:15 p.m. <i>Lunch</i>	
<hr/>	
01:15 p.m. <i>End of ATAS 2014</i>	

ORAL PRESENTATIONS

- Invited Talks
- Regular Presentations

Mechanism and products of U(VI) reduction in the subsurface

R. Bernier-Latmani,¹ J. R. Bargar,² D. S. Alessi,¹ P. S. Shao,¹ M. Stylo,¹ N. Neubert,³ S. Weyer³

¹ Ecole Polytechnique Federale de Lausanne (EPFL), Lausanne, Switzerland

² Stanford Synchrotron Radiation Lightsource, Menlo Park, CA, U.S.A.

³ Leibniz Universität Hannover, Hannover, Germany

Microorganisms are capable of transforming soluble and mobile hexavalent uranium [U(VI)] to sparingly soluble and relatively immobile tetravalent uranium [U(IV)] through the transfer of two electrons or one electron followed by disproportionation [1]. This process can be carried out directly, enzymatically, by the microorganisms or indirectly, through the reduction of iron or sulfate. Fe(II) bearing minerals produced through the microbial reduction of Fe(III) or sulfide-bearing minerals produced through microbial sulfate reduction are both likely routes for U(VI) reduction in the environment. Uranium reduction by microbes is relevant for the bioremediation of the subsurface contaminated with hexavalent uranium [2], for the formation of uranium ore roll front deposits and for the mobility of uranium in radioactive waste geological repositories. In particular, engineered remediation of the U(VI)-contaminated subsurface relies on the immobilization of uranium, which is achieved by its reduction to U(IV) and its persistence as an insoluble species. There are two main questions remaining in our understanding of U(VI) reduction: (a) what is the mechanism of U(VI) reduction in the subsurface? Do biotic or abiotic processes dominate the reduction?; (b) what is the *in situ* product of U(VI) reduction and how stable is it in the subsurface?

For the past two decades, the product of U(VI) reduction was thought to be the crystalline U(IV) oxide mineral, uraninite (UO₂). Using X-ray Absorption Spectroscopy, we characterized the product(s) of direct and indirect microbial uranium reduction and find that while crystalline nanoparticulate uraninite (UO₂) is a product of the reduction process, another product, an amorphous, phosphate-coordinated or carbonate-coordinated U(IV) species is more predominant in many environments [3,4]. The formation of this product was controlled by the solute composition of the aqueous solution. Another synchrotron technique, Scanning Transmission X-ray Microscopy (STXM), enabled the identification of microbial biofilms as the controlling factor for the formation of this non-crystalline species referred to as non-uraninite U(IV) (Fig. 1).

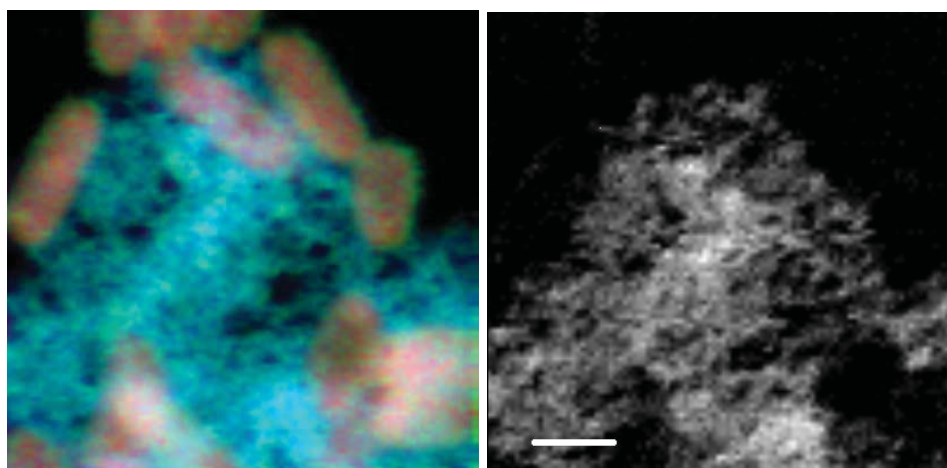


Fig. 1: STXM images of *Shewanella oneidensis* cells reducing U(VI) under conditions yielding non-uraninite U(IV). The left image shows a tricolor map indicating carbon speciation with red = protein, blue = polysaccharide and green = lipid. The corresponding U map on the right side shows that U is primarily associated with the extracellular polymeric substances rather than the cells.

Furthermore, U isotope fractionation studies investigated the isotopic signature of biotic vs. abiotic reduction. The results clearly show that abiotic reduction exhibits minimal isotope fractionation while enzymatically mediated U(VI) reduction has a clear signature indicating that the heavy U isotope is preferentially reduced.

[1] Wall J. D. and Krumholz L. R. (2006) Annual Reviews of Microbiology 60, 149–166.

[2] Anderson R. T., et al. (2003) Applied and Environmental Microbiology 69, 5884–5891.

[3] Bernier-Latmani R., et al. (2010) Environmental Science and Technology 44, 9456–9462.

[4] Boyanov M. I., et al. (2011) Environmental Science and Technology 45, 8336–8344.

Theoretical actinide molecular science: aqueous species, macrocycles, mineral surfaces

G. Schreckenbach

Department of Chemistry, University of Manitoba, Winnipeg, MB, Canada

Over the last decades, computational chemistry has seen continuous and rapid development that is driven both by the sustained development of computer technology (exemplified by Moore's Law [1]) and by significant advances in theory and methodology [2]. Computational chemistry has reached a point where it can be used as "just another spectrometer" in a "black-box" fashion for certain areas and applications, while it continues its fast development in other areas.

Theoretical and computational actinide chemistry [3], application of the tools of computational chemistry to the early actinides (typically Th to Am), is an area that is still a frontier area, despite having seen impressive advances over the last several years. This is due to challenges arising from the size of typical systems, the need to include relativistic effects, and technical difficulties such as the large number of closely spaced electronic states, amongst others. This, combined with the *experimental* challenges of actinide (and particularly trans-uranium) chemistry, makes the actinides a particularly fruitful area for collaborations between theoretical and experimental research.

We will begin this presentation by discussing some aspects of the computational methodology as applied to actinides (and thus, we will "take a look inside the black box"). We will then focus on some applications from our recent work. In this manner, we hope to illustrate the scope of questions that can be addressed, and the kind of unique insight that computational chemistry might provide. Specifically, we will discuss representative results from the following areas:

- (i) Aqueous chemistry: Plutonyl hydroxide complexes (Fig. 1) [4];
- (ii) Macrocycles: Uranium-uranium interaction and other unique bonding schemes of bimetallic actinide complexes inside a "pacman" polypyrrolic macrocycle (Fig. 2) [5, 6];
- (iii) Mineral surface interactions: Adsorption of uranyl species onto TiO_2 surfaces (Fig. 3) [7, 8].

In each case, we will attempt to draw specific as well as general conclusions regarding the methodology employed and the chemistry involved.

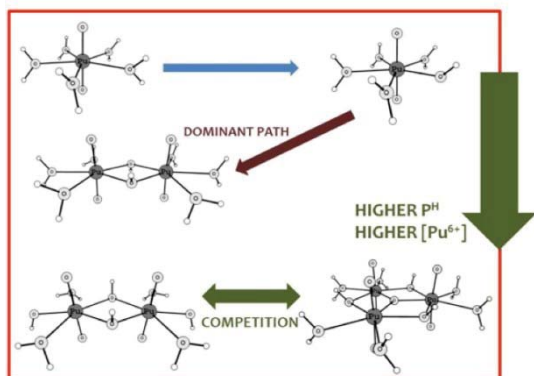


Fig. 1: Summary of plutonyl hydroxide speciation [4].

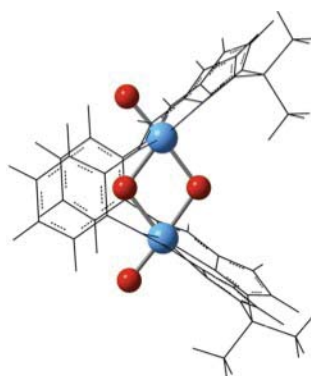


Fig. 2: Computationally predicted "butterfly" U_2O_4 structure within the framework of the 'pacman' ligand [5].

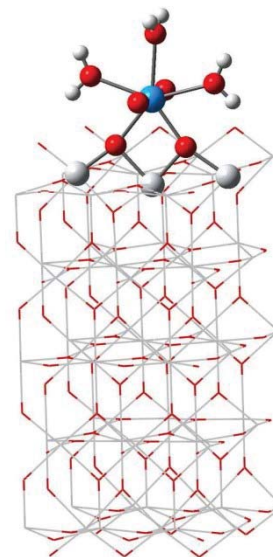


Fig. 3: Uranyl aquo complex adsorbed on a TiO_2 surface [7,8].

[1] http://en.wikipedia.org/wiki/Moore%27s_law, accessed June 24, 2014.

[2] Cramer, C. J. (2004) *Essentials of Computational Chemistry: Theories and Models*; 2nd ed.; Wiley, New York.

[3] Schreckenbach, G. and Shamov, G. A. (2010) *Acc. Chem. Res.* 43, 19–29.

[4] Odoh, S. O.; Reyes, J. A.; Schreckenbach, G. (2014) *Inorg. Chem.*, submitted.

[5] Pan, Q.-J.; Shamov, G. A.; Schreckenbach, G. (2010) *Chem. Eur. J.* 16, 2282–2290.

[6] Arnold, P. L. et al. (2012) *Nature Chem.* 4, 221–227.

[7] Odoh, S. O. et al. (2012) *Chem. Eur. J.* 18, 7117–7127.

[8] Pan, Q.-J. et al. (2012) *Chem. Eur. J.* 18, 1458–1466.

Uptake, reduction, and reoxidation mechanisms of uranium in biogeochemical systems studied by X-ray absorption spectroscopy

M. I. Boyanov,^{1,2} D. E. Latta,^{1,3} B. Mishra,^{1,4} E. J. O'Loughlin,¹ K. M. Kemner¹

¹ Biosciences Division, Argonne National Laboratory, Argonne, U.S.A.

² Institute of Chemical Engineering, Bulgarian Academy of Sciences, Sofia, Bulgaria

³ Department of Civil and Environmental Engineering, The University of Iowa, Iowa City, U.S.A.

⁴ Physics Department, Illinois Institute of Technology, Chicago, U.S.A.

Uranium (U) is a contaminant of current concern at several sites in the United States, such as the former nuclear materials production site at Hanford, Pacific Northwest National Laboratory (PNNL); the closed U mine at Rifle, CO, and the former U enrichment facility at the Oak Ridge National Laboratory (ORNL). Uranium is also an emergent contaminant worldwide from fracking processes and from nuclear energy production. When contaminated groundwater passes through subsurface regions it can encounter both reducing and oxidizing zones that contain various biological and mineral surfaces. The molecular-level interactions of the dissolved contaminant with the subsurface components determine its overall propagation rate, so a certain degree of mechanistic understanding of the uptake processes is needed to be able to include appropriate reactions in a chemical model and to provide accurate predictions of contaminant transport at the field scale.

To this end, various spectroscopies are currently being employed to obtain the necessary information. X-ray absorption fine-structure spectroscopy (XAFS) is well-suited to the study of U transformations in environmental systems, due to its chemical selectivity, its sensitivity to valence state and local atomic structure, and its ability to probe the U atoms in an arbitrary hydrated matrix. Uranium redox transformations are of particular interest, since a significant decrease in dissolved U concentration is observed when oxidized U^{VI} is reduced to U^{IV} through chemical or biological processes. We will present results from XAFS measurements in systems where U^{VI} was reacted with biotic and abiotic reductants that are relevant to iron- or sulfate-reducing conditions in subsurface environments (e.g., reactions with bacteria or Fe^{II} -containing phases). We find that the redox reactivity between Fe^{II} and U^{VI} increases with increased clustering of the Fe^{II} atoms (i.e., when Fe^{II} polymerizes in minerals or when the Fe^{II} content of magnetite increases). We also find that reduction to U^{IV} does not necessarily lead to the formation of the lowest solubility mineral uraninite (UO_2). Factors such as the presence of phosphate or Ti^{IV} in the system, or the ratio of U to high-affinity binding sites on magnetite and TiO_2 lead

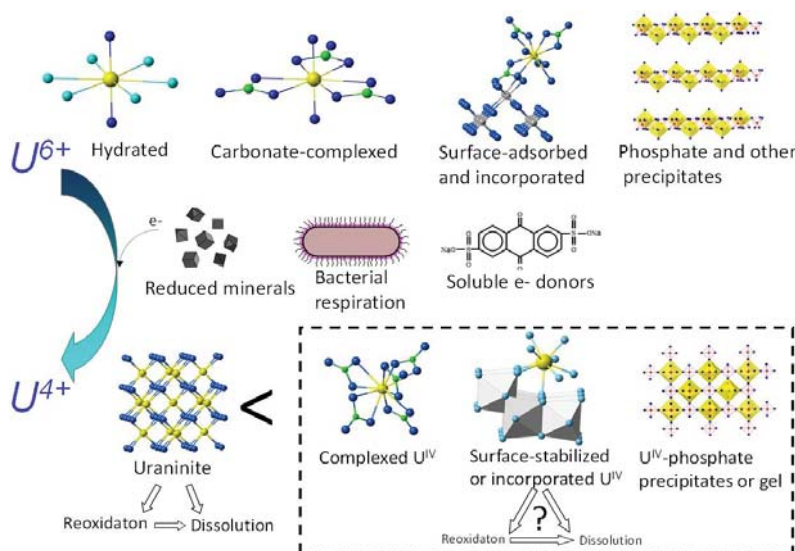


Fig. 1: Schematic illustration of the major processes responsible for U uptake in environmental systems. The importance and the current scarcity of information on reduced non-uraninite U^{IV} phases are highlighted by the dashed-line box.

to different adsorbed (i.e. non-uraninite) U^{IV} species. These findings provide an explanation for the recently observed predominance of non-uraninite U^{IV} species in contaminated sediments under reducing conditions and suggest the need for refinement of reactive transport models that only use thermodynamic and kinetic parameters derived for nanoparticulate uraninite. The use of XAFS was instrumental in obtaining these insights, highlighting the importance of spectroscopic techniques in providing an improved understanding of contaminant transport.

Bose-Einstein-Hubbard condensate-type behavior *via* a novel mechanism in the *f* electron Mott insulator $\text{UO}_{2(+x)}$

S. D. Conradson,^{1,2} D. A. Andersson,² T. Durakiewicz,² S. M. Gilbertson,² G. Rodriguez,² M. L. Neidig,³ S. Daifuku,³ J. Kehl³

¹ Synchrotron Soleil, Gif-sur-Yvette, France

² Los Alamos National Laboratory, Los Alamos, New Mexico, U.S.A.

³ University of Rochester, Rochester, New York, U.S.A.

The requirement for coherence among its constituent particles renders condensation an ultralow temperature phenomenon in systems comprised of atoms. However, condensates have also been prepared from several different types of quasiparticles, with high temperatures associated with ones with very

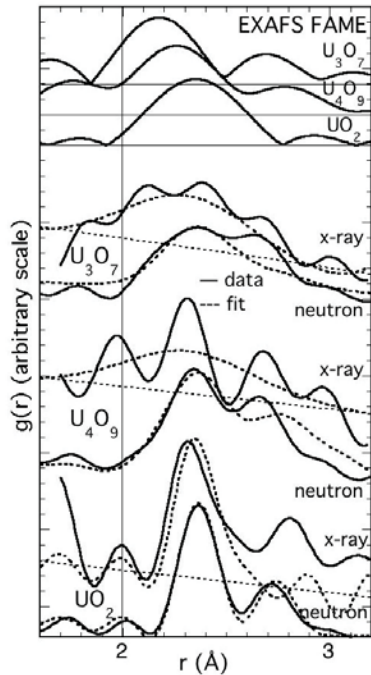


Fig. 1: XAFS, X-ray pdf and neutron pdf results from UO_{2+x} compounds.

low masses. None have yet been prepared from polarons, which would be of substantial interest because of their inclusion of charge and spin and direct association with the fully dense crystal lattice. Formation from polarons could also possibly give some of the unique properties of condensates at higher temperatures if the coherence originated in a collective excitation that could occur in a mixed valence oxide. Using a large number of structural and spectroscopic probes, we now have a number of bizarre and unique experimental results that are best interpreted as being signatures of a quantum phase composed of polaronic carriers in the Mott insulator UO_2 . Differences between the structures of doped UO_{2+x} determined by neutron scattering vs. X-ray scattering and absorption demonstrate that this system exhibits intrinsic dynamics analogous to this property in cuprates. They also show (Fig. 1) a much more complicated excitation that includes charge transfer between U(IV) and (VI) states with the accompanying atom displacements far too large for the tunnelling polaron process. Accompanying O XAS measurements support this interpretation, showing the broadening of the electronic states expected with intrinsic dynamics. EPR measurements demonstrate that the spins as well as the charges display collective behavior that is neither superconductivity nor ferromagnetism. The properties of unpinned carriers were examined with optical pump-optical/THz probe spectroscopy. These experiments show that the photoinduced charged quasiparticles created by relaxation from the $5f$ portion of the UHB aggregate and organize to form their own quantum phase separate from the UO_2 host that undergoes a gap opening phase transition at 50–60 K (Fig. 2). The <1.5 THz probe also is consistent with quasiparticle condensation, and a 2 THz signal gives oscillations that could only occur with a condensate. The best and perhaps only explanation for these properties is that the domains containing the charges and spins are droplets of superfluid formed by the U(V)-U(IV/VI) charge transfer excitation made coherent within these domains by its coupling to a (111)-oriented phonon that changes the spacing between the U planes and the relative stability of these two forms of the material.

low masses. None have yet been prepared from polarons, which would be of substantial interest because of their inclusion of charge and spin and direct association with the fully dense crystal lattice. Formation from polarons could also possibly give some of the unique properties of condensates at higher temperatures if the coherence originated in a collective excitation that could occur in a mixed valence oxide. Using a large number of structural and spectroscopic probes, we now have a number of bizarre and unique experimental results that are best interpreted as being signatures of a quantum phase composed of polaronic carriers in the Mott insulator UO_2 . Differences between the structures of doped UO_{2+x} determined by neutron scattering vs. X-ray scattering and absorption demonstrate that this system exhibits intrinsic dynamics analogous to this property in cuprates. They also show (Fig. 1) a much more complicated excitation that includes charge transfer between U(IV) and (VI) states with the accompanying atom displacements far too large for the tunnelling polaron process. Accompanying O XAS measurements support this interpretation, showing the broadening of the electronic states expected with intrinsic dynamics. EPR measurements demonstrate that the spins as well as the charges display collective behavior that is neither superconductivity nor ferromagnetism. The properties of unpinned carriers were examined with optical pump-optical/THz probe spectroscopy. These experiments show that the photoinduced charged quasiparticles created by relaxation from the $5f$ portion of the UHB aggregate and organize to form their own quantum phase separate from the UO_2 host that undergoes a gap opening phase transition at 50–60 K (Fig. 2). The <1.5 THz probe also is consistent with quasiparticle condensation, and a 2 THz signal gives oscillations that could only occur with a condensate. The best and perhaps only explanation for these properties is that the domains containing the charges and spins are droplets of superfluid formed by the U(V)-U(IV/VI) charge transfer excitation made coherent within these domains by its coupling to a (111)-oriented phonon that changes the spacing between the U planes and the relative stability of these two forms of the material.

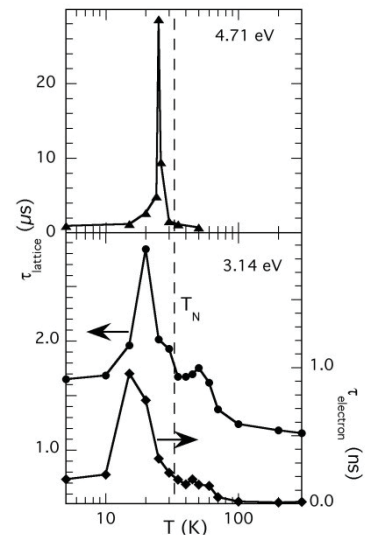


Fig. 2: Quasiparticle lifetimes following optical pumping at listed energies.

[1] Conradson, S. D., et al. (2013) Phys. Rev. B 88, 115135/1-22.

[2] Conradson, S. D., et al. (2014) J. Phys. Chem. C, submitted.

Mineral surface hydroxo group identity and reactivity

J.-F. Boily

¹ Department of Chemistry, Umeå University, Umeå, Sweden

Mineral surfaces are geochemically important reaction centres and sinks for gases, solutes and solvents. These surfaces are populated by (hydr)oxo functional groups that can undergo protonation, ligand exchange, and form extensive networks of hydrogen bonds. Knowledge of the types, distributions and orientations of these groups is essential for understanding molecular-scale processes taking place at mineral surfaces.

Fourier transform infrared spectroscopy is used to probe different types of hydroxo groups at mineral surfaces of geochemical importance. The strong sensitivity of the O-H bond strength to changes in bonding environment (*ca.* 150 cm⁻¹ per pm change in O-H bond length) imparts substantial changes in the O-H stretching region when mineral surfaces are exposed to reactive species. In this work we resolve interactions between these groups at surfaces of synthetic nano-sized (α , β , γ)-FeOOH particles with atmospheres containing water vapor and carbon dioxide to illustrate this principle. Vibration spectroscopic signatures of isolate and hydrogen bonded hydroxo groups at these mineral surfaces will be presented alongside structural and spectroscopic predictions from molecular modelling efforts. This body of work forms the basis for a molecular-scale understanding of key reactions taking place at surfaces of geochemically relevant mineral particles that are not only exposed to the gas phase but also to aqueous solutions.

Monitoring redox and separation behavior of actinide ions by a combination of NMR and Emission Spectroscopy

L. S. Natrajan,¹ S. D. Woodall,¹ A. N. Swinburne,¹ S. Randall,¹ A. Geist,² P. J. Panak,² B. B. Beele,² N. Banik,² C. Adam,² P. Kaden,² A. Kerridge³

¹ The Centre for Radiochemistry Research, The University of Manchester, Manchester, U.K.

² Institute for Nuclear Waste Disposal, Karlsruhe Institute of Technology, Eggenstein-Leopoldshafen, Germany

³ Department of Chemistry, University College London, London, U.K.

Europe currently holds a substantial nuclear legacy arising from fission activities, with a large proportion of high activity wastes that pose a radiological threat to natural and engineered environments. The decision to dispose of these high level wastes (following separation) in a suitable geological disposal facility (GDF) has provided some of the most demanding technical and environmental challenges facing the EU in the coming century. In order to address these issues, we have begun a program of work to establish a comprehensive understanding of the electronic properties and physical and chemical properties of the radioactive actinide meta ls us ing state of the art emission spectroscopic techniques in combination with NMR and computational methods [1].

Our approach to this is to firstly use coordination chemistry to synthesize uranium compounds with ligands that model environmentally complexed species and use optical spectroscopy to understand and map both the chemical and physical behavior of these species (Figure 1). We have recently established that U(IV) complexes are emissive and will demonstrate that uranium in the +IV and +VI oxidation states can be detected simultaneously at relatively low concentrations. Time gating techniques enable the long lived uranyl(VI) species to be separated from the shorter lived uranium(IV) species. Furthermore, the form of the emission spectra of uranyl(VI) compounds are extremely sensitive to the nature of the ligand bound in the equatorial plane and the complex nuclearity (extent of aggregation), potentially giving a sensitive method of assessing the solution forms of uranium in environmental conditions. We will next discuss how the optical properties of these model compounds can be extended to the *trans*-uranics and applied to disproportionation reactions and redox events in solution. Finally, we will discuss the development of new polyaminocarboxylate ligands that are effective in lanthanide/actinide separation technologies.

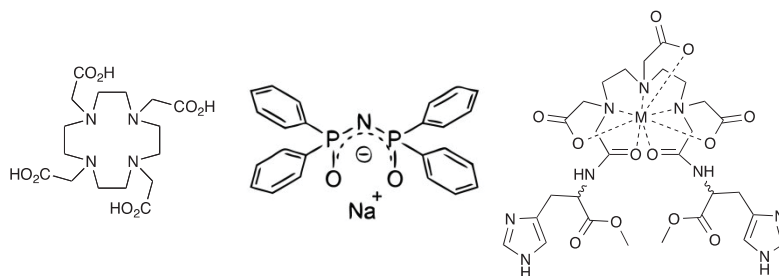
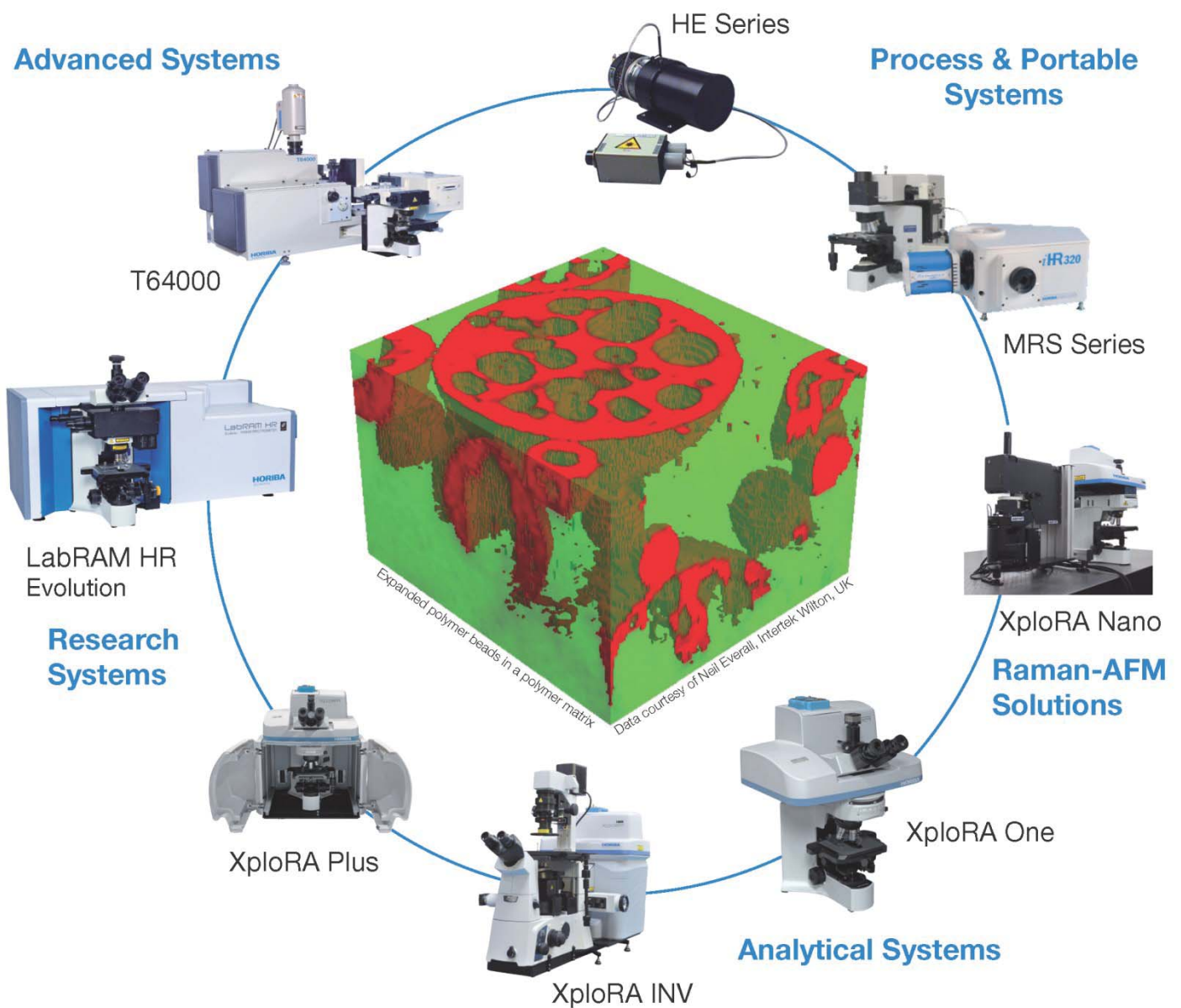


Fig. 1: Ligands chosen as models for carboxylate and phosphate actinide species with U, Np, Am and Cm.

[1] L. S. Natrajan, (2012) *Coord. Chem. Rev.* 256, 1583; *Coord. Chem. Rev.* (2014), 266–267, 171.

The Most Complete Line of Solutions from the World Leader in **3D** Raman Spectroscopy



Importance of actinides-organic complexes in biodegradation and bioreduction

T. Ohnuki,¹ Y. Suzuki,² T. Nankawa,¹ K. Tanaka³

¹ Advanced Science Research Center, Japan Atomic Energy Agency, Japan

² School of Bioscience and Biotechnology, Tokyo University of Technology, Tokyo, Japan

³ Institute for Sustainable Sciences and Development, Hiroshima University, Hiroshima, Japan

When multivalent actinides (Ans) and lanthanides (Lns) released from the HLW and TRUW disposal sites migrate through geologic formation, some fraction of Ans and Lns were sorbed by the geological compositions, such as inorganic and organic materials [1,2]. Among the geological compositions, microorganisms are ubiquitous and are well known to sorb radionuclides [3,4]. TRU wastes contain cellulosic materials, scintillation fluids, waste oils, decontamination reagents, and chemical reagents. Among them, organic acids may form stable complexes with multivalent actinides (Ans) and lanthanides (Lns). Citric acid, which is a low molecular organic substance ubiquitously found in the environment [5], affects the sorption of metal ions on inorganic substances. Redden et al. [6] reported that citric acid enhances the sorption of U(VI) on goethite, but reduces its sorption on kaolinite at acidic pH. These findings demonstrate that the presence of organic acids affects the mobility of metal ions. However, little is known of the effect of organic materials on the sorption behavior of Ans and Lns by microorganisms.

We have examined the chemical species change of Eu(III) and U(VI) complexes with citric acid and malic acid during the degradation and reduction by *Pseudomonas fluorescens* and *Shewanella putrefaciens*. We have also studied Ce(III) accumulation by the mixture of biogenic Mn oxides and fungus hyphae. The oxidation states of Ce and U were determined by XANES and UV-Vis. The solid phase was analyzed by SEM and EDS. The chemical species of Eu- and U-citrate or malic complexes were analyzed by ESI-MS. The exudates of fungus binding with Ce was measured by SEC-HPLC coupled with ICP-MS.

P. fluorescens degraded Eu-citrate and -malate complexes. In the degradation of Eu-citrate complexes, excess citrate was degraded until the citrate/Eu ratio was ca. 1. ESI-MS analysis revealed that remained citrate was formed 2:2 complex with Eu, indicating that bi-nuclear Eu-citrate complex is recalcitrant. In the degradation of Eu-malate complex, one of the metabolites associated with Eu was determined as pyruvic acid by ESI-MS. In the reduction of U(VI) by *S. putrefaciens* without citrate, most of the dissolved U was precipitated to form UO₂ by SEM and XANES analyses. With citrate, most of U was dissolved after the reduction to U(IV) by UV-Vis spectra. The reduction rate of U(VI) to U(IV) with citrate was smaller than that with EDTA. ESI-MS analysis indicated the presence of multi-nuclear complexes, suggesting that the bio-reduction of U(VI) slows by the formation of multi-nuclear complexes. Ce(III) was oxidized to Ce(IV) by the association with biogenic Mn oxides by XANES analysis, and the associated Ce(IV) was released into the solution with the organic exudates of the fungal hyphae by SEC-HPLC-ICPMS analysis.

These results indicate that biotransformation of Lns and Ans strongly depends on the chemical species.

[1] N. Kozai, et al. (2014) J. Radioanal. Nucl. Chem. 299, 1581–1587.

[2] N. Kozai, et al. (2014) J. Radioanal. Nucl. Chem. 299, 1571–1579.

[3] K. Tanaka, et al. (2010) Geochimica et Cosmochimica Acta 74, 5463–5477.

[4] M. Jiang, et al. (2010) Chem. Geology 277, 61–69.

[5] S. Buruckert (1970) Ann. Agron. 21, 725–757.

[6] G.D. Redden, et al. (1998) Adsorption of Metals by Geomedia, Ch. 13 (E. A. Jenne, ed.), Academic Press, USA.

TRLFS studies on biosorption of uranium on halophilic archaea at high ionic strength (3 M NaCl)

M. Bader,¹ A. Cherkouk,¹ B. Drobot,¹ T. Stumpf¹

¹ Institute of Resource Ecology, Helmholtz-Zentrum Dresden-Rossendorf, Dresden, Germany

Salt rock is one of the three potential host rock types for long-term storage of radioactive waste in a deep geological repository in Germany. To date little is known about the interactions of halophilic microorganisms which are indigenous in salt rock and radionuclides under these extreme conditions. The microorganisms can impact the oxidation state, speciation and solubility of radionuclides and hence their mobility. This information is necessary to improve the safety assessment of a geological repository.

To characterize the interactions between radionuclides and microorganisms under high saline conditions biosorption experiments with *Halobacterium noricense* DSM 15987 and uranium were done. This halophilic archaea is used because of its ubiquitous occurrence in salt rock [1].

Due to its halophilicity the working concentration of NaCl was 3 M. The batch experiments have shown that 90% of U(VI) was bound to the cells after 48 h. The formed uranium complexes were characterized by the use of infrared-spectroscopy and time-resolved laser-induced fluorescence spectroscopy (TRLFS). Despite the high concentration of chloride a luminescence spectrum could be recorded. The spectra of the salt solutions (3 M NaCl)

with different uranium concentrations (10 μ M, 50 μ M, 100 μ M; pH 6) without cells have the same emission maxima (512, 536, 560 nm; see Fig. 1). Comparing the position of this bands with literature they can be assigned to the $(\text{UO}_2)_3(\text{OH})_5^+$ complex [2]. In contrast, the suspension consisting of *Halobacterium noricense* cells and U(VI) in 3 M NaCl lead to a red-shift of the spectra where the emission bands (501, 522, 550 nm; see Fig. 1) indicate the uranyl phosphate complex UO_2PO_4^- [3]. It can be concluded that uranium binds to phosphate groups which are located on the cell wall or inside the cells. Further investigations (e.g. TEM/EDX) are required for differentiation. These first results show that the characterization of the formed complexes is possible with TRLFS despite the high chloride concentration and can be used for further examinations.

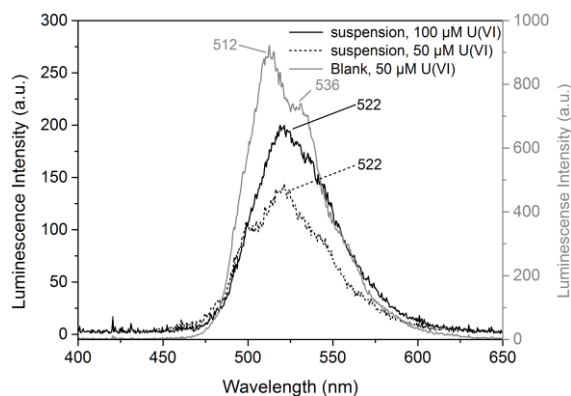


Fig. 1: TRLFS spectra of samples after biosorption experiments from *Halobacterium noricense* with uranium (pH 6, 3 M NaCl, 48 h). Grey: Blank 50 μ M U(VI); dotted line: cell suspension, 50 μ M U(VI); black: cell suspension, 100 μ M U(VI).

[1] Swanson, J.S., et al. (2012) Status Report Los Alamos National Laboratory

[2] Moulin, C., et al. (1998) Appl. Spectrosc. 52, 528–535.

[3] Bonhoure, I., et al. (2007) Radiochim. Acta. 95, 165–172.

Uranium Redox processes – initiated by plant cells

G. Geipel,¹ K. Viehweger²

¹ Institute of Resource Ecology, Helmholtz-Zentrum Dresden-Rossendorf, Dresden, Germany

² Institute Radiopharmaceutical Cancer Research, Helmholtz-Zentrum Dresden-Rossendorf, Dresden, Germany

Recently we have shown that uranium can be taken up by plant cells. Fractionation studies showed that the uranium was present in nearly all cell compartments. Nevertheless, luminescence measurements showed that the speciation of the uranium in the several cell compartments differs from each other.

One of the major remaining questions concerns to the ways of uranium uptake. Recently published work [1, 2] proposed that the uranium uptake is influenced by the iron uptake. As it is known that the iron uptake occurs via reduction of the iron(III) into iron(II), we conclude that uranium uptake should also be accompanied by a redox process. First measurements by laser-induced photo-acoustic spectroscopy gave evidence for the presence of uranium(IV) inside the cells.

The formation of uranium(IV) from uranium(VI) is a more complicated redox process, as the oxo-cation uranium(VI) has to be transformed into an oxo-hydrate form. Electrochemically this process is irreversibly. In systems existing at nearly neutral pH additionally hydrolysis or complex formation of the uranium ions occur.

On the other hand the formed uranium(IV) can also be formed by a disproportionation step from uranium(V).



From electrochemical point of view the formation of uranium(V) is a reversible process and the redox potential uranium(VI)/uranium(V) is of the same order as the redox potential iron(III)/iron(II) (values for acidic solution).

The evaluation of Laser-Induced Photoacoustic Spectra (LIPAS) in the wavelength range 620 nm to 680 nm gave evidence for the formation of both reduced oxidation states in the media studied. The uranium(V) is assigned to an absorption at around 637 nm [3] while uranium(IV) absorbs light at ~660 nm.

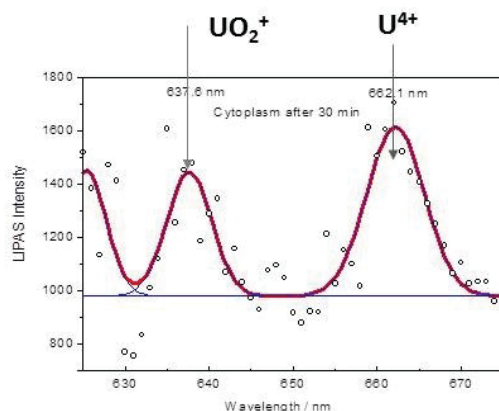


Fig. 1: LIPAS spectrum of the cytoplasm fraction.

To prove the proposed mechanism of uptake in addition to the cytoplasm fraction both oxidation states should exist also in the nutrient medium. Examples will be shown.

[1] F. Doustaly et al. (2014) Uranium perturbs signaling and iron uptake response in *Arabidopsis thaliana* roots, *Metallomics* 6, 809–821.

[2] K. Viehweger, G. Geipel (2010) Uranium accumulation and tolerance in *Arabidopsis halleri* under native versus hydroponic conditions, *Environmental and Experimental Botany* 69, 39–46.

[3] T. Ogura et al. (2010) Spectroelectrochemical identification of a pentavalent uranyl tetrachloro complex in room-temperature ionic liquid, *Inorganic Chemistry* 50, 10525–10527.

Mechanisms of uranium and thorium accumulation in the bone matrix

G. Creff,¹ S. Safi,² P. Lorenzo Solari,³ C. Vidaud,⁴ C. Den Auwer¹

¹ Institut de Chimie de Nice (ICN), Université Nice Sophia Antipolis, Nice, France

² Institut de Physique Nucléaire d'Orsay (IPNO), Université Paris-Sud, Orsay, France

³ Synchrotron SOLEIL, Gif-sur-Yvette, France

⁴ Laboratoire d'étude des protéines cibles, CEA Centre de Marcoule, Bagnols-sur-Cèze, France

In case of release of actinides in the environment, contamination of the living organisms can occur and induce radiological and chemical toxicities. Whatever the way of integration, the radioelement is absorbed, then either directly excreted, or transported by blood, linking with different biological ligands (amino acids, peptides, proteins), toward target organs. While at the macroscopic scale many studies have described the impact of such elements on animals (biokinetics studies), quantified the excretion and the retention rates and identified the main target organs, the information concerning the mechanisms of transport, accumulation and storage of actinides at the molecular level still remain very scarce mainly because of the difficulty to combine the actinide chemistry (strong tendency to hydrolysis) with the physiological conditions (around pH 7).

Regarding the possible target organs and based on several different studies, the bone matrix appears as a privileged target for most of the actinides (it retains 70% of Th(IV), 10–15% of U(VI) 30–50% of Np(IV) and (V), 50% of Pu(IV) and 30% of An(III)). The objective of our research work is to elucidate the mechanisms of interaction of thorium and uranium with the bone matrix at the molecular scale. The bone is composed of a cellular matrix (osteocytes and osteoblasts) and an extra cellular matrix (ECM), presenting a mineral and an organic phase. The mineral part of ECM consists of hydroxyapatite (HAP) crystals and calcium carbonate. On the other hand, the organic part of ECM is composed of various proteins, including osteopontin. This hyper-phosphorylated and non-structured macromolecule, which has recently been identified, is particularly important in the process of osteogenesis (providing the link between HAP and bone cells) and might play a crucial role in the *in vivo* accumulation of actinides in the regions of bone growth, capable of inducing bone cancer. Moreover it is well known that actinides present a very strong chemical affinity for phosphate groups, whether from organic or mineral origin. We have studied the interaction of the osteopontin protein with two selected actinides: uranium, at oxidation state (VI) because it is the radioelement which presents the largest “natural” exposure risk (especially for the workers of the extraction uranium mines) but also because it is a good representant of the γ actinide cations; and thorium, at oxidation state (IV), because it represents a possible new combustible for future nuclear plants and also because it is a less radioactive surrogate with simpler RedOx chemistry than for all the other actinides (IV) (such as Pu).

For that purpose, we have implemented a combination of experimental and theoretical techniques. Among the different experimental techniques used to probe the structure of the complexes between actinides and their biological environment (molecule, protein, matrix), X-ray Absorption Spectroscopy (XAS) is an ideal tool. By probing the local environment of the targeted cation, this spectroscopy allows to overcome the size, chemical and physical forms of the considered system. XAS experiments were thus performed on the Mars beamline of SOLEIL synchrotron (French synchrotron radiation source facility) and were combined with density functional theory calculations (DFT), time resolved luminescence spectroscopy (TRLS, for uranium only), attenuated total reflection Fourier transform infrared (ATR-FTIR) and isothermal titration calorimetry (ITC) experiments in order to determine the local organization around the actinide cation¹. In order to complement these structural data, a study of ²³⁸Pu complexation by osteopontin at the actinide trace scale and at physiological pH is currently ongoing. We have used size dependant micro filtration and alpha spectrometry to determine the plutonium behavior towards OPN uptake. This approach complements the structural data obtained on Th(IV) with pseudo physiological conditions that mimic possible Pu(IV) contamination.

[1] S. Safi, G. Creff, A. Jeanson, L. Qi, C. Basset, J. Roques, P. Lorenzo Solari, E. Simoni, C. Vidaud, C. Den Auwer (2013) *Chem. Eur. J.* 19, 11261.

Chelation of uranyl by variants of the calmodulin EF-hand motif

R. Pardoux,¹ S. Sauge-Merle,¹ D. Lemaire,¹ M. R. Beccia,¹ N. Bremond,¹ C. Battesti,¹ M. L. Merroun,² P. L. Solari,³ P. Delangle,⁴ P. Guilbaud,⁵ C. Berthomieu¹

¹ CEA, DSV, IBEB, UMR7265 CNRS CEA Aix-Marseille Univ, St Paul-lez-Durance, France

² Dept. of Microbiology, Univ. of Granada, Spain

³ Synchrotron SOLEIL, Gif-sur-Yvette, France

⁴ CEA, INAC, Service de Chimie Grenoble, France

⁵ DRPCPC, SMCS, LILA, CEA-Marcoule, Bagnols-sur-Cèze, France

Proteins or peptides are very versatile metal ligands, as illustrated by the large number of metalloproteins which catalyze a wide range of highly selective reactions through a restricted number of metal ions. Metal sites are ‘designed’ for selective uptake and catalytic activity.

We chose a protein engineering approach to analyze structural factors governing uranyl binding and thermodynamic stabilization in proteins and to develop affine and specific ligands for selective uptake that could be used for bioremediation.

Uranyl properties present similarities with those of calcium. The EF-hand motif is the most prevalent Ca^{2+} -binding site in proteins. All metal ligands are located within a 12 amino acid loop (Fig. 1). We selected the recombinant N-terminal domain of calmodulin from *A. thaliana* as a structured template that contains two EF-hand Ca^{2+} binding motifs to engineer peptide variants with increased uranyl affinity and specificity. By combining site directed mutagenesis to substitute Ca^{2+} ligands and/or the introduction of phosphoryl groups (Fig. 1), we could modulate uranyl binding properties as well as the U/Ca selectivity.

The protein variants have been studied by fluorescence spectroscopy and microcalorimetry to obtain thermodynamic parameters of the uranyl-protein complexation. In addition a modeling approach based on molecular dynamics was used together with FT-IR and EXAFS spectroscopies to identify structural characteristics of the protein-uranyl complexes.

We showed that the introduction of a phosphoryl group at threonine-9 in the metal binding loop increases the affinity of the peptide for uranyl by almost two orders of magnitude at pH 7.[1] FT-IR spectra indicated that the phosphoryl group is deprotonated at pH 7 and is involved in uranyl coordination. We also obtained a uranyl binding motif with dissociation constants K_d of 200 pM at pH 6 and pH 7 without phosphorylation ($K \sim 5 \times 10^9$) and a uranyl/calcium specificity of 10^7 . [2] The uranyl-protein complexes have been studied using FT-IR and EXAFS spectroscopy to analyze the structure of the uranyl binding site.

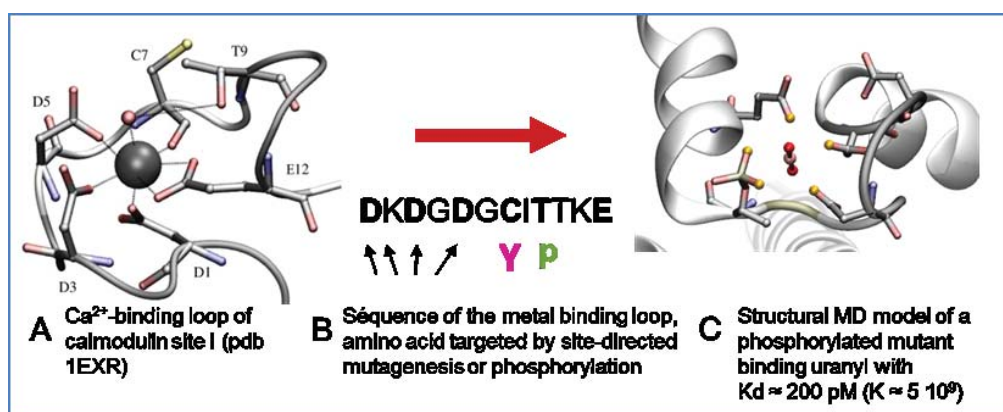


Fig. 1: Illustration of the strategy used to engineer a uranyl binding site in the EF-hand motif of calmodulin.

[1] Pardoux R. et al. (2012) Modulating uranium binding affinity in engineered calmodulin EF-hand peptides : effect of phosphorylation, PLoS One 7, e41922.

[2] New uranium-chelating peptides derived from EF-hand calcium-binding motif useful for uranium biodetection and biodecontamination, R. Pardoux, et al... patent submitted 28 march 2013, n° 13305400.7.

Study of paramagnetic actinide complexes with dipicolinate ligands

M. Autillo,¹ C. Berthon,¹ P. Moisy²

¹ CEA Marcoule, DEN/DRCP/SMCS/LILA, Bagnols sur Cèze CEDEX, France

² CEA Marcoule, DEN/DRCP, Bagnols sur Cèze CEDEX, France

The actinide (An) solution chemistry has been the subject of many studies over the last years, particularly in order to understand the behavior difference between An(III) and Ln(III). This research conducted in the nuclear fuel processing has led to consider a covalent part in ligand – actinide bonds [1]. Despite many efforts to prove and quantify this phenomenon, it is still difficult to explain the chemical properties of these elements in solution. In this context, the study of actinide paramagnetic behavior can be a "simple" method to analyze the electronic properties of actinide elements and obtain information on the ligand – actinide interaction. This information may be obtained from a NMR chemical shift study of actinide complexes. Indeed, modifications induced by a paramagnetic complex can be divided into two components (see [eq. 1]). A Fermi contact contribution (δ_c), which represents the covalence degree of coordination bonds with the actinide ions and a dipolar contribution (δ_{pc}), which accounts for the complex structures. The paramagnetic induced shift (δ_{para}) can be used only if we can isolate these two terms.

$$(\delta_{para})_{i,j} = (\delta_{pc})_{i,j} + (\delta_c)_{i,j} = G_i C_j^D + F_i \langle S_z \rangle_j \quad [\text{eq. 1}]$$

$$(\delta_{para})_{i,j} = \frac{F_i'}{T} \langle S_z \rangle_j + \frac{G_i'}{T^2} C_j^D \quad [\text{eq. 2}]$$

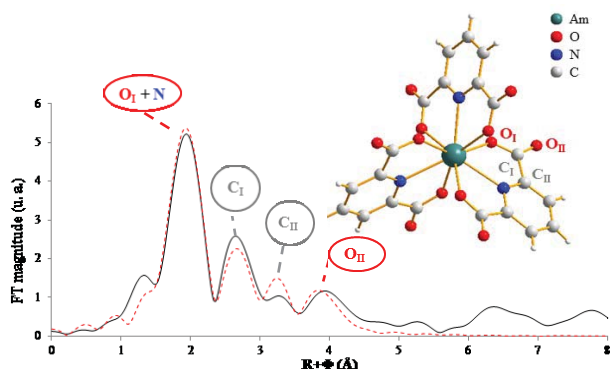


Fig. 1: Fourier transform of experimental and fitted spectra on crystallographic data of $\text{Am}(\text{DPA})_3(\text{C}_3\text{H}_5\text{N}_2)_3 \cdot 3\text{H}_2\text{O}$.

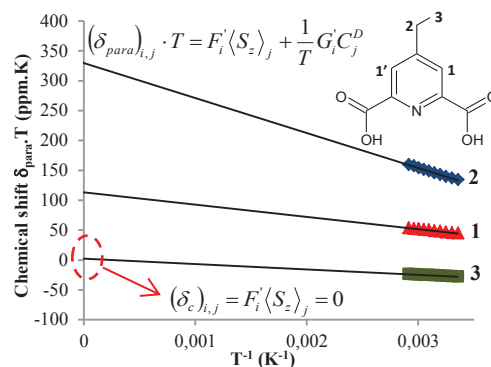


Fig. 2: Plot of $\delta_{para} \cdot T = f(1/T)$ for $\text{Am}(\text{DPA})_3^{3-}$ complex in DMSO.

Empirical separation methods (*i*) have been proposed for lanthanide complexes and are based on a graphical separation [2]. Another approach consists in using the temperature dependence difference of chemical shifts (see [eq. 2]) (*ii*) or an induced shift “purely dipolar” (*iii*) [2].

To achieve this study on actinide elements, we chose to work with complexes of dipicolinic acid (DPA). They are stable and form rigid structures in solution. First, in order to determine the structure factor G_i (see [eq. 2]), a crystallographic study was performed on An(III) complexes with the DPA ligand and through cooperation with FIPCE Moscow (A. Fedosseev). Then, the solid state structure conservation in solution has been proved by an EXAFS study (Fig. 1). Finally, various separation methods (*ii* and *iii*) involving NMR spectroscopy were applied to actinide elements. Unlike with Ln(III) ions [3], the An(III) paramagnetic induced shift on NMR ^1H signals and their temperature dependence suggest a major Fermi contact contribution (δ_c), showing a higher covalent part for An(III). However, the temperature study of ethyl-DPA ligand (Fig. 2) with more expanded protons seems to reveal a major dipolar contribution (δ_{pc}) for the CH_3 group and a paramagnetic shift separation can be proposed. Thus, it appears that the study of the paramagnetic behavior of these ions with a specific ligand (^1H up to six bonds from the paramagnetic center) allows to separate these contributions from the total paramagnetic shift and to obtain contact and dipolar information.

[1] (a) R. E. Cramer, et al. (1983) *Organometallics* 2, 1336–1340. (b) J. G. Brennan, et al. (1989) *Journal of the American Chemical Society* 111, 2373–2377 (c) N. Kaltsoyannis (2000) *Inorganic Chemistry* 39, 6009–6017.

[2] C. N. Reilley, et al. (1976) *Analytical Chemistry*, 1446–1458.

[3] J. F. Desreux and C. N. Reilley (1976) *Journal of the American Chemical Society* 98, 2105–2109.

Plutonium oxidation state speciation in aqueous solution studied by Pu L and M edge high energy resolution XANES technique

I. Pidchenko, D. Fellhauer, T. Prüßmann, K. Dardenne, J. Rothe, E. Bohnert, B. Schimmelpfennig, T. Vitova

Institute for Nuclear Waste Disposal, Karlsruhe Institute of Technology, Eggenstein-Leopoldshafen, Germany

In this work four electrochemically aqueous plutonium (Pu) species prepared in perchloric acid solution at different oxidation states (III, IV, V, VI) as well as Pu(IV) colloids are characterized for the first time by Pu L₃ and M₅ edge high energy resolution X-ray absorption near-edge structure spectroscopy (HR-XANES). A Johann type five-analyzer crystal spectrometer [1–5] recently installed and commissioned at the INE-Beamline for actinide research at the ANKA synchrotron radiation facility, Karlsruhe, Germany, [6] was applied. Different to conventional XANES, several spectral features could be identified. The most intense absorption resonances (White Line, WL) have higher intensities for all Pu L₃ HR-XANES spectra compared to the conventional XANES. Additionally, the Pu(V) and Pu(VI) L₃ HR-XANES spectra exhibit better resolved post-edge features. The energy distance between the WL and this resonance is sensitive to the bond distance between the Pu and axial O atoms in Pu(V) and Pu(VI). Extended X-ray absorption fine structure (EXAFS) investigation is performed to correlate oxidation states with average Pu–O bonding distances. For the Pu(VI) M₅ edge HR-XANES a feature at higher energy is well resolved, which might be sensitive to changes in Pu–O bond length and to the level of hybridization of metal and axial oxygen valence orbitals. A pre-edge ‘shoulder’ is detected in the Pu(III) spectrum. The origin of hitherto unresolved features is elucidated by quantum chemical calculations using the FEFF9.5 code. The HR-XANES experimental technique provides new insights into the actinides electronic structure and allows detection of minor contributions of Pu oxidation states in oxidation state mixtures.

-
- [1] Glatzel, P., et al. (2009) *Catalysis Today* 145 (3–4).
[2] Klymenov, E., et al. (2011) *Review of scientific instruments*, 82.
[3] Vitova, T., et al. (2010) *PRB*, 82 (23).
[4] Vitova, T., et al. (2013) *J. Physics: Conf. Series*, 430 (1).
[5] Walshe, A., et al. (2014) *Dalton Transactions*, DOI: 10.1039/c3dt52437j.
[6] Rothe, J., et al. (2012) *Review of scientific instruments*, 83.

Coordination of actinyl ions to nitrogenous heterocyclic ligands: a joint theoretical and experimental study

P. Yang,¹ Z. Wang,¹ D. Pan,¹ Y. Gong,² J. Gibson²

¹ Pacific Northwest National Laboratory, Richland, Washington, U.S.A.

² Lawrence Berkeley National Laboratory, Berkeley, California, U.S.A.

Nuclear energy represents a critical tool available to meet the demand of increasing energy supply, at the same time reducing greenhouse gas emission. To reduce the need for long-term nuclear waste storage, it is important to develop efficient strategies for selective separation. A better molecular-level understanding of the coordination modes and affinity of ligands with multiple binding sites to actinyl ions can pave the way to designing new ligand with improved extraction efficiency and selectivity. We will discuss the coordination chemistry to actinyl ions with ligands composed of multiple competitive binding sites including sulfur, nitrogen and oxygen chelating groups. We will present the interactions between actinide centers and the selected nitrogenous heterocyclic ligands using first-principle methods that include relativistic effects and electron correlation. The theoretical results will be further validated by gas phase collision-induced dissociation experiments and solution spectroscopic characterizations.

Nuclear magnetic resonance spectroscopy in Ln/An research

J. Kretzschmar,¹ J. Schott,¹ S. Tsushima,¹ A. Barkleit,¹ S. Paasch,² E. Brunner,²
G. Scholz,³ V. Brendler¹

¹ Institute of Resource Ecology, Helmholtz-Zentrum Dresden-Rossendorf, Dresden, Germany

² Bioanalytical Chemistry, Technische Universität Dresden, Dresden, Germany

³ Department of Chemistry, Humboldt-Universität Berlin, Berlin, Germany

Since signal separation by lanthanide shift reagents [1,2] has been replaced by elaborate pulse sequences and high-field spectrometers, lanthanides have advanced from auxiliaries to real objects of interest, also as inactive analogues for trivalent actinides in consequence of their similar chemistry.

Here we report on interactions and structures of the Ln(III) (La^{3+} , Eu^{3+} and, where applicable, Y^{3+}) with selected systems, *i.e.*, L-lactate [3], inorganic (poly)borates [4] and organoborates [5]. Small organic molecules such as lactate are important as model molecules and potential complexing agents found throughout the biosphere. Borates are ubiquitous in nature. In the context of nuclear waste disposal they occur in remarkable amounts in salt formations being potential host rocks for nuclear waste repositories, but also in boron containing cooling water or borosilicate glass coquilles for spent nuclear fuel. Organoborates are considered due to possible reaction of the former compounds and, additionally, suggested as analogues to model the interaction between Ln/An and borates in general.

Among several possible structures, infrared (IR) and NMR measurements, supported by density functional theory (DFT) calculation, revealed that lactate forms Ln(III) (and Am^{3+}) complexes with both the carboxyl and hydroxyl group involved. Polyborates, *i.e.*, triborate and pentaborate form soluble weak aqueous Ln(III) complexes prior to precipitation as amorphous white solids, whereas condensation to higher polyborates can be excluded. Two signals in both the ^{89}Y and the ^{11}B NMR spectra probably arise from two coordination sites, which may reflect the polyborate species found in the supernatant solution. The organoborates formed by the reaction of boric acid and, *e.g.*, lactate or salicylate also possess a tetra-coordinated boron atom $[\text{BO}_4]$, considered as the responsible site for Ln(III) interaction in inorganic (poly)borates. Since the (poly)borate/boric acid equilibrium is strongly concentration and pH dependent, their replacement by organic analogues allows investigations at both lower total boron concentrations and pH values.

[1] Hinckley, C. C. (1969) *J. Am. Chem. Soc.* 91, 5160–5162.

[2] Gansow, O. A.; Willcott, M. R.; Lenkinski, R. E. (1971) *J. Am. Chem. Soc.* 93, 4295–4297.

[3] Barkleit, A.; Kretzschmar, J.; Tsushima, S.; Acker, M. (2014) *Dalton Trans.* DOI: 10.1039/c4dt00440j.

[4] Schott, J.; Kretzschmar, J.; Acker, M.; Eidner, S.; Kumke, M. U.; Drobot, B.; Barkleit, A.; Taut, S.; Brendler, V.; Stumpf, T. (2014) *Dalton Trans.* DOI: 10.1039/c4dt00843j.

[5] Schott, J.; Kretzschmar, J.; Acker, M.; Tsushima, S.; Barkleit, A.; Taut, S.; Brendler, V.; Stumpf, T. (2014) in preparation.

Theoretical studies of excited states and electronic spectra of uranyl complexes

J. Li,¹ J. Su,^{1,2} F. Wei,¹ W. H. E. Schwarz¹

¹ Department of Chemistry, Tsinghua University, Beijing, China

² Division of Nuclear Materials Science and Engineering, Shanghai Institute of Applied Physics, Chinese Academy of Sciences, Shanghai, China

Uranyl dication (UO_2^{2+}) is the most stable form of uranium in nature. Uranyl compounds exhibit characteristic optical properties in absorption and emission which has been utilized to study speciation of uranyl in natural and artificial environments.[1] Theoretical explorations of the coordination structure, electronic structure, and excited states of uranyl compounds are essential to understanding of the nature of electronic spectra. However, interpretation of the electronic spectra of actinide complexes is difficult due to complicated electron correlation and relativistic effects, especially spin-orbit coupling effects. Here, we report the relativistic quantum chemistry studies on the excited states, electronic spectra, and photoelectron spectra of the gas-phase uranyl halides, including $[\text{UO}_2(\text{H}_2\text{O})_5]^{2+}$, $[\text{UO}_2(\text{H}_2\text{O})_3(\text{glycine})_1]^{2+}$, $[\text{UO}_2(\text{H}_2\text{O})_1(\text{glycine})_2]^{2+}$, UO_2Cl_2 , $\text{UO}_2\text{F}_2(\text{H}_2\text{O})_n$ ($n = 0-3$), UO_2X_3^- ($X = \text{F}, \text{Cl}, \text{Br}, \text{I}$), $\text{UO}_2\text{X}_4^{2-}$ ($X = \text{F}, \text{Cl}$), and $[\text{UO}_2\text{F}_4(\text{solvent})_n]^{2-}$ (solvent = $\text{H}_2\text{O}, \text{CH}_3\text{CN}$; $n = 1, 2$) [2–7].

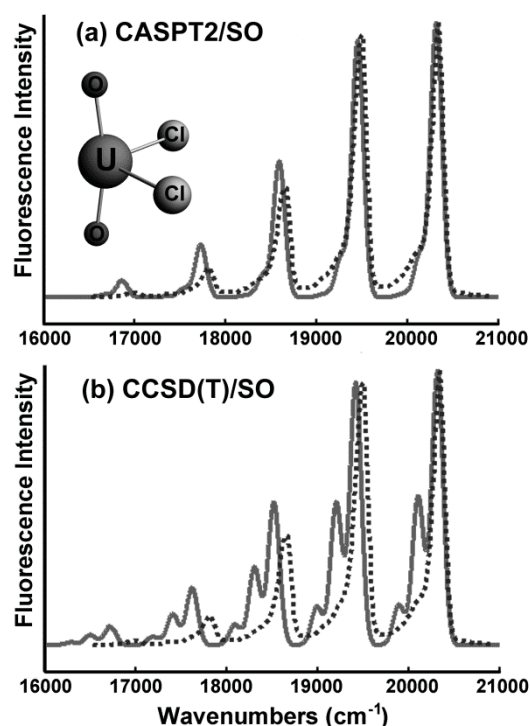


Fig. 1: Theoretical (solid) and experimental (dotted) luminescence spectra of UO_2Cl_2 : (a) CASPT2/SO and (b) CCSD(T)/SO.

While density functional theory (DFT) provides reasonable geometries and ground-state properties, *ab initio* wavefunction theory (WFT) is needed for accurate account of the electronic excited states of actinide systems. We adopted a restricted-active-space based state-interacting spin-orbit (RAS-SI/SO) approach using excited-states energies calculated via scalar relativistic WFT approaches, including CASPT2, CCSD(T), and CR-EOM-CCSD(T). These WFT methods provide accurate excited-states energies for both intra-atomic and ligand-to-metal charge transfer states of uranium compounds. With these excited states data, the electronic spectra and photoelectron spectra of actinide compounds can be well interpreted.

While density functional theory (DFT) provides reasonable geometries and ground-state properties, *ab initio* wavefunction theory (WFT) is needed for accurate account of the electronic excited states of actinide systems. We adopted a restricted-active-space based state-interacting spin-orbit (RAS-SI/SO) approach using excited-states energies calculated via scalar relativistic WFT approaches, including CASPT2, CCSD(T), and CR-EOM-CCSD(T). These WFT methods provide accurate excited-states energies for both intra-atomic and ligand-to-metal charge transfer states of uranium compounds. With these excited states data, the electronic spectra and photoelectron spectra of actinide compounds can be well interpreted.

- [1] Rabinowitch, E.; Belford, R.L. (1964) in: Spectroscopy and Photochemistry of Uranyl Compounds, Oxford University Press, Oxford, U.K.
- [2] Su, J.; Zhang, K.; Schwarz, W.H.E. and Li, J. (2011) *Inorg. Chem.* 50, 2082–2093.
- [3] Su, J.; Wang, Y.L.; Wei, F.; Schwarz, W.H.E. and Li, J. (2011) *J. Chem. Theory Comput.* 7, 3293–3303.
- [4] Su, J.; Wang, Z.; Pan, D. and Li, J. (2014) *Inorg. Chem.*, submitted.
- [5] Su, J.; Dau, P.D.; Qiu, Y.H.; Liu, H.T.; Xu, C.F.; Huang, D.L.; Wang, L.S. and Li, J. (2013) *Inorg. Chem.* 52, 6617–6626.
- [6] Dau, P.D.; Su, J.; Liu, H.T.; Liu, J.B.; Huang, D.L.; Li, J. and Wang, L.S. (2012) *Chem. Sci.* 3, 1137–1146.
- [7] Dau, P.D.; Su, J.; Liu, H.T.; Huang, D.L.; Li, J. and Wang, L.S. (2012) *J. Chem. Phys.* 137, 064315.

Uranyl minerals as models for the long term storage of spent nuclear fuels

A. Walshe,¹ E. D. Spain,² T. A. Keys,² R. A. Forster,² T. Prüßmann,³ T. Vitova,³ R. J. Baker¹

¹ School of Chemistry, Trinity College, Dublin, Ireland

² School of Chemical Sciences, Dublin City University, Dublin, Ireland

³ Institute for Nuclear Waste Disposal, Karlsruhe Institute of Technology, Eggenstein-Leopoldshafen, Germany

Storage of Spent Nuclear Fuels (SNF) in geological repositories is the favored method for a number of EU countries. Under moist oxidizing conditions, UO_2 will likely oxidize to uranyl compounds via a number of phase changes. These have been characterized on the weathering of uranium ores and the surface of UO_2 and SNF [1]. These phases can sorb radionuclides such as neptunium and therefore alter the migration rates into the near-field.

We will present our recent work on the characterization of the unusual mineral studtite, $[\text{UO}_2(\eta^2\text{-O}_2)(\text{H}_2\text{O})_2] \cdot 2\text{H}_2\text{O}$, using solid-state electrochemistry [2] and X-ray spectroscopy (EXAFS and HR-XANES) [3] (Fig. 1); both techniques have the potential to give important information on the electronic structure of actinide complexes but are not currently well utilized. We will also present results on an electrochemical study of uranyl (oxy)hydroxides, phosphates and carbonates. These results suggest that uranyl minerals are redox non-innocent that may have implications for Np migration in that they could oxidize geostable Np(IV) to soluble $[\text{NpO}_2]^+$ with concomitant reduction of the uranyl minerals to UO_2 .

We will also discuss the use of Eu as a model for Am in the sorption onto the surface of selected minerals using emission spectroscopy.

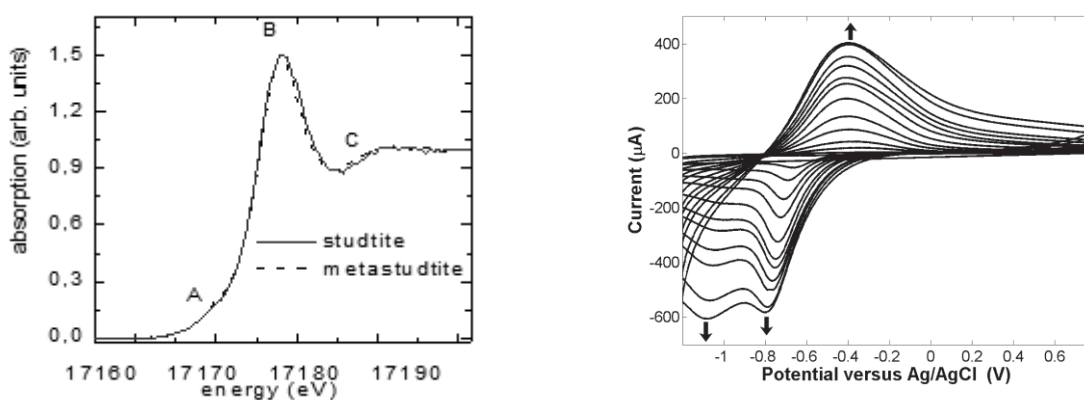


Fig. 1: U L_{3} -edge HR-XANES spectrum (left) and solid state cyclic voltammogram (right) of studtite.

[1] R. J. Baker (2014) *Coord. Chem. Rev.* 266-267, 123–136.

[2] C. Mallon, A. Walshe, R. J. Forster, T. E. Keyes, and R. J. Baker (2012) *Inorg. Chem.* 51, 8509.

[3] A. Walshe, T. Prüßman, T. Vitova, R. J. Baker (2014) *Dalton. Trans.* 43, 4400.

Cryogenic Laser-Induced Time-Resolved Luminescence Spectroscopy of U(VI) in mineral mixtures and natural sediments

Z. Wang,¹ J. M. Zachara,¹ C. T. Resch,¹ D. Pan,² W. Wu,² J.-F. Boily,³ C. Liu¹

¹ Pacific Northwest National Laboratory, Richland, WA, U.S.A.

² Radiochemistry Laboratory, School of Nuclear Science and Technology, Lanzhou University, Lanzhou, China

³ Department of Chemistry, Umeå University, Umeå, Sweden

Uranium is a major subsurface contaminant at many uranium processing facilities across the world [1,2]. Depending on the chemical composition and uranium concentration of the waste solution as well as aging time, uranium may exist in various forms from precipitated U(VI)-silicates, phosphates, carbonates, and -oxyhydroxides, to adsorbates on a suite of soil and mineral phases from iron oxides, calcium carbonate, quartz/amorphous silica to phyllosilicates. The migration of uranium in the natural environment will be dictated by the dissolution-precipitation and sorption-desorption equilibria in natural waters. As subsurface sediments are heterogeneous mixtures of different mineral phases with varying mineralogical compositions at different contamination sites, an improved understanding of uranium speciation in complex host mineral assemblages will not only provide sound scientific basis for the development of cleanup techniques but also offer critical information to assess its future environmental risks. Such knowledge will also aid in the evaluation of nuclear waste repositories.

Uranium(VI) absorbs in the broad wavelength range from deep UV to visible and displays bright luminescence emission in the visible wavelength range with characteristic O=U=O vibronic features [3]. The luminescence spectral profiles such as spectral origin, vibronic band spacing and relative intensity of the vibronic bands as well as luminescence lifetime vary as ligand coordination in the equatorial plane changes, allowing identification of U(VI) coordination environment and the corresponding chemical species. Time-resolved luminescence measurement under cryogenic conditions in combination with chemometric analysis further broadens the applicability of uranium(VI) luminescence analysis of U(VI) speciation in natural sediments in which luminescence spectroscopic analysis is often hindered by strong luminescence quenching effect, weak spectral intensity and poor spectral resolution.

In this work, qualitative and semi-quantitative analysis of U(VI) speciation in contaminated sediments at the US Hanford site, in quartz-chlorite mixtures and in natural granitic materials by cryogenic time-resolved U(VI) luminescence spectroscopic measurement are presented. Batch adsorption and spectral analysis of U(VI) adsorbed on phlogopite, muscovite and other phyllosilicates such as chlorite, illite and montmorillonite are compared by their affinity to U(VI) adsorption and surface speciation characteristics. Challenges in both luminescence spectral and lifetime analysis in samples with unknown luminescence quenching effect and uncertainties in their application in the prediction of uranium speciation in natural sediments are discussed.

[1] Bernhard, G., Geipel, G., Brendler, V., and Nitsche, H. (1996) Speciation of Uranium in Seepage Waters of a Mine Tailing Pile Studied by Time-Resolved Laser-Induced Fluorescence Spectroscopy (TRLFS) *Radiochim. Acta* 74, 87–91.

[2] Zachara, J.M., Brown, C., Christensen, J., Dresel, E., Kelly, S., Liu, C., McKinley, J., and Um, W. (2007) *A Site-Wide Perspective on Uranium Geochemistry at the Hanford Site*. Pacific Northwest National Laboratory, Richland, WA.

[3] Rabinowitch, E. and Belford, R.L. (1964) *Spectroscopy and Photochemistry of Uranyl Compounds*.

Eu³⁺ binding to deep groundwater humic substances studied by time resolved laser fluorescence spectroscopy and factor analysis

T. Saito

Nuclear Professional School, School of Engineering, The University of Tokyo, Tokai, Ibaraki, Japan

Time-resolved laser fluorescence spectroscopy (TRLFS) is a valuable tool for speciation of fluorescent actinide and lanthanide ions. Discrimination capability of TRLFS for co-existing species of a target ion originates from a multivariate data structure of TRLFS and can be further reinforced by combining with multi-mode factor analysis. PARAFAC (parallel factor analysis) is a multi-mode factor analytic technique and has been successfully applied for data reduction of TRLFS of Eu³⁺, a known chemical homologue of trivalent actinide ions, complexing with simple ligands [1], adsorbing on mineral surfaces [2], and binding to humic substances (HS) [3]. In this study binding of Eu³⁺ to HS extracted from deep groundwater was studied by TRLFS-PARAFAC. HS is ubiquitous in various environments and plays an important role in speciation of metal ions through their binding to the functional groups of HS. Although metal binding to HS has been studied over decades for HS from surface environments, our knowledge on metal binding to deep groundwater HS is rather limited. This is the first attempt to reveal metal binding behaviors of groundwater HS through TRLFS and compare them with those of surface HS.

Humic and fulvic acid were extracted from sedimentary groundwater collected at the -250-m gallery of the Horonobe underground research laboratory operated by the Japan Atomic Energy Agency. The Horonobe humic and fulvic acids are called HHA and HFA hereafter. Europium binding to HHA and HFA was studied with 50 mg/L HS samples containing 70 μM Eu³⁺ at 0.1 or 0.01 M NaClO₄ as a function of pH. TRLFS measurements were performed by a Ti:sapphire laser operating at 394 nm and 1 kHz, a spectrograph, and an ICCD camera. A series of TRLFS data was simultaneously analyzed by PARAFAC [3].

Two factors were found for both HHA and HFA regardless of the salt concentrations employed. Considering the spectral shapes and decay lifetimes, Factor A, which existed at relatively low pH, is attributed to a free Eu³⁺ aquo ion, and factor B, which predominates at circumneutral pH, to Eu³⁺ bound to the Horonobe HS. Based on the concentrations of these species, the distribution coefficients (K_d) were calculated as a function of pH (Fig. 1). Binding of Eu³⁺ to the Horonobe HS increases with pH and decreases with salt concentration, suggesting its binding to acidic (most likely carboxylic) functional groups of negatively charged HS molecules. The K_d values are comparable to those of HS with surface origin. This is surprising as HHA and HFA are thought to have rather different chemical structures from surface HS. In the conference the fluorescence spectra and decay lifetimes of Eu³⁺ bound to the Horonobe HS will be compared with those to surface HS in details.

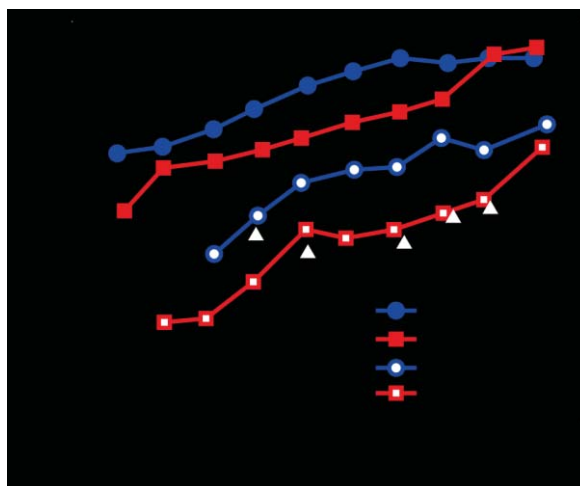


Fig. 1: Distribution coefficients (K_d) of Eu³⁺ bound to HHA and HFA at 0.1 and 0.01 M NaClO₄ as function of pH.

- [1] Saito, T., et al. (2009) *Environ. Sci. Technol* 44, 5055–5060.
- [2] Ishida, K., et al. (2012) *J. Colloid Interface Sci.* 374, 258–266.
- [3] Lukman, S., et al. (2012) *Geochim. Cosmochim. Acta* 88, 199–215.

Elemental analysis of simulated debris of nuclear fuel in water by fiber-coupled Laser Induced Breakdown Spectroscopy

M. Saeki,¹ C. Ito,¹ I. Wakaida,¹ B. Thornton,² T. Sakka,³ H. Ohba¹

¹ Japan Atomic Energy Agency, Tokai-mura, Japan

² The University of Tokyo, Meguro, Japan

³ Kyoto University, Nishikyo-ku, Japan

Focusing of powerful laser pulses onto a material generates ablation plasma that is composed of excited atoms. Analysis of emission from the excited atoms gives us information on the elemental compositions of the ablated material. This technique is called laser induced breakdown spectroscopy (LIBS), and is attractive as elemental analysis method because real-time, in-situ and remote observation is possible without any sample preparation. These advantages are available in elemental analysis in a high-radiation field, such as the post-accident environment inside the TEPCO Fukushima Daiichi nuclear power plant (F1-NPP) in Japan, which was seriously damaged by the tsunami on March 11, 2011. In the F1-NPP, debris of the nuclear fuel (mixture of melted fuel core, fuel cladding and construction material) is submerged in water from the reactor pressure vessel to the primary containment one in the reactor core [1]. The decommissioning needs information on elemental component of the debris. Thus, we have developed the fiber-coupled LIBS in order to apply it to remote sensing in the post-accident environment [2].

Considering that our fiber-coupled LIBS system is applied to the monitoring inside the F1-NPP, we established important matters for investigation. One matter is the optical condition that is used for the laser induced breakdown and the emission spectroscopy. This condition is dominated by the transmissivity of optical fiber, which is changed by radiation exposure. To get information the transmissivity, we exposed the optical fiber to ⁶⁰Co gamma-ray with total doses over 1 MGy and compared the optical transmissivity between before and after the radiation dose in the region of 400–1100 nm. As the result of this, the transmissivity decreased to 0–30% in the region of 400–650 nm, while the transmissivity before the radiation dose was kept with the efficiency of ~100% in the region of 730–1100 nm. Thus, we designed to generate the breakdown plasma by the fundamental of Nd: YAG laser (1064 nm) and to observe the emission spectrum in the region of 730–1060 nm. Another is technique to analysis the underwater sample. In the underwater LIBS there is difficulty in detection of the plasma emission, because the breakdown plasma is confined in very small volume by the water and the surrounding water distorts the plasma emission. We overcome this difficulty by creating quasi-atmospheric environment around the breakdown plasma by gas-flow or double-pulse technique [2].

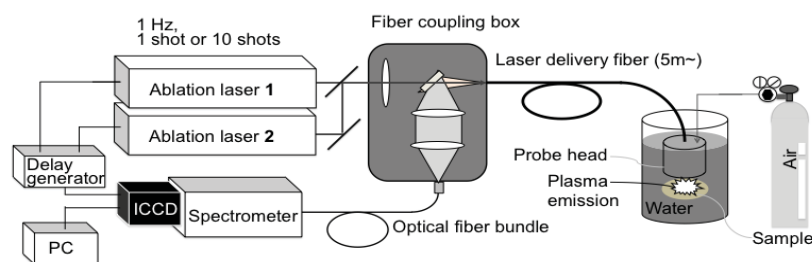


Fig. 1: Experimental set-up of fiber-coupled LIBS system.

Figure 1 shows an experimental set-up of our fiber-coupled LIBS system. The system consists of ablation lasers, fiber-coupling box, laser delivery fiber, and probe head. To check radiation resistivity of this system, we measured the emission spectrum of simulated debris (mixture of Ce, Zr and Fe)

under gamma-ray radiation dose of 15 kGy/hour. As a result, we obtained the emission spectrum with same pattern as before the gamma-ray radiation, although the emission intensity decreased. We also check the ability of our fiber-coupled LIBS system in analysis of underwater sample. In analyzing zirconium alloy in the water, we observed emission spectrum with same quality as in atmosphere. By using the developed fiber-coupled LIBS instrument, we have analyzed simulated debris (mixture of U and Zr) and have assured that qualitative measurement is possible.

[1] http://www.tepcoco.jp/en/nu/fukushima-np/review/review3_2-e.html.

[2] Saeki, M. et al (2014) J. Nucl. Sci. Technol. 51, 930–938.

Structure and inclusions in bulk and dispersed samples of Chernobyl “lava”: data from vibrational spectroscopy, XAFS and X-ray tomography

A. A. Shiryaev,^{1, 2, 3} I. E. Vlasova,³ Y. V. Zubavichus,⁴ R. A. Senin,⁴ A. A. Averin,¹
A. Pakhnevich,⁵ B. I. Ogorodnikov,⁶ B. E. Burakov⁷

¹ Institute of Physical Chemistry and Electrochemistry RAS, Moscow, Russia

² Institute of Ore Geology, Petrography, Mineralogy and Geochemistry RAS, Moscow, Russia

³ Chemistry Department, Moscow State University, Moscow, Russia

⁴ National Research Center “Kurchatov Institute”, Moscow, Russia

⁵ Paleontological Institute RAS, Moscow, Russia

⁶ Karpov Physical Chemistry Institute, Moscow, Russia

⁷ Khlopin Radium Institute, St. Petersburg, Russia

The major fraction of radioactivity from destroyed 4th Unit of Chernobyl NPP is assumed to remain inside confinement building called “Shelter” or “Sarcophagus” and it is primarily accumulated in glassy fuel-containing materials called Chernobyl “lava”. The lava samples have been studied very actively during the first decade after the accident, but later intensity of these works decreased. However, long term stability of lava streams is still the subject of high interest because future engineering solutions strongly depend on realistic models of lava’s interaction with environment. We report the results of complex investigation of bulk lava samples collected in 1991 from famous black lava stream, so-called “Elephants foot” (level 0 m), and relatively modern samples of aerosols and disperse particles collected in rooms on the level +6 m inside the “Shelter” in 2011–2013. Information about structure of aluminosilicate lava matrix was assessed using multiwavelength Raman and infra-red microspectroscopy. Vibrational spectroscopy also provides information about water content in lava matrix and inclusions, which is critically important for modeling of evolution of mechanical properties and weathering process. Speciation of two important elements – Zr and U – was studied in the bulk lava sample using X-ray Absorption Spectroscopy (XAFS). Spatial distribution of inclusions was investigated in 2D and 3D using electron microscopy and X-ray tomography. Distribution of radionuclides was monitored by digital and alpha-track autoradiography.

The most common inclusions are represented by UO_x (often with dendrite morphology); high-uranium zircon crystals (usually faceted) and spherical Fe-Cr-Ni droplets. Despite presence of U-rich inclusions, autoradiography shows rather uniform distribution of α -emitters, suggesting that significant fraction of alpha-emitting radionuclides was dissolved in the glass matrix. XAFS at U L_{3-} and Zr K-edges revealed partitioning of these elements between the principal mineral phases present; attempts to analyze their speciation in the glassy matrix as well are currently underway.

The matrix represents a moderately polymerized aluminosilicate glass: Raman spectroscopy shows presence of Q^3 and Q^2 silicate units. Remarkably, obvious signatures of heterogeneously distributed OH-groups are observed both in the glass matrix and in zircon inclusions. As it is known, water often deteriorates mechanical properties of silicate glasses.

Important fraction of radioactivity of the aerosols is related to UO_x particles less than 5 μm in size. They may represent dispersed fuel and (or) they may originate from mechanically destroyed lava. Larger glass particles may reach 150 microns in the longest dimension and they often contain inclusions of UO_x with Zr admixture.

The resistance of the lava flows against weathering is likely very non-uniform: whereas some of the samples are stable mechanically and chemically; other flows rapidly deteriorate.

The work was partly supported by RSCF grant 14-13-00615.

AMS of actinides in ground- and sea-water: a new procedure for simultaneous trace analysis of U, Np, Pu, Am and Cm isotopes

F. Quinto,¹ M. Lagos,¹ M. Plaschke,¹ T. Schäfer,¹ P. Steier,² R. Golser,² H. Geckeis¹

¹ Institute for Nuclear Waste Disposal, Karlsruhe Institute of Technology, Eggenstein-Leopoldshafen, Germany

² VERA Laboratory, Faculty of Physics, University of Vienna, Vienna, Austria

Challenges for the analysis of actinides in the environmental are their occurrence at concentrations below ppq level, and the rare availability of isotopic tracers for mass spectrometric measurements of ²³⁷Np and ²⁴³Am. We present an analytical protocol suited to the measurement by Accelerator Mass Spectrometry (AMS) of U, Np, Pu, Am and Cm without previous chemical separation from each other, and to the use of ²³⁹Pu and ²⁴⁸Cm as non-isotopic tracers for ²³⁷Np and ²⁴³Am, respectively. The detection limits of AMS at VERA [1] for actinide nuclides allow accurate determinations down to 10⁵ atoms, corresponding to ~40 ag and to ~9 × 10⁻⁸ Bq of ²³⁹Pu or to ~9 × 10⁻¹¹ Bq for ²³⁶U. AMS determination of ²³⁷Np and ²⁴³Am using ²³⁹Pu and ²⁴⁸Cm as non-isotopic tracers, requires estimating the ionization yield of the sputtered NpO⁻, PuO⁻, AmO⁻ and CmO⁻ in the given sample matrix.

Groundwater, seawater (250 mL), and MilliQ water samples are spiked with known amounts of Np, Pu, Am and Cm isotopes, their concentrations spanning from ~3 × 10² to ~4 × 10⁶ atoms/mL. The actinides are co-precipitated with Fe(OH)₃. This procedure allows the pre-concentration of the actinides from the bulk elements, and, at the same time after conversion of the Fe-hydroxides to Fe-oxides, their incorporation into the sample matrix suited to the AMS measurements. The actinide nuclides are measured employing stripping with helium to the 3+ charge state at 1.65 MV terminal voltage.

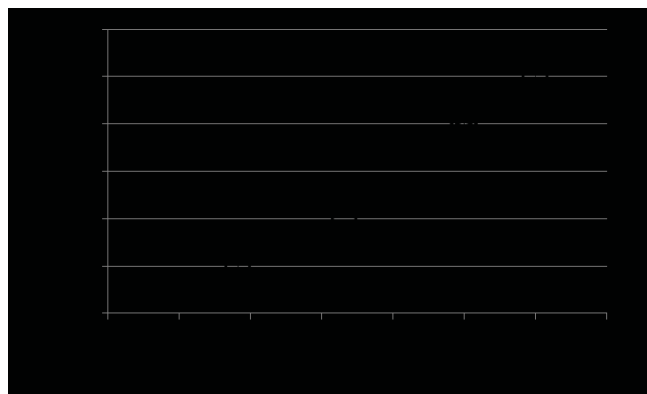


Fig. 1: Count rates (s⁻¹) of ²⁴⁵Cm (~0.03 fg), ²⁴⁰Pu (~0.8 fg), ²⁴⁶Cm (~2 fg), ²³⁹Pu (~40 fg), ²⁴³Am (~40 fg), ²⁴⁸Cm (~40 fg) and ²³⁷Np (~400 fg) from the same cathode produced from a 250 mL groundwater sample.

Figure 1 highlights how a reliable determination of up to seven actinide nuclides with concentrations from ~2 ppq down to ~0.0001 ppq is possible without previous chemical separation of the actinides from each other.

Preliminary results indicate a dependency of the ionization yield of the actinides on the sample matrix, with average ²³⁷Np/²³⁹Pu and ²⁴⁸Cm/²⁴³Am atom ratios of 12.0 ± 1.6 and 1.6 ± 0.1, respectively for the groundwater samples, and 11.7 ± 0.4 and 1.4 ± 0.1 for the MilliQ water samples. The measured ²³⁷Np/²³⁹Pu ratios are lower than their nominal value of 14.2 ± 0.4, and the measured ²⁴⁸Cm/²⁴³Am atom ratios higher than their nominal value of 1.38 ± 0.02, indicating a

higher ionization yield in the AMS ion source of PuO⁻ relative to NpO⁻, as well as a higher ionization yield of CmO⁻ relative to AmO⁻, in agreement with previous observations [2,3]. The use of ²³⁹Pu and ²⁴⁸Cm as non-isotopic tracers for ²³⁷Np and ²⁴³Am, respectively, is possible in AMS measurements when an accurate estimate of the relative ionization yields of the various actinides is carried out.

In order to test the performances of the method when analyzing an existing nuclear contamination in water samples, measurements of ²³⁶U/²³⁸U isotopic ratios were carried out. The ²³⁶U/²³⁸U isotopic ratios measured in 250 mL groundwater samples from the Grimsel test site (GTS), (2.5 ± 0.1) × 10⁻⁷ and (3.4 ± 0.3) × 10⁻⁷, as well as in tap water from Karlsruhe, (5.0 ± 0.6) × 10⁻⁹, are consistent with the global fallout origin [4]. These findings indicate the mobility of global fallout ²³⁶U, which apparently is able to migrate together with meteoric water from the surface to depths down to the level of the GTS groundwater at 450 m. Interestingly, fallout Pu could not be detected indicating a much lower mobility under given conditions.

[1] Steier, P. et al. (2013) Nucl. Instr. Meth. Phys. Res., Sect. B 294, 160–164.

[2] Fifield, L.K. et al. (1997). Nucl. Instr. Meth. Phys. Res., Sect. B 123, 400–404.

[3] Christl, M. et al. (2014) Nucl. Instr. Meth. Phys. Res. Sect. B 331, 225–232.

[4] Quinto, F. et al. (2013) Environ. Sci. & Technol., 47, 5243–5250.

Site-selective TRLFS of Eu(III) doped rare earth phosphates for conditioning of radioactive wastes

N. Huittinen,¹ Y. Arinicheva,² J. Holthausen,² S. Neumeier,² T. Stumpf¹

¹ Institute of Resource Ecology, Helmholtz-Zentrum Dresden-Rossendorf, Dresden, Germany

² Forschungszentrum Jülich, Jülich, Germany

Crystalline ceramic materials show promise as potential waste forms for immobilization of high-level radioactive wastes. Rare earth (RE) phosphate ceramics have been found to be extremely stable over geological time scales [1] and they show good tolerance to high radiation doses [2]. These ceramics are able to incorporate radionuclides in well-defined atomic positions within the crystal lattice [3] up to high (~25%) loadings [4], which will reduce the volume of waste in the radionuclide conditioning process. The dehydrated RE phosphates are known to crystallize in two distinct structures, depending on the ionic radius of the cation: the larger lanthanides from La³⁺ to Gd³⁺ crystallize in the nine-fold coordinated monazite structure, while the smaller lanthanides such as Lu³⁺ form eight-fold coordinated xenotime structures (Fig. 1).

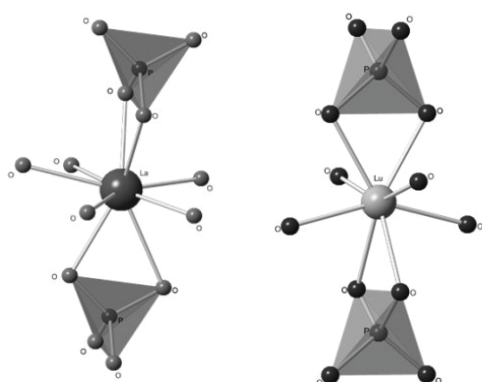


Fig. 1: Nine-fold coordinated LaPO₄ monazite (left) and eight-fold coordinated LuPO₄ xenotime (right).

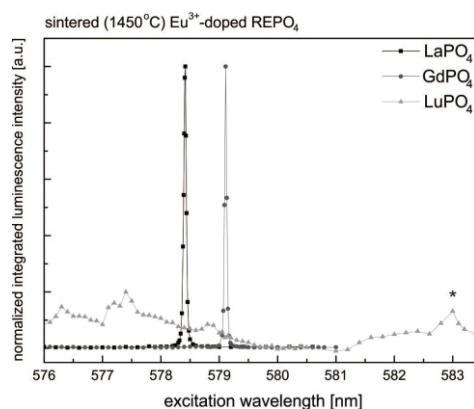


Fig. 2: Excitation spectra of Eu³⁺-doped REPO₄. The peak corresponding to Eu³⁺ incorporation in LuPO₄ is indicated with an asterisk.

In the present work we have used site-selective time-resolved laser fluorescence spectroscopy (TRLFS) to investigate the structural incorporation of Eu³⁺, an analogue for the actinides Pu³⁺, Am³⁺ and Cm³⁺, in rare earth phosphate ceramics. The very narrow excitation spectra of LaPO₄ and GdPO₄ monazites doped with 500 ppm Eu³⁺ (Fig. 2) indicate that Eu³⁺ is fully incorporated on the host cation sites in the highly ordered ceramic materials independent of the ionic radii of the host cations. The LuPO₄ xenotime phase, however, shows a very low incorporation of the Eu³⁺ ion within the crystal lattice (incorporation site indicated in Fig. 2 with an asterisk). The majority of the signal in the Eu³⁺-LuPO₄ excitation spectrum could be assigned to partly hydrated europium in the LuPO₄ ceramic. In experiments where we increased the dopant concentration up to 50% in the xenotime host matrix, a larger amount of Eu³⁺ incorporation within the crystal structure in relation to the hydrated species could be seen. A similar increase of the dopant concentration in the monazite phases caused a broadening of the excitation spectra as a result of local disordering of the crystal structures. This disordering, however, had no influence on the Ln³⁺ site symmetry in the monazites. Our site-selective TRLFS investigations have shown that the host cation size in the monazites has very little influence on the Eu³⁺ incorporation into these materials. The structure of the ceramic, however, seems to play a decisive role in how well the dopant is substituted within the crystal lattice.

[1] Donald, I.W. et al. (1997) *J. Mater. Sci.* 32, 5851–5887.

[2] Luo, J.S. and Liu, G.K. (2001) *J. Mater. Res.* 16, 366–372.

[3] Holliday, K.S. et al. (2012) *Radiochim. Acta* 100, 189–195.

[4] Bregiroux, D. et al. (2007) *Inorg. Chem.* 46, 10372–10382.

Spectroscopic and microscopic characterization of U bearing multicomponent borosilicate glass

S. Bahl,¹ V. Koldeisz,² K. Kvashnina,³ T. Yokosawa,¹ I. Pidchenko,¹ H. Geckeis,¹ T. Vitova¹

¹ Institute for Nuclear Waste Disposal, Karlsruhe Institute of Technology, Karlsruhe, Germany

² Department of Inorganic and Analytical Chemistry, Budapest University of Technology and Economics, Budapest, Hungary

³ European Synchrotron Radiation Facility, Grenoble, France

Highly radioactive liquid waste (HLW) from nuclear fuel reprocessing is commonly incorporated in borosilicate glass matrices to generate a disposable waste form [1]. The long term radiotoxic U is of great concern in safety concepts for a nuclear waste repository. In case of water intrusion different corrosion processes take place and release of radioactivity into the environment can be facilitated. U can be immobilized by precipitation on mineral surfaces or incorporation in the mineral structure by forming stable oxidation states like U(IV) [2]. However, this actinide (An) element can be also highly mobile in the environment in a form of colloids or higher oxidation states in water soluble complexes like U(VI) [3].

In this work a multi-component borosilicate glass [4] with varying U loading and Mo/waste simulate in addition to U was prepared (see Tab. 1) to serve as a simplified reference system in structural studies of vitrified reprocessed HLW. The structure and morphology of the glass products, local chemical environment of U and U oxidation state are under investigation by several experimental techniques.

Raman spectroscopy and scanning electron microscopy (SEM) in combination with energy-dispersive X-ray spectroscopy (EDX) reveal homogeneous amorphous glass in samples 1–3. Raman spectra display U–O vibrational bands at 769 cm^{-1} gaining in intensity

with increasing U concentration. Raman and SEM-EDX identify CaMoO_4 rich regions with $1.5\ \mu\text{m}$ average size embedded in the amorphous glass matrix of samples 4–6.

By U M_4 edge high energy resolution X-ray absorption near edge structure (HR-XANES) and valence band resonant inelastic X-ray scattering (VB-RIXS) spectroscopy techniques U is found to occur in oxidation state VI in all samples likely due to the oxidizing conditions of the synthesis process. The comparison of U M_4 edge HR-XANES glass spectra with spectra of natural U minerals suggests dominating uranyl type of short U–O_{axial} bonding. However, a weak pre-edge feature in the U M_4 HR-XANES spectra with increasing intensity as a function of U loading might indicate local structural distortions around U or uranium oxide clusters with growing size. Ongoing analysis of U L_3 edge extended X-ray absorption fine structure (EXAFS) spectra will help to verify these assumptions and particularly the concentration dependent U–U interaction in the glass matrix. *Ab initio* multiple scattering calculations using FEFF9.6 code of HR-XANES spectra will be performed to support the experimental observations. Incorporation of U into the CaMoO_4 crystalline phases will be validated by transmission electron microscopy (TEM), EDX and EXAFS.

Tab 1: Multi component borosilicate glass samples; *(Fe_2O_3 5.43 wt%, MoO_3 2.72 wt%, ZrO_2 1.51 wt%, BaO 1.51 wt%, Sm_2O_3 0.60 wt%, Cr_2O_3 1.51 wt%).

Sample	UO ₂ [wt%]	MoO ₃ [wt%]	waste simulate* [wt%]
sample 1	1.19	–	–
sample 2	3.00	–	–
sample 3	5.00	–	–
sample 4	1.19	8.00	–
sample 5	5.00	8.00	–
sample 6	2.72	8.00	16.00

[1] R.J. Short, G. Möbus, G. Yang, R.J. Hand, N. Hyatt, W.E. Lee (2004) Materials Research Society Symposium Proceedings.

[2] F. Huber, D. Schild, T. Vitova, J. Rothe, R. Kirsch, T. Schäfer (2012) *Geochimica et Cosmochimica Acta* 96, 154–173.

[3] P. Zhao, M. Zavarin, R.N. Leif, B.A. Powell, M.J. Singleton, R.E. Lindvall, A.B. Kersting (2011) *Applied Geochemistry* 26, 308–318.

[4] W. Grünewald, G. Roth, S. Hilpp, W. Tobie, A. Salimi, S. Weisenburger, B. Brendebach (2009) *Proceedings of Global 2009*, Paris.

Hydrolysis of tetravalent cerium (Ce(IV)) – A multi-spectroscopic study on nanocrystalline CeO₂ formation

A. Ikeda-Ohno,¹ S. Weiss,¹ S. Tsushima,¹ C. Hennig^{1,2}

¹ Institute of Resource Ecology, Helmholtz-Zentrum Dresden-Rossendorf, Dresden, Germany

² The Rossendorf Beamline (ROBL), ESRF, Grenoble, France

Because of the flexibility between the tri- and tetravalent oxidation states, cerium (Ce) is known to be the only rare earth element (REE) forming a stable pure stoichiometric dioxide compound (CeO₂). Owing to this chemical specificity along with the highest natural abundance of Ce among all REEs, the application of CeO₂ has spread over a variety of fields. More recently, CeO₂ has been employed as nanoparticles with many technological applications, which include the catalysts for harmful gas treatment the water gas shift reaction, electrodes for solid oxide fuel cells and a medical use as an artificial superoxide dismutase. These versatile and still emerging applications of CeO₂ still require a simpler and more efficient synthetic strategy, particularly for manufacturing CeO₂ nanoparticles.

The hydrolysis of tetravalent cerium (Ce(IV)) is a primary step of many wet syntheses for fabricating CeO₂ nanoparticles, although all the reported synthetic methods require additional processes, such as heating, adding organic solvents or calcination, subsequent to the initial hydrolysis step to finally yield CeO₂ nanoparticles. This means that understanding of the hydrolysis mechanism of Ce(IV) would be beneficial to developing a new concept for the efficient production of CeO₂ nanoparticles. Based on this background, this study focuses on the systematic investigation of the hydrolysis behaviour of Ce(IV) using synchrotron-based X-ray techniques (X-ray absorption spectroscopy (XAS) and high energy X-ray scattering (HEXS)), dynamic light scattering (DLS) and transmission electron microscopy (TEM).

Ce K-edge XAS combined with DFT calculations has revealed that the primary aquo species of Ce(IV) is not a mononuclear species, but dinuclear species in which two Ce(IV) are bridged by oxo- or hydroxo groups.[1] Further XAS and HEXS study has suggested that, as an increase in pH, these dinuclear species are evolved into larger oligomer species, which finally form nano-sized crystalline CeO₂ (Fi. 1).[2] These results demonstrate that simple hydrolysis of Ce(IV) with careful pH adjustment could yield well-crystalline CeO₂ nanoparticles with an uniform size distribution.

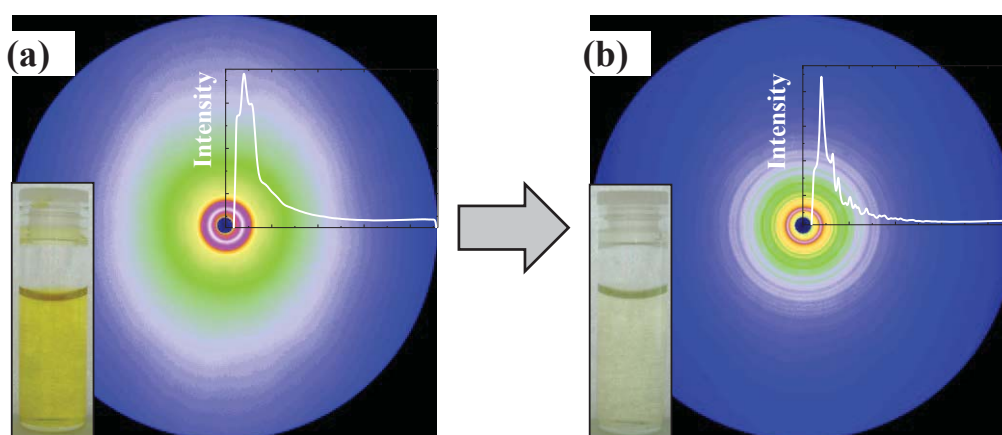


Fig. 1: (a) 0.5 M Ce(IV) in 1.0 M HNO₃ at pH = 0.0 (inset photo), its two-dimensional X-ray scattering image (circular image) and integrated scattering curve (insert graph with a white line), and (b) those for 0.5 M Ce(IV) in 1.0 M HNO₃ at pH = 1.0. Clear ring patterns observed in (b) indicate the presence of crystalline substances in the sample.

[1] Ikeda-Ohno, A.; Tsushima, S.; Hennig, C.; Yaita, T. and Bernhard, G. (2012) Dalton Trans. 41, 7190–655.

[2] Ikeda-Ohno, A.; Hennig, C.; Weiss, S.; Yaita, T. and Bernhard, G. (2013) Chem. Eur. J. 19, 7348–7360.

XPS and UPS study on the electronic structure of ThO_x (x ≤ 2) and (U,Th)O_x (x ≤ 2) thin films

P. Çakir,^{1,2} R. Eloirdi,¹ F. Huber,¹ R. J. M. Konings,³ T. Gouder¹

¹ European Commission, Joint Research Centre (JRC), Institute for Transuranium Elements (ITU), Actinide Research Unit, Karlsruhe, Germany

² Delft University of Technology, Faculty of Applied Sciences, Delft, The Netherlands

³ European Commission, Joint Research Centre (JRC), Institute for Transuranium Elements (ITU), Material Research Unit, Karlsruhe, Germany

To be evaluated as model system for surface corrosion studies of spent nuclear oxide fuels [1–3], ThO₂ films have been prepared in-situ by adsorption of molecular and atomic oxygen on Th metal films, and by sputter deposition of Th metal in an Ar/O₂ gas mixture. Surface composition and electronic structure were compared to bulk oxide compounds. X-ray and Ultraviolet photoemission spectroscopy (XPS and UPS, respectively) were used to measure Th-4*f*, O-1*s* core levels and the valence band region. The Th-4*f* line was analyzed in terms of the final-state screening model. Evolution of the binding energies with oxygen concentration has been studied and Figure 1 reports the results obtained on films prepared by sputtering. On Th metal, molecular oxygen adsorption stopped after the formation of a ThO₂ surface layer. In presence of atomic oxygen, oxidation proceeded into the underlying bulk. Formation of oxygen interstitials was shown by the broadening of the O-2*p* and O-1*s* lines and by the increase of the O-1*s*/Th-4*f* ratio. Once all metal has disappeared forming pure ThO₂, all photoemission peaks from Th and O undergo a rigid shift to low binding energy (BE).

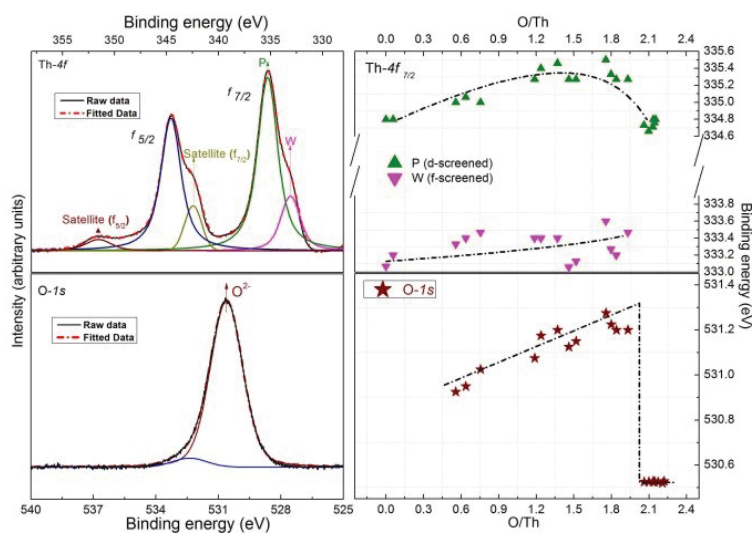


Fig. 1: Left: Fit of Th-4*f* (up) and of O-1*s* (down) core level peaks with Gaussian curves. Right: Binding energy shift of W and P peaks present in Th-4*f*_{7/2} (up) and of O-1*s* peak (down) as a function O/Th ratio in ThO_x (0 ≤ x ≤ 2) thin films.

Thin films of ThO_x (x ≤ 2) were also produced by DC sputtering Ar plasma in presence of O₂. The film was continuously oxidized during formation and there was no oxygen concentration gradient between surface and bulk. The Th-4*f* core level spectrum could be fitted by two peaks corresponding to *f*-screened (W) and *d*-screened peak (P). While the *f*-screened peak is the main peak for the thorium metal, its BE shifts and its intensity decreases at the expense of the *d*-screened peak which is the main peak in ThO₂. The Th-4*f* and O-1*s* peaks both increase to higher binding energy till an O/Th ratio of about 2, and then drop suddenly to a lower and constant energy corresponding to the formation of ThO₂

which cannot further oxidized. The sudden drop of the binding energy observed for ThO₂ thin film is also attributed to the decrease of the Fermi-energy. Also first results obtained on the electronic structure of (U,Th)O_x (x ≤ 2) films analyzed by UPS and XPS will be reported.

[1] S. Stumpf et al. (2010) *J. Nucl. Mater.* 397, 19–26.

[2] T. Gouder (1998) *J. Alloys Compd.* 271–273, 841–845.

[3] F. Miserque et al. (2001) *J. Nucl. Mater.* 298, 280–290.

Molecular insights into actinide speciation at interfaces and nanoparticles

A. Campbell, N. Hess

Environmental Molecular Sciences Laboratory, Pacific Northwest National Laboratory, Richland, U.S.A.

Critical determinants of radionuclide mobility are oxidation state, chemical speciation, nanoparticle formation and formation of surface and aqueous complexes at interfaces with solid phases. Understanding how environmental conditions impact these determinants is key to predictive modelling of radionuclide fate and transport in environmental systems and under repository conditions as well. We present the results of some recent studies of actinide incorporation in secondary mineral phases, oxidation of uranium oxide, and structural characterization of actinide nanoparticles conducted by scientist utilizing the unique set of capabilities of the Radiochemistry Annex at EMSL. The Radiochemistry Annex, a new state-of-the-art laboratory to facilitate application of advanced analytical methods to environmental samples containing radionuclides, has been established at EMSL, a U.S. Department of Energy Office of Biological and Environmental Research user facility located at Pacific Northwest National Laboratory in Richland, Washington. A major objective of EMSL's Radiochemistry Annex is to provide a specialized environment where scientists can apply advanced experimental resources for imaging and spectroscopy to studies of radionuclides in environmental samples and waste forms. The user facility consists of approximately 6000 sq ft of lab space for NMR, EPR, XPS spectroscopies and AFM, EMP, FIB/SEM, SEM, and TEM imaging. Together with NWChem, EMSL's premier computational modelling code, users are able to address radionuclide systems from both experimental and computational vantage points.

Mechanistic understanding of mineral reactivity toward trace metals through density functional theory

K. D. Kwon

Department of Geology, Kangwon National University, Chuncheon, Korea

Minerals greatly impact diverse phenomena from climate change to contaminant dynamics via sorption and redox chemistry with trace metals. Surface spectroscopy has enhanced our understanding of the mineral reactivity by elucidating the molecular-level species of trace metals sorbed on mineral surfaces, but there are often ambiguities in the interpretation of spectra and guiding principles to rationalize observed trends. Density functional theory (DFT) provides highly detailed information about structure, energetics, and electronic properties of minerals and trace metals. DFT can reduce the ambiguities in the spectrum interpretation and tests hypotheses that are formulated by experimental observation. New properties of minerals are often revealed by DFT computations [1, 2]. In this presentation, two examples are shown how DFT can be synergistic with spectroscopy to understand the mineral reactivity. First example is about layer-type Mn oxide (e.g., birnessite) which exhibits an extremely high sorption capacity for metal cations. Spectroscopy found different trends in Co, Ni, Cu, and Zn partitioning between surface complexes above Mn(IV) vacancies and species incorporated into them (Fig. 1). DFT rationalizes the partitioning trends based on atomic force and electronic structure analysis [3]. In the second example, DFT results are introduced to examine the relationship between composition and structure of transition-metal incorporated mackinawite (layer-type Fe sulfide), which is still ambiguous in experiments. Application of DFT computations to understanding of the mineral reactivity toward actinide elements is further discussed.

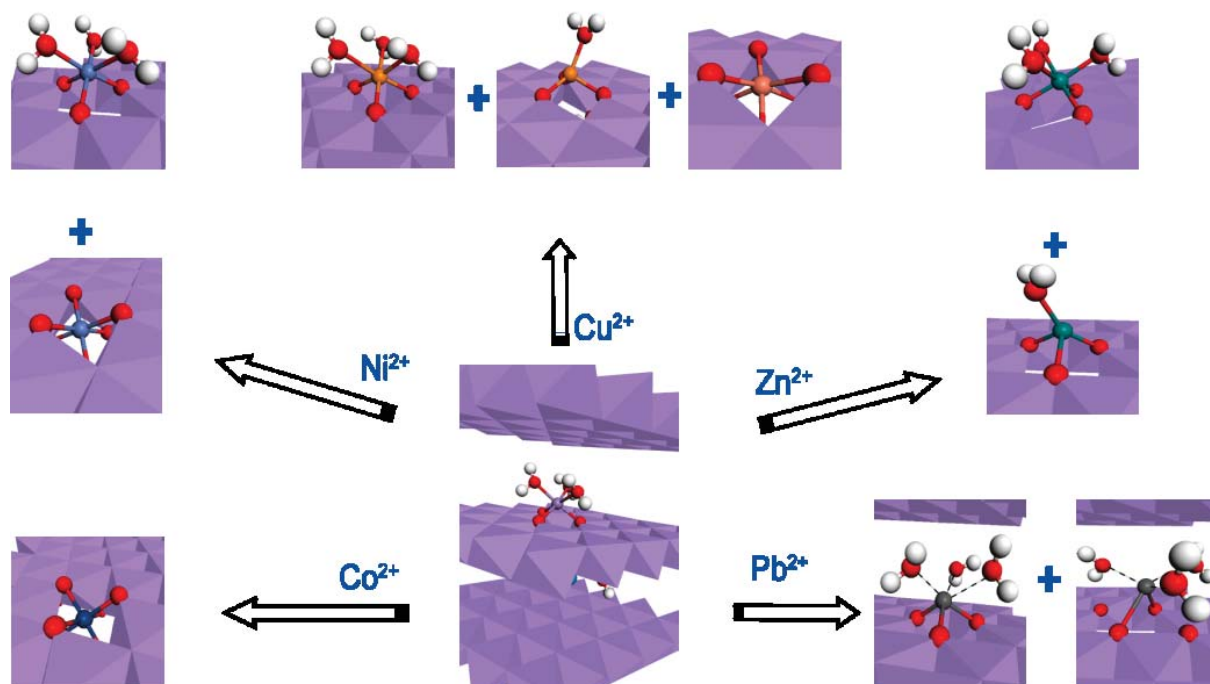


Fig. 1: Partitioning trends of trace metals at Mn(IV) vacancies in birnessite.

- [1] Kwon K. D., Refson K. and Sposito G. (2008) Defect-induced photoconductivity in layered manganese oxides: A density functional theory study, *Physical Review Letters* 100, 146601.
- [2] Kwon K. D. et al. (2011) Magnetic ordering in mackinawite (tetragonal FeS): evidence for strong itinerant spin fluctuations, *Physical Review B* 83, 064402.
- [3] Kwon, K. D., Refson, K. and Sposito, G. (2013) Understanding the trends in transition metal sorption by vacancy sites in birnessite, *Geochimica et Cosmochimica Acta* 101, 222–232.

Surface interaction of actinide oxides and mixed oxides with ice under UV light: an UPS, XPS investigation

P. Çakir,^{1,2} R. Eloirdi,¹ F. Huber,¹ R. J. M. Konings,³ T. Gouder¹

¹ European Commission, Joint Research Centre (JRC), Institute for Transuranium Elements (ITU), Actinide Research Unit, Karlsruhe, Germany

² Delft University of Technology, Faculty of Applied Sciences, Delft, The Netherlands

³ European Commission, Joint Research Centre (JRC), Institute for Transuranium Elements (ITU), Material Research Unit, Karlsruhe, Germany

Interaction of actinide oxides (AnO_2 , $An = U, Pu, Np$) and U mixed oxides with Pu and Th with adsorbed ice under UV light was studied by Ultra-violet and X-ray photoelectron spectroscopy (UPS and XPS, respectively). The oxides were produced as thin films by reactive sputter deposition in the presence of O_2 . Water was condensed as thick ice film on the surface at low temperature. Results were compared before and after warming up of ice layer under UV light (HeI and HeII radiation). NpO_2 was reduced to surface Np_2O_3 . Np_2O_3 was reported [1] to be stable only as a layer on the surface of Np metal; however our findings show the possibility to reduce NpO_2 to a stable Np_2O_3 on the surface under UV light and in the presence of ice layer (Fig. 1). In the co-deposited U-Pu Mixed Oxide thin film, Pu was reduced from PuO_2 to Pu_2O_3 . In U-Th Mixed Oxide, the U was reduced from hyperstoichiometric UO_{2+x} to stoichiometric UO_2 but not to the lower oxides: the lowest thermodynamically stable oxides are formed. In the mixed oxides, U reduction seems to be activated both for oxides with Th and with Pu. The role of UV light on the reduction process was also investigated by measuring on irradiated and dark areas of the films.

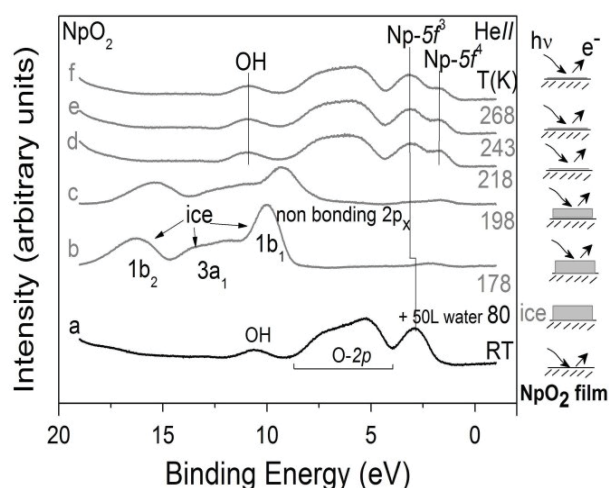


Fig. 1: HeII valence band spectra of a NpO_2 film cooled down, then covered by ice (b) and warmed up (c till f). After ice desorption the $5f^4$ emission of reduced Np_2O_3 appears (d).

Surface reduction is explained as a photocatalytic reaction of the surface, triggered by the excitation of electrons from the valence (or impurity) band into the conduction band. The enhancement of reactivity of the mixed oxides compared to pure uranium is explained by the higher band gap of ThO_2 and PuO_2 compared to UO_2 . The UV light used in this study has energy sufficient to enable the transfer of electron from valence band to conduction band of the actinide oxides.

[1] J. R. Naegele, L. E. Cox, and J. W. Ward (1987) *Inorg Chim Acta* 139, 32.

Computational modeling of actinide adsorption on edge surfaces of 2:1 clay minerals

A. Kremleva, S. Krüger

Theoretische Chemie, Department Chemie, Technische Universität München, Garching, Germany

Clays are considered as favorable host rock formations for highly radioactive waste. Adsorption of actinides on clay minerals, representing the dominant fraction of the mineral content of clay rocks, is regarded as efficient retardation mechanism. Thus, a mechanistic understanding of actinide adsorption on clay mineral surfaces at the atomic level is an important prerequisite for thoroughly modeling the actinide distribution in the environment.

We study uranyl adsorption on clay minerals at the density functional level with the plane-wave based projector augmented wave (PAW) approach as implemented in the program VASP [1], applying a periodic supercell approach. The reactive edge surfaces of the neutral 2:1 clay mineral pyrophyllite are characterized and the corresponding surfaces of permanently charged model smectite minerals are created by two types of cation substitutions: (i) $\text{Si}^{4+} \rightarrow \text{Al}^{3+}$ in the tetrahedral sheet (beidellitic) and (ii) $\text{Al}^{3+} \rightarrow \text{Mg}^{2+}$ in the octahedral sheet (montmorillonitic). Surface solvation is approximated by 1–2 layers of explicit water molecules. For all model smectite minerals, we studied bidentate uranyl(VI) adsorption on various adsorption sites of the (010), (110), and (100) edge surfaces.

The structural parameters of the adsorbed species are very similar for adsorption on pyrophyllite and smectite minerals when their substitutions lie below the surface. Noticeable variations appear only when cations of adsorption sites are substituted. This finding agrees with our previous result that U–O bond lengths to the surface correlate with the formal charge of the corresponding surface O centers [2]. In agreement with this paradigm, significant structural effects are lacking in case of sub-surface substitutions. In contrast, substitutions on the surface lower the formal charges of surface O centers and thus, in most cases, result in shorter U–O bonds to the surface. The types of adsorption complexes determined depend on the orientation of the edge surfaces. The characteristics of these complexes depend on the surface structure and the corresponding adsorption site. A change of coordination number of uranyl from 5 to 4 appears for sites with rather long O–O distances. Hydrolysis of adsorbed uranyl is obtained when there are unsaturated surface aluminol groups close to the adsorption site.

Adsorption energies are rather sensitive to the modeling procedure. Simple optimization of the adsorption complexes at a mineral surface solvated by explicit water molecules results in a wide scattering of adsorption energies. The energies vary by up to 150 kJ mol^{-1} , which can be rationalized by variations in the structure of the solvation layer. To achieve more reliable adsorption energies, we applied a simulated annealing procedure to equilibrate the solvent structure prior to optimization. Most systems were found to equilibrate and converge after 3 ps to an almost stable total energy (variations smaller than 10 kJ mol^{-1}). Adsorption energies determined in this way for uranyl on various sites of the same surface vary by 50 kJ mol^{-1} only. On average, adsorption on montmorillonite surfaces is about $20\text{--}30 \text{ kJ mol}^{-1}$ more favorable than on neutral pyrophyllite. Structural parameters of the adsorption complexes agree with results from simple optimization. Overall we demonstrate that species and their structures are, independent of the mineral model, determined by the surface chemical groups, while the energies for forming surface complexes vary slightly with the type of mineral.

[1] a) G. Kresse, J. Hafner (1993) Phys. Rev. B 47, 558; b) G. Kresse, J. Hafner (1994) Phys. Rev. B 49, 14251; c) G. Kresse, J. Furthmüller (1996) J. Comput. Mat. Sci. 6, 15; d) G. Kresse, J. Furthmüller (1996) Phys. Rev. B 54, 11169.

[2] A. Kremleva, S. Krüger, N. Rösch (2013) Surf. Sci. 615, 21.

Interaction of U(VI) with aluminium(hydr)oxides: structural analysis combining EXAFS and artificial intelligence

A. Rossberg,^{1,2} A. C. Scheinost^{1,2}

¹ Rossendorf Beamline at ESRF, Grenoble, France

² Institute of Resource Ecology, Helmholtz-Zentrum Dresden-Rossendorf, Dresden, Germany

U(VI) can form various binary, ternary and polynuclear sorption complexes with Al(hydr)oxides [1]. Depending on physicochemical parameters (P) like pH, $p\text{CO}_2$, surface area, and surface loading (Γ) these sorption complexes can coexist, hence the spectroscopic signal will be the weighted sum of the spectra of the single complexes in their actual fractions. Inherent to EXAFS spectroscopy, however, the spectroscopic resolution is often not high enough to separate the complex spectra from each other. In this case, the spectroscopic identification of the complexes and the determination of their speciation becomes a challenging task. The un-mixing of the spectroscopic signal into the signals of the pure complexes is currently performed with common statistical methods [2]. However, these methods comprise the major problem that they cannot include additional information like P , which is often available. While this additional information can help to enhance the reliability and the uniqueness of the so-

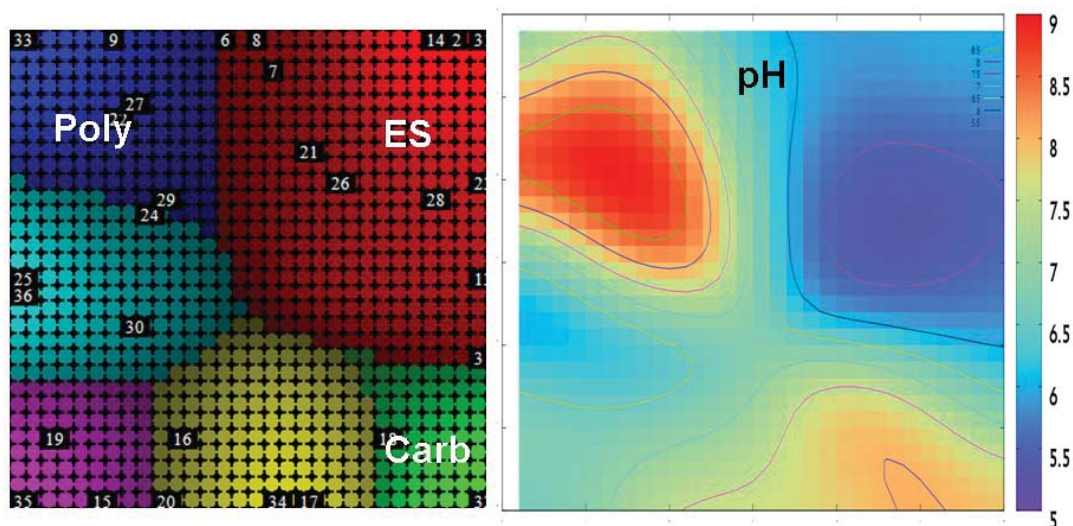


Fig. 1: Example for the influence of the pH on the formation of polynuclear (Poly), edge-sharing (ES) and ternary carbonato (Carb) sorption complexes. Left: Self-organizing map after learning, each point (30x30) correspond to a neuron which contains a EXAFS spectrum and the values of the parameter space P (see definition of P in the text), each color corresponds to one sorption complex, as darker the color as more the complexes are mixed, small numbers are the identifier of the included samples at the determined positions (neurons), 31–36 are the pure sorption complexes. Right: Complementary map for the distribution of the pH.

lution, we propose the use of modified [3] self-organizing maps (SOM) [4], as a variant of an artificial neural network, since SOM can handle any kind of information. Results will be shown for theoretical chemical systems and for UL_{III} -edge EXAFS spectra of twenty-nine samples of U(VI) reacted with Al(hydr)oxides. SOM predicts the spectra of six acting sorption complexes together with their fractions for each sample. Moreover, due to the fact that SOM infers a functional relationship between the spectra (sp) and the additionally included P (simplified: $sp = F(P)$), predominance fields as function of P can be established for the sorption complexes. Figure 1 exemplarily shows the correlation between the six sorption complexes and pH: the higher the pH, the higher the probability of formation of polynuclear (Poly) and ternary carbonato (Carb) sorption complexes, whereas at low pH the formation of edge-sharing (ES) sorption complexes is favored. We will also discuss the influence of other parameters such as $p\text{CO}_2$ and Γ .

[1] Hattori, T. et al. (2009) *Geochim. Cosmochim. Acta.* 73, 5975–5988.

[2] Rossberg, A. et al. (2009) *Environ. Sci. Technol.* 43, 1400–1406.

[3] Domaschke, K. et al. (2014) *Proceedings of ESANN.*

[4] Kohonen, T. (1982) *Biological Cybernetics* 43, 59–69.

Using CLSM and TRLFS analysis to describe spatial distributions of Eu surface complexes – Future perspectives

S. Britz,¹ A. Schulze,¹ R. Steudtner,² K. Großmann²

¹ GRS mbH, Braunschweig, Germany

² Institute of Resource Ecology, Helmholtz-Zentrum Dresden-Rossendorf, Dresden, Germany

Surface reactions on mineral-water interfaces such as sorption processes are one important retardation process for radionuclide transport to be considered in long-term safety assessments. These surface reactions are correlated with geochemical conditions of the surrounding environment that vary in time and space. For long-term safety analysis for e.g. radioactive waste repositories it is of great interest to understand and to realistically assess these geochemically driven surface and transport processes.

In the present study sorption reactions are modeled using so-called surface complexation parameters (SCP) referring to mineral-specific constants such as protolysis constants, surface site areas, surface site densities, and stability constants of surface complexes. Many studies have dealt with the development of surface complexation models and SCP in the past [1,5,6]. In this research, it is the aim to assess SCP and to apply surface complexation models to describe retardation of long-term safety relevant elements via the application of mechanistic geochemical speciation codes. The knowledge of the surface complex(es) is a prerequisite for the application of these models. Therefore, we have developed a method to identify spatial distributions of surface complexes over varying geochemical conditions directly on the minerals' surfaces. This method offers the possibility to collect experimental data to back-up widely accepted surface complexation reactions on the one hand, but also to possibly emphasize neglected and/or not existing surface processes.

To validate the new approach uranium is chosen for first experiments since a vast amount of spectroscopic data is available for this element. Column experiments with Uhry quartz (G20 EAS extra) and U(VI) 10^{-5} mol L⁻¹ are performed. A constant pH of 4.9 is applied. Two U(VI) peaks develop throughout the experiment: The first fraction travels quite fast through the column and coincidences with the breakthrough curve of the applied NaBr tracer (10^{-5} mol L⁻¹). The second U fraction, which is stronger retarded, due to an increase of pH, is kept in column by stopping the experiment after a defined amount of background solution passed the column. Samples are prepared by slicing the column horizontally. Via the application of a confocal laser scanning microscope (CLSM) and time-resolved laser fluorescence spectroscopy (TRLFS) spatial distributions of U(VI) surface complexes are collected. The application of both spectroscopic and microscopic methods offers the possibility to develop 3D spatial distributions of surface complexes for relevant elements for any geochemical system. First results of the conducted U(VI)-quartz system show good agreements with literature values and offer promising results [2–4]. In future, it is one aim to collect spatial distributions of Eu surface complexes under varying geochemical conditions (variation of pH, ionic strength, ligand concentration in natural sediments). Eu is considered to be a homologue for the long-term safety relevant trivalent actinides such as Am and Cm. For flow systems of (i) different pure mineral phases and (ii) natural sediments we want to determine different surface complexes, possible preferred sorption sites on mineral surfaces and composite sediments. We want to identify potential niches of geochemical variable conditions in combination with e.g. precipitation reactions, and potentially preferred flow paths.

Future aspects and first research developments are introduced and we would like to offer an outlook how next steps are intended to be addressed.

[1] Bradbury, M., Baeyens, B. (2001) *Geochimica et Cosmochimica Acta* 66, 2325–2334.

[2] Davies, J. A. (2001) *Surface complexation modelling of uranium(VI) adsorption on natural mineral assemblages*, US Nuclear Regulatory Commission, Washington DC, 214 p.

[3] Gabriel, U., Charlet, L., Schlöpfer, C. W., Vial, J. C., Brachmann, A., Geipel, G. (2001) *Journal of Colloid and Interface Science* 239, 358–368.

[4] Ilton, E. S., Wang, Z., Boily, J. F., Qafoku, O., Rosso, K. M., Smith, S. C. (2012) *Environmental Science & Technology* 46, 6604–6611.

[5] Kitamura, A., Fujiwara, K., Yamamoto, T., Nishikawa, S., Moriyama, H. (1999) *Journal of Nuclear Science and Technology* 36, 1167–1175.

[6] Stumpf, S., Stumpf, T., Lützenkirchen, J., Walther, C., Fanghänel, T. (2008) *Journal of Colloid and Interface Science* 318, 5–14.

A joint photoelectron spectroscopy and theoretical study on uranium halide complexes

J. Su,^{1,2} P. D. Dau,³ H.-T. Liu,^{1,3} L.-S. Wang,³ J. Li²

¹ Division of Nuclear Materials Science and Engineering, Shanghai Institute of Applied Physics, Chinese Academy of Sciences, Shanghai, China

² Department of Chemistry, Tsinghua University, Beijing, China

³ Department of Chemistry, Brown University, Providence, U.S.A.

Uranium halides are important for fundamental actinide chemistry and a variety of nuclear technologies from uranium enrichment to separation. Investigations of such complexes and their stabilities are critical in understanding the chemical transformation and coordination chemistry in recycling spent nuclear fuels in dry process.[1] Anion photoelectron spectroscopy (PES) together with electrospray ionization (ESI) is a powerful spectroscopic experimental technique in probing electronic structures of solution species in the gas phase. Here, we report the electronic structures and spectroscopy of gas-phase uranium halides UF_n^- ($n = 1-6$) [2] and UX_5^- ($X = F, Cl$) [3,4] using ESI-PES and relativistic quantum chemistry.

The UF_n^- ($n = 1-6$) anions were systematically studied by using PES. Theoretical investigations show that the adiabatic electron detachment energies (i.e., electron affinities of the neutrals) of UF_n^- ($n = 1-6$) increase from $n = 1$ to $n = 6$. Chemical bonding analyses of UF_n^- indicate that the U-F bond lengths increase for $n = 2-4$ and decrease for $n = 5-6$, while the bond strengths decrease monotonically. The

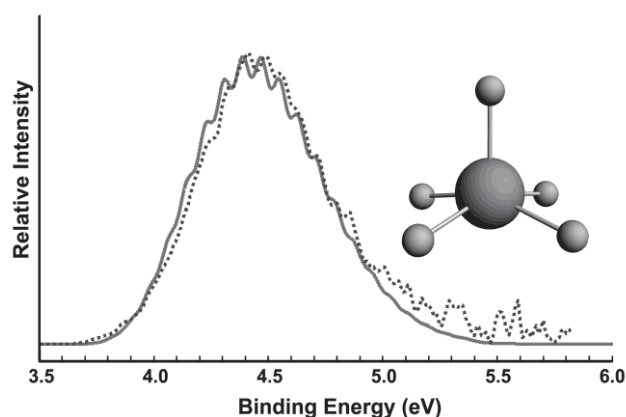


Fig. 1: Calculated (solid) and experimental (dotted) photoelectron spectra of UF_5^- at 213 nm.

ground states of UX_5^- ($X = F, Cl$) have an open shell with two unpaired electrons occupying two primarily U ($5f_{xyz}$ and $5f_z^3$) based molecular orbitals. The structures of both UX_5^- and UX_5 ($X = F, Cl$) are theoretically optimized and confirmed to have C_{4v} symmetry. The UX_5^- anions are highly electronically stable with adiabatic electron binding energies of 3.82 ± 0.05 eV and 4.76 ± 0.03 eV for $X = F$ and Cl , respectively. An extensive vibrational progression from U-F symmetrical stretching mode is observed in the spectra of UF_5^- , which is well reproduced by a Franck-Condon simulation (see Fig. 1). Systematic chemical bonding analyses are performed on all the uranium pentahalide complexes UX_5^- ($X = F, Cl, Br, I$). The results indicate that the U-X interactions in

UX_5^- are dominated by ionic bonding with increasing covalent contributions for the heavier halogen complexes. Our study shows that the synergy of experimental and theoretical investigations can provide an in-depth understanding of the complex electronic structures and chemical bonding of actinide compounds.

[1] Morss, L.R.; Edelstein, N.M.; Fuger, J. (2006) in: The Chemistry of the Actinide and Transactinide Elements, Vols. 1 and 2, Springer, Dordrecht, The Netherlands.

[2] Li, W.-L.; Hu, H.-S.; Jian, T.; Lopez, G.-V.; Su, J.; Li, J. and Wang, L.S. (2013) *J. Chem. Phys.* 139, 244303.

[3] Dau, P.D.; Su, J.; Liu, H.T.; Huang, D.L.; Wei, F.; Li, J. and Wang, L.S. (2012) *J. Chem. Phys.* 136, 194304.

[4] Su, J.; Dau, P.D.; Xu, C.F.; Huang, D.L.; Liu, H.T.; Wei, F.; Wang, L.S. and Li, J. (2013) *Chem. Asian J.* 8, 2489.

ATR-FTIR and UV-Vis spectroscopic studies of aqueous U(IV)-oxalate complexes

W. Cha, E. C. Jung, Y.-S. Park, H.-R. Cho, Y.-K. Ha

Nuclear Chemistry Research Division, Korea Atomic Energy Research Institute, Daejeon, Republic of Korea

Understanding the behaviors of actinide ions interacting with organic molecules is essential to the assessment of the geochemical migration of actinide species in the environment. Tetravalent uranium (U(IV)) is one of major redox states of uranium under anoxic and reducing conditions of deep groundwater systems. Soluble or dissolved U(IV) species may play key roles during the U(VI)/U(IV) transformation processes resulting from the complexation of U(IV) with chelating or multi-functional ligands. In this study, a U(IV)-oxalate (Ox) complex system is examined using attenuated total reflection (ATR)-FTIR and UV-Vis absorption spectroscopy to identify the complexation behaviors at a wide range of pH (0–6) and their impact on the U(IV) solubility.

Information of molecular structures of dissolved complexes and their quantitative ligand-metal binding can be obtained by ATR-FTIR spectroscopy [1]. A solid standard, $\text{UOx}_2 \cdot 2\text{H}_2\text{O}(\text{s})$ was prepared in this study by thermally dehydrating $\text{UOx}_2 \cdot 6\text{H}_2\text{O}(\text{s})$ and confirming the structure by XRD analysis [2]. ATR-FTIR measurements using a flow setup provide clear evidence for the formation of both $\text{U}(\text{Ox})_3^{2-}$ and $\text{U}(\text{Ox})_4^{4-}$ at pH 3–6 up on dissolution of $\text{UOx}_2 \cdot 2\text{H}_2\text{O}(\text{s})$ (Fig. 1), and allow the estimation of species distribution. The characteristic carboxylate vibration (ν_1 and ν_2) of the complexes are thought to represent the five-membered ring bidentate complex structure as reported for aqueous transition metal-oxalate complexes [3].

Complexation of U(IV) with oxalate is characterized by the formation of crystalline $\text{UOx}_2 \cdot 6\text{H}_2\text{O}(\text{s})$ in acidic solutions and the enhanced solubility of U(IV) with the excess amount of the ligand at higher pH (up to ~6). The solubility of $\text{UOx}_2 \cdot 6\text{H}_2\text{O}(\text{s})$ is estimated by UV-Vis absorption measurements using a liquid-waveguide capillary cell with a 1-m optical pathlength and ICP-AES analysis after the solid phase removal. It was revealed that each U(IV)-Ox complex has a unique UV-Vis absorption spectrum, as shown in Fig. 2, although the spectral overlap is significant. Therefore, both results of ATR-FTIR and UV-Vis absorption measurements were used to reduce the uncertainty for estimating the thermodynamic data of the U(IV)-Ox complex system. The temperature-dependent speciation and molecular structures of the individual complex species will be discussed in connection to their aqueous chemistry in a geochemical system.

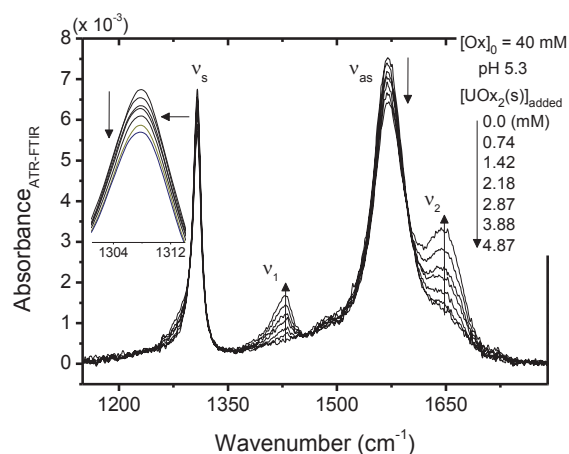


Fig. 1: ATR-FTIR spectra showing the consumption of free oxalate (Ox^{2-}) at ν_s and ν_{as} for carboxylate vibration, and the formation of UOx_n^{4-2n} ($n \geq 3$) at ν_1 and ν_2 upon further complexation of dissolved $\text{UOx}_2 \cdot 2\text{H}_2\text{O}(\text{s})$ in a solution containing oxalate (40 mM) at pH 5.3 ($I = 0.1 \text{ M}$).

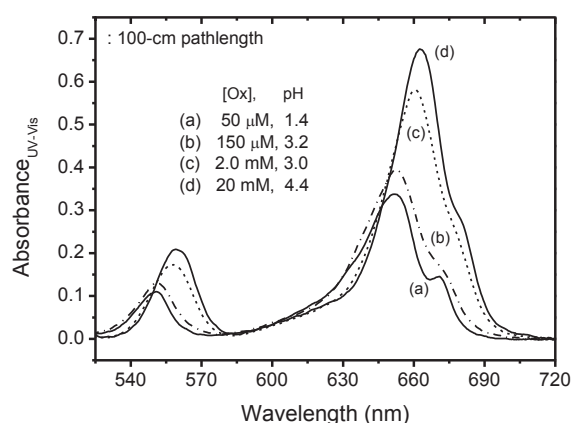


Fig. 2: UV-vis absorption spectra measured from solutions containing U(IV) (56 μM) under various conditions, i.e., (a), (b), (c) and (d) as noted; in each of which the distinct spectral feature of the 1:1, 1:2, 1:3 and 1:4 U(IV)-Ox complex is displayed, respectively.

[1] Müller, K. et al. (2008) Inorg. Chem. 47, 10127–10134.

[2] Duviolbourg-Garela, I. et al. (2008) J. Solid State Chem. 181, 1899–1908.

[3] Axe, K. and Persson, P. (2001) Geochim. Cosmochim. Acta 65, 4481–4491.

Luminescence of lanthanides in aqueous solutions in the presence of small organic molecules

K. Burek, S. Eidner, K. Brennenstuhl, M. U. Kumke

¹ Institute of Chemistry (Physical Chemistry), University of Potsdam, Potsdam, Germany

Luminescence spectroscopy has proven to be a powerful tool in the speciation analysis of actinides and lanthanides. Based on the spectroscopic properties, a wealth of information on the species of these ions present in the sample can be obtained. In particular, the evaluation of the spectral intensity distribution as well as the luminescence decay kinetics was successfully applied to extract information from the experimental data. The data analysis relies on the exact knowledge of the intra- and intermolecular processes involved in the luminescence of the actinide (An(III)) and lanthanide (Ln(III)) ion. Since the luminescence of An(III) and Ln(III) ions originates from electronic transitions within the f-orbitals, which are shielded by outer s- and p-shells and which are only slightly (if any) involved in the binding of ligands, the effective changes in the photophysical properties are sometimes small and require high-end high resolution spectroscopic approaches such as fluorescence line narrowing (FLN) spectroscopy carried out at ultralow temperature. Moreover, the situation may become more complicated when the electronic system of a ligand can interact with the electronic system of the Ln(III) or An(III) ions. Here, several different deactivation processes may come into play resulting in a significant alteration of the photophysics observed. As a consequence, a proper knowledge about the contribution of such ligand-related deactivation processes is indispensable for a correct speciation analysis. A prominent example is the influence of OH-vibrations and the induced fluorescence quenching of such. Based on the fundamental understanding, an analysis yields the number of water molecules coordinated in the first (and second) coordination sphere of the Ln(III) ions. Energy transfer to certain ligand-related vibrational modes or to the ligand triplet state and electron transfer in combination with the formation of a charge-transfer-transition state are possible radiationless deactivation processes leading to a change in the luminescence characteristics of Ln(III) complexes. Therefore, the interplay between the electronic levels of Ln(III) ion and ligands need to be understood in detail in order to use the full potential of luminescence as a speciation tool.

In our experiments, we investigated the luminescence of Eu(III), Tb(III), Dy(III), and Sm(III) in the presence of small aromatic carboxylic acids (SACA). In previous experiments with Eu(III) it was observed that the luminescence (especially the luminescence kinetics) was distinctly changed – in some cases an unexpected significant decrease in the luminescence decay time of the complexes in comparison to the aquo-complex was observed. In our work, the temperature dependence of the luminescence decay time of different Ln(III)-SACA complexes was evaluated in order to shed more light on the radiationless deactivation processes involved. Depending on the specific properties of the combination between metal ion and ligand, in particular the redox chemistry and the relative energy difference between the triplet energy of the SACA and the emitting energy level of the Ln(III), different deactivation processes are active resulting in an effective quenching of the Ln(III) luminescence. While for Tb(III) the triplet energy of the ligand showed to be the major factor, for Eu(III) the formation of an intermediate charge transfer state was identified as the main deactivation process. In our experiments also the influence of the ionic strength ($0 < I < 4$ M) was investigated.

Synthesis and laser spectroscopy of uranium(IV, VI) complexes in ionic liquids

N. Aoyagi,¹ M. Watanabe,¹ T. Kimura,¹ A. Kirishima,² N. Sato²

¹ Nuclear Science and Engineering Center, Japan Atomic Energy Agency (JAEA), Tokai, Ibaraki, Japan

² Institute of Multidisciplinary Research for Advanced Materials, Tohoku University, Sendai, Japan

The nature of uranium compounds has potential applications in developing their utilities as catalytic, magnetic, and chromic materials [1,2]. Among them the control of the valence is a key issue for the in-depth understanding of a particular function. In our recent study, the thermochromic property of uranium containing ionic liquids, $[\text{C}_n\text{mim}]_3[\text{U}^{\text{VI}}\text{O}_2(\text{NCS})_5]$: 1-alkyl-3-methylimidazolium pentakis-(isothiocyanate), was examined by ^{15}N NMR spectroscopy and time-resolved laser-induced spectroscopy (TRLFS) [3]. It is a change of coordination number around a uranyl moiety that explains the yellow-to-orange color alteration due to increase of temperature. The lower oxidation state of uranium is of another interest lately and a series of compounds has been investigated by Hashem et al. [4]; other spectroscopic properties such as UV-Vis-NIR absorption spectra and luminescence spectra are studied in the present work using U^{IV} complexes in ionic liquids [5].

Synthesis of uranium tetrahalides was performed in the preliminary test. Uranium metal or oxides were contacted to an excess amount of halogen, HF or CX_4 ($\text{X} = \text{Cl}, \text{Br}$) in a quartz reaction tube at an elevated temperature such as $420\text{ }^\circ\text{C}$ – $500\text{ }^\circ\text{C}$ for 3–6 hours, affording a series of UX_4 , where $\text{X} = \text{F}, \text{Cl}, \text{Br},$ and I . The crude product was added to the acetonitrile with a proper amount of $[\text{C}_1\text{mim}]\text{Cl}$ and KSCN to give the green powder of $[\text{C}_1\text{mim}]_4[\text{U}^{\text{IV}}(\text{NCS})_8]$ (**1**).

The complex **1** exhibits pale luminescence in light yellow at room temperature. Luminescence intensity at 77 K enhances and time-resolved luminescence spectra are shown in Fig. 1. Broad bands are observed during 5–25 ns after a short excitation pulse generated by Ti:sapphire regenerative amplifier (a). The fluorescence lifetime of this species was around 10 ns. In contrast, there are sharp and well-defined multiple peaks appearing after a couple of hundreds of microseconds as a delay time (b). These are assigned as a $\text{U}^{\text{VI}}\text{O}_2(\text{NCS})_5^{3-}$ species having phosphorescence lifetime around 100 μs in imidazolium-based ionic liquids[1]. It means this ionic product is a mixture of U^{IV} and a trace amount of U^{VI} by origin or U^{VI} is formed in the chemical treatment in an Ar glove box. Moreover, the large difference of luminescence intensity gives rise to a highly-sensitive detection of coexisting U^{VI} species.

Therefore, further purification by sublimation is still needed in order to obtain the uranium compounds at the spectroscopic quality. The purification was conducted in a vacuum-sealed quartz tube kept at $500\text{ }^\circ\text{C}$. The impurities are greatly removed by this method. Spectroscopic properties of synthesized ionic liquids containing uranium(IV) are to be discussed in detail.

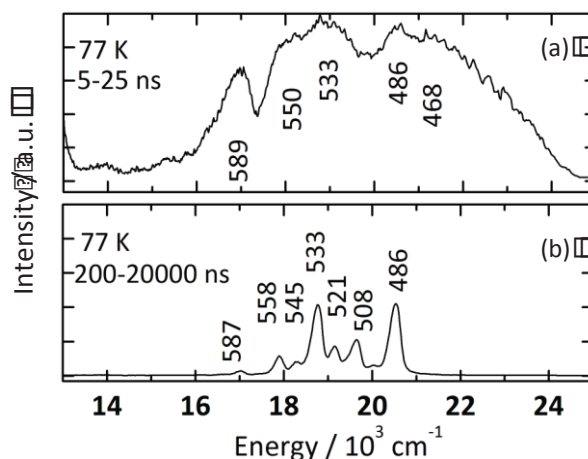


Fig. 1: Time-resolved luminescence spectra of $[\text{C}_2\text{mim}][\text{U}(\text{NCS})_8]$ at 77 K. The temporal gate widths are 5–25 ns (a) and 20 ns–20 μs (b), respectively. Peak positions in nanometer are also shown.

- [1] K. Binnemans, (2007) Chem. Rev. 107, 2592–2614.
[2] K. Takao, et al. (2013) Inorg. Chem. 52, 3459–3472.
[3] N. Aoyagi, et al. (2011) Chem. Commun. 47, 4490–4492.
[4] E. Hashem, et al. (2013) RSC Adv. 3, 4350–4361.
[5] N. Aoyagi, et al. J. Radioanal. Nucl. Chem., accepted.

Development of accurate force field parameters for An(III)/Ln(III) ions in aqueous solution

B. Schimmelpfennig,¹ M. Trumm,¹ P. J. Panak,^{1,2} A. Geist¹

¹ Institute for Nuclear Waste Disposal, Karlsruhe Institute of Technology, Karlsruhe, Germany

² Institute for Physical Chemistry, University of Heidelberg, Heidelberg, Germany

Over the last years classical force fields have been employed regularly to investigate certain properties of metal ions in aqueous solution [1–4]. Especially in actinide chemistry, a theoretical approach is desirable due to the difficulties in handling radioactive materials. Despite good agreement of most studies with experimental results, the derivation of the force-field parameters, the analytical form of the interaction terms and the length of the simulation often vary and leave doubt in the reliability and the predictive character of such approaches. Especially for systems containing counter-ions or complexing ligands, most classical force fields are not accurate enough to reproduce data derived from ab initio methods. The POLARIS(MD) software package [5] includes a polarizable force field and a charge-transfer term [3], both in a many-body form, able to reproduce quantum-chemical data with an accuracy of more than 99% of the total binding energy for a large number of reference points.

We will present the results of our study on the 1:3 complex (Fig. 1) of the Cm(III) ion with the iPr-BTP and nPr-BTP extraction ligands [6] which play a major role in the separation of the minor actinides from the lanthanides. Measured data show an increased stability constant for iPr-BTP by a factor of 100 compared to nPr-BTP [7], but up to now no explanation could be proved experimentally. Results from our molecular dynamics (MD) simulations suggest that the difference originates from a shielding effect induced by the side-chains. The n-propyl side-chains allow about two more water molecules to occupy the area between the aromatic ring-systems, leading to a change in the thermodynamic behavior (Fig. 2). Based on the MD results new EXAFS and NMR experiments are being designed to confirm the theoretical predictions.

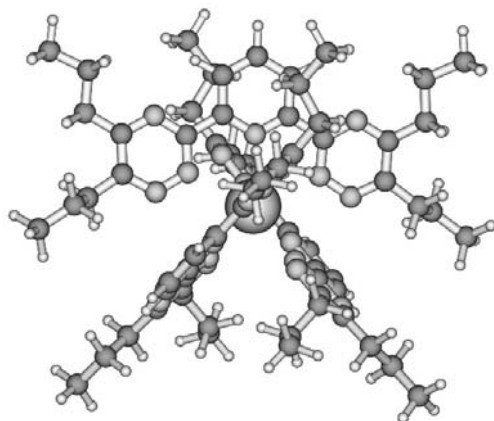


Fig. 1: Optimized gas-phase structure of the Cm(III) nPr-BTP 1:3 complex.

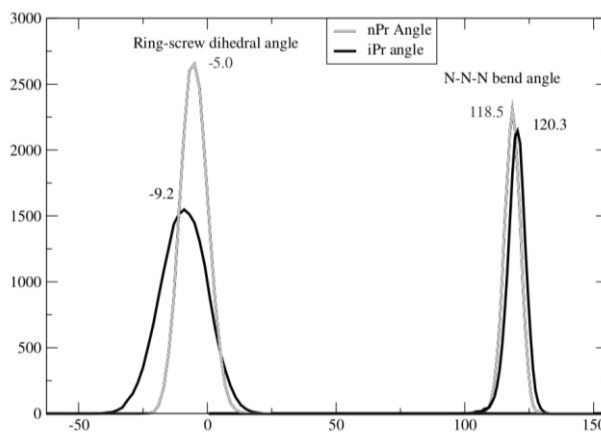


Fig. 2: Distribution of the screw- and bend-angles for the iPr- and nPr-BTP complexes in the MD simulation.

- [1] M. Trumm et al., *J Chem Phys* 136 (2012).
- [2] C. Beuchat et al., *J Phys Chem B* 114 (2010).
- [3] F. Réal et al., *J Comp Chem* 34 (2013).
- [4] R. Spezia et al., *J Phys* 190 (2009).
- [5] M. Masella et al., *J Chem Phys* 119 (2003).
- [6] S. Trumm et al., *EJ Inorg Chem* (2010).
- [7] P. J. Panak et al., *Chem. Rev.* 113 (2013).

ABSTRACTS

POSTER PRESENTATIONS

Structural studies on (La,Eu)PO₄ solid solutions by infrared, Raman and X-ray absorption spectroscopy

Y. Arinicheva,¹ M. J. Lozano-Rodriguez,^{2,3} S. Neumeier,¹ A. C. Scheinost,^{2,3}
N. Clavier,⁴ D. Bosbach¹

¹ Institute of Energy and Climate Research, Nuclear Waste Management and Reactor Safety (IEK-6),
Forschungszentrum Jülich, Jülich, Germany

² Institute of Resource Ecology, Helmholtz-Zentrum Dresden-Rossendorf, Dresden, Germany

³ The Rossendorf Beamline at ESRF, Grenoble, France

⁴ Institut de Chimie Séparative de Marcoule, UMR 5257 CEA/CNRS/UM2/ENSCM, Bagnols-sur-Cèze, France

Phosphate ceramics with monazite structure are promising materials as potential nuclear waste forms for the conditioning of minor actinides, because of such properties as high loading, high chemical stability and irradiation resistance [1]. Rhabdophane is a hydrous phosphate phase produced by a low temperature synthesis route and serves as precursor material for monazite formation. It also can be formed due to aqueous alteration of monazite [2].

This study is established with the overall objective to reveal the changes in the crystal structure of rhabdophane and monazite. A refined understanding concerning the formation of rhabdophane and monazite lanthanides/actinides solid solutions and phase stability is of great importance with regard to the long term stability of ceramic materials for safe nuclear disposal.

La_{1-x}Eu_xPO₄ rhabdophane and monazite solid-solutions were synthesized by wet chemical methods (precipitation and hydrothermal synthesis). Eu serves as surrogate for trivalent actinides. Samples were characterized by Scanning Electron Microscopy with Energy Dispersive X-ray spectroscopy (SEM/EDX), X-Ray Diffraction (XRD), Raman and Infrared (IR) spectroscopy, as well as Extended X-ray Absorption Fine-Structure (EXAFS) spectroscopy at La and Eu L-edges. Additionally, *in-situ* Raman spectroscopic measurements were performed in order to observe structural changes by rhabdophane-monazite phase transformation during heat treatment.

Structural refinement of X-ray diffraction data showed a Vegard-like behavior of lattice parameters, i.e. a linear decrease with increasing Eu loading. A linear shift of Raman and IR bands towards higher wavenumbers with increasing Eu content is also consistent with the lattice shrinkage.

In contrast, EXAFS analysis revealed that only the La–O distances in the first coordination shell and the first metal-metal distances decrease according to Vegard's law, while the Eu–O local coordination remains unchanged. These new EXAFS results provide important insight into the structural basis of the stability of monazite solid-solutions; they will be used in the future to develop the thermodynamic constants needed for long-term stability predictions.

[1] Lumpkin, G.R. (2006) Elements 2, 365–372.

[2] Du Fou de Kerdaniela, E. et al. (2007) Journal of Nuclear Materials 362, 451–458.

Europium(III) lactate structure determination using spectroscopic (ATR FT-IR, NMR) and theoretical (DFT) methods

A. Barkleit,^{1,2} J. Kretzschmar,¹ S. Tsushima,¹ M. Acker³

¹ Institute of Resource Ecology, Helmholtz-Zentrum Dresden-Rossendorf, Dresden, Germany

² Radiochemistry, Department of Chemistry and Food Chemistry, Technische Universität Dresden, Dresden, Germany

³ Central Radionuclide Laboratory, Technische Universität Dresden, Dresden, Germany

Small organic molecules like lactic acid ($\text{HO-CH}(\text{CH}_3)\text{-COOH}$), which can bind heavy metal ions, are ubiquitous in nature. They can be found in nearly all biological systems as a product of various biochemical processes and in the geosphere as well, *i.e.* as part of organic matter of argillaceous rocks. This renders lactate a suitable model molecule for a multi-technique structure determination. Eu(III) was chosen as non-radioactive model for trivalent actinides.

Current structural suggestions for the Eu(III) lactate are only assumptions from indirect methods [1,2]. We want to provide direct structural information. ATR FT-IR spectroscopy combined with calculations of structure and spectroscopic data using DFT reveals structural features. Lanthanide induced shifts (LIS) in NMR spectroscopy as caused by the interaction of nuclear spins with electronic unpaired spins can be used as a helpful tool for signal separation, probing the potential binding sites and structure including geometries and distances [3].

The combination of all these methods offers new insights concerning the structure of the Eu(III) lactate 1:1 complex thereby resolving contradictions in the previous works whether the hydroxyl group is protonated or not.

From ATR FT-IR measurements, bidentate coordination of exclusively the carboxylate group could be ruled out because of the characteristic degree of spectral splitting of the asymmetric and symmetric stretching vibrations ν_{as} and ν_{s} of the carboxylate group. The best accordance of the DFT calculated vibrational spectra to the measured spectrum is given for monodentate coordinating carboxylate group and additional coordination of the deprotonated hydroxyl group (Fig. 1). NMR findings strongly support the results obtained from ATR FT-IR measurements in combination with DFT calculations. The correlation between the chemical shift changes of the ^{13}C NMR signals and the Eu-C distances calculated by DFT suites perfectly this structure model [4].

The finding that the hydroxyl group seems to be deprotonated under complex formation [4] contradicts former structure suggestions, which suppose a coordination of the trivalent metal ion with the protonated hydroxyl group [1,2]. Both experimental methods, ATR FT-IR and NMR, as well as the DFT calculations yielded an impressively homogeneous structural explanation of the investigated Eu(III) lactate 1:1 species.

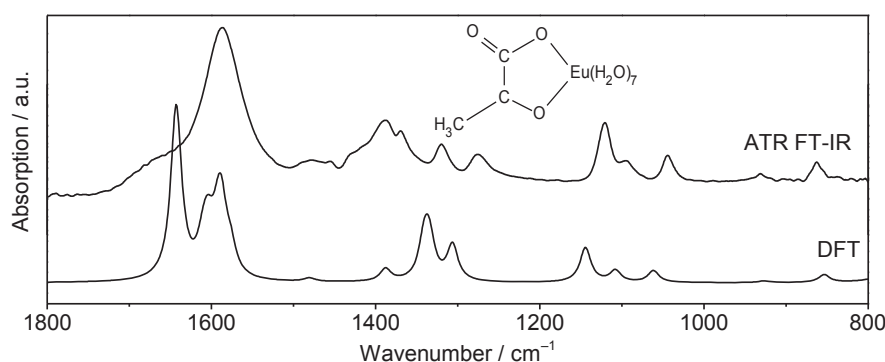


Fig. 1: Experimental (ATR FT-IR) and calculated (DFT) spectra of Eu(III) lactate.

[1] Tian, G.X. et al. (2010) Inorg. Chem. 49, 10598-10605.

[2] Dickins, R.S. et al. (2002) J. Am. Chem. Soc. 124, 12697-12705.

[3] Mayo, B.C. (1973) Chem. Soc. Rev. 2, 49-74.

[4] Barkleit, A. et al. (2014) Dalton Trans. DOI: 10.1039/c4dt00440j.

Investigation of new Mo fuel matrices for Generation IV Reactors by Electrospray Ionization Mass-Spectrometry

M. Cheng,^{1,2} M. Steppert,¹ C. Walther¹

¹ Institut für Radioökologie und Strahlenschutz, Leibniz Universität Hannover, Hannover, Germany

² Institute for Nuclear Waste Disposal, Karlsruhe Institute of Technology, Eggenstein-Leopoldshafen, Germany

Even though Germany opted out the nuclear energy program, efforts are made worldwide to develop Generation IV reactors. The new reactor concepts should provide higher safety and sustainability and close the nuclear fuel cycle. These new types of reactors demand thermally stable and inert fuel matrices. Within the scope of the development of new reactors molybdenum is investigated as inert matrix to embed the fissile material. The application of these matrices should enhance the retention of radionuclides, especially of Pu(IV) and Am(III), during operation, is investigated in the ASGAR-project (Advanced fuels for Generation IV reactors: Reprocessing and Dissolution). To properly design the reprocessing procedures of the spent fuel, it is important to understand the solution behavior of the Mo-Matrix and the influence of the fissile material on the dissolution processes. To this end the solution species of Mo in strongly acidic media have to be characterized and quantified comprehensively. For this purpose electrospray ionization mass spectrometry [1, 2], which can probe the stoichiometry and relative abundances of solution species, was applied [3].

Isotopically pure ⁹⁸Mo was dissolved in nitric acid ([HNO₃] = 0.5 M, 1 M and 3 M), resulting in a solution with [Mo] = 10 mM. The solutions were measured with the ALBATROS ESI-TOF [4], at low declustering conditions and with a mass resolution of about $m/\Delta m = 16000$. Furthermore, in order to clarify whether the Mo-Matrix forms mixed species with actinides from the fuel, mixtures of ⁹⁸Mo and ⁹⁰Zr as analogue for Pu (IV) with [⁹⁸Mo] = 8 mM and [⁹⁰Zr] = 8 mM were investigated by ESI-MS.

An example of an ESI TOF spectrum in logarithmic representation is shown in Fig. 1. The mass spectra clearly show that besides the expected pure Mo and Zr species mixed Mo-Zr species with the stoichiometries $[\text{MoZrO}_4(\text{NO}_3)_2\text{H}]^+(\text{H}_2\text{O})_n$,

$[\text{Mo}_2\text{ZrO}_7(\text{NO}_3)_2\text{H}]^+(\text{H}_2\text{O})_n$ and $[\text{Mo}_3\text{ZrO}_{10}(\text{NO}_3)_2\text{H}]^+(\text{H}_2\text{O})_n$ are present in solution. The relative abundances of the mixed species are altogether 33% with respect of Mo in this sample. The investigation includes different ratios of the ⁹⁸Mo and ⁹⁰Zr 1:1, 2:1 and 10:1 at different acidic strengths ([HNO₃] = 0.5 M, 1 M) that are better comparable to these of the real reprocessing of the spent nuclear fuel.

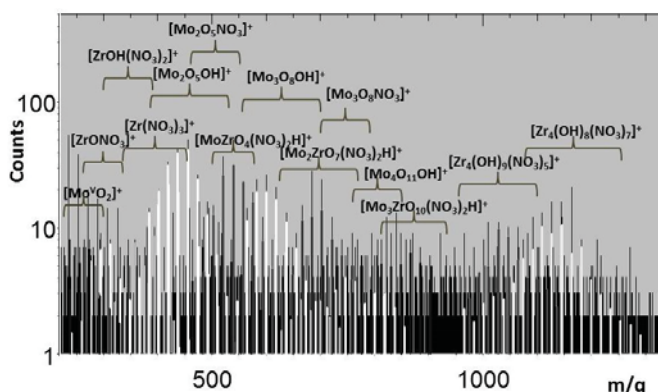


Fig. 1: Time-of-Flight Mass spectrum of a sample with [Mo] = 8 mM, [Zr] = 8 mM, [HNO₃] = 3 M.

[1] Wilm, M. and M. Mann, (1996) Anal. Chem. 68, 1–8.

[2] Cole, R.B. (1997) Electrospray ionization mass spectrometry, John Wiley and Sons, New York.

[3] Walther, C., et al. (2007) Anal. Bioanal. Chem. 388, 409–431.

[4] Bergmann, T. et al. (1989) Rev. Sci. Instrum. 60, 347–349.

Speciation of uranyl(VI) using combined theoretical and luminescence spectroscopic methods

B. Drobot, S. Tsushima, R. Steudtner, J. Raff

Institute of Resource Ecology, Helmholtz-Zentrum Dresden-Rossendorf, Dresden, Germany

Speciation constitutes the basis for actinide complexation studies. These systems can be very complex and challenging especially because of the polynuclear species. An advanced combination of theoretical and experimental methods is proposed here. Continuous wave (CW) and Time-Resolved Laser-induced Fluorescence Spectroscopy (TRLFS) data of uranyl(VI) hydrolysis were analyzed using Parallel Factor Analysis (PARAFAC). Distribution patterns of five major species were thereby derived under a fixed uranyl concentration (10^{-5}) over a wide pH range from 2 to 11. UV (180 nm to 370 nm) excitation spectra were extracted for individual species. Time-dependent density functional theory (TD-DFT) calculations revealed ligand excitation (water, hydroxo, oxo) in this region and ligand-to-metal charge transfer (LMCT) responsible for luminescence. Thus, excitation in the UV is extreme ligand sensitive and highly specific. Combining findings from PARAFAC and DFT the $[\text{UO}_2(\text{H}_2\text{O})_5]^{2+}$ cation (aquo complex, 1:0) and four hydroxo complexes (1:1, 3:5, 3:7 and 1:3) were identified. Refined structural and thermodynamic data of uranyl(VI) hydrolysis is thus acquired.

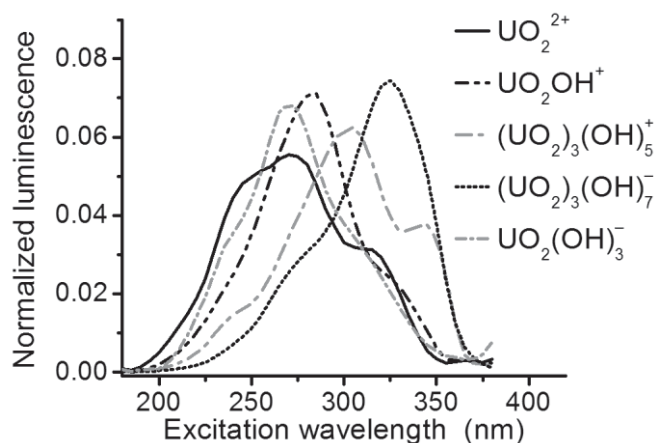


Fig. 1: Extracted excitation spectra for 5 major complexes of uranyl(VI) hydrolysis. Excitation maxima shift from 270 nm (free uranyl) to 325 nm ($(\text{UO}_2)_3(\text{OH})_7^-$).

Np-237 sorption onto montmorillonite and corundum

O. Elo,¹ N. Huittinen,² K. Müller,² K. Heim,² P. Hölttä,¹ J. Lehto¹

¹ Laboratory of Radiochemistry, University of Helsinki, Finland

² Institute of Resource Ecology, Helmholtz-Zentrum Dresden-Rossendorf, Dresden, Germany

The bentonite buffer in Engineered Barrier Systems (EBS), planned for spent nuclear fuel (SNF) repositories, consists mainly of the clay mineral montmorillonite. Montmorillonite and other aluminosilicates are known to retain radionuclides found in the SNF, thus, contributing to the retention or immobilization of these metal ions in the environment. The neptunyl cation, NpO_2^+ , is rather soluble, poorly sorbed, and readily mobile under environmental conditions making it highly relevant for research concerning SNF repository safety.

In the present study we have investigated the sorption of neptunium on the clay mineral montmorillonite under carbonate free, but environmentally relevant conditions. The interaction of neptunium with $\alpha\text{-Al}_2\text{O}_3$ (corundum) has also been investigated in order to study the aluminol surface sites present on clay minerals, which are regarded as the main adsorption sites for radionuclide attachment [1]. We have performed batch sorption studies both as a function of pH and as a function of neptunium concentration $5 \times 10^{-10} \text{ M} - 5 \times 10^{-6} \text{ M}$. The NpO_2^+ uptake on the two different minerals is rather weak. Sorption on the mineral surfaces begins at pH 7, and at pH 8 which is the pH-value expected to prevail in the deep underground in Olkiluoto, Finland, the final disposal site for the Finnish SNF, only $\sim 10\%$ of the actinyl ion is retained (Fig. 1). To gain insight into the surface speciation of neptunium on the two minerals, we performed *in situ* ATR-FT-IR spectroscopic investigations at pH 9 and 10. Upon NpO_2^+ sorption onto corundum and montmorillonite we observe a shift of the asymmetric stretch vibration of the neptunyl ion from 818 cm^{-1} obtained for the free aquo ion to 790 cm^{-1} (Fig. 2). The large shift of the asymmetric stretching vibration indicates the formation of an inner-sphere bound neptunium complex on the mineral surface. A similar shift has previously been observed for NpO_2^+ sorption onto gibbsite ($\alpha\text{-Al(OH)}_3$) [2]. In contrast to the results obtained in Gückel et al., where neptunium desorption could not be observed after flushing the mineral film on the ATR crystal, we observe a high reversibility of the sorption on both corundum and montmorillonite (Fig. 2). This high reversibility of the sorption process speaks for a weaker bonding to the surface. In upcoming EXAFS (Extended X-ray Absorption Fine Structure) measurements, we hope to be able to find an explanation for the deviating desorption behavior of NpO_2^+ on montmorillonite and corundum in comparison to gibbsite. In addition, information on structural parameters and the complexation mechanism of neptunium sorption onto montmorillonite and corundum will be obtained.

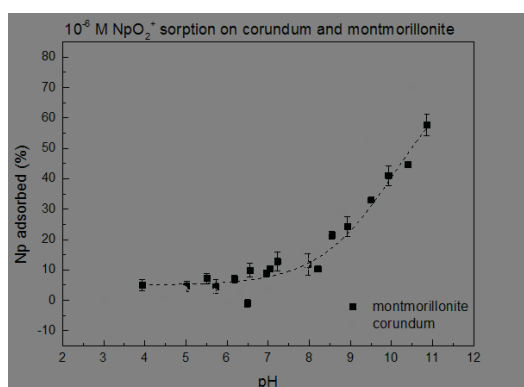


Fig. 1: Sorption of $10^{-6} \text{ M NpO}_2^+$ on 0.5 g/L montmorillonite and corundum in 0.01 M NaClO_4 .

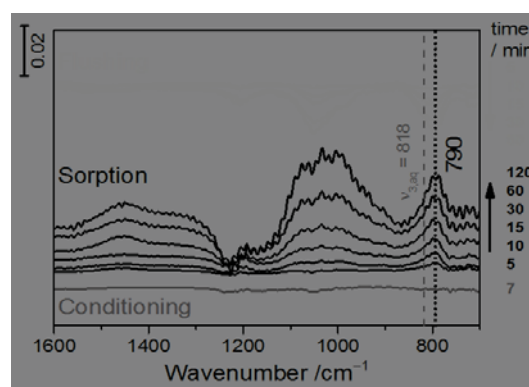


Fig. 2: Sorption of $50 \mu\text{M NpO}_2^+$ in 0.01 M NaCl in D_2O on corundum at $\text{pD} = 9.6$, flow rate 0.1 mL/min.

[1] Turner, D.R. (1998) Neptunium(V) sorption on montmorillonite: An experimental and surface complexation modeling study. *Clays and Clay Minerals*, 46, 256-269.

[2] Gückel, K. et al. (2013) Spectroscopic identification of binary and ternary surface complexes of Np(V) on gibbsite. *Environmental Science & Technology*, 47, 14418-25.

The surface speciation of the ternary sorption system U(VI)/phosphate/silica

H. Foerstendorf,¹ R. Steudtner,¹ M. J. Comarmond,² K. Heim,¹ K. Müller¹

¹ Institute of Resource Ecology, Helmholtz-Zentrum Dresden-Rossendorf, Dresden, Germany

² Australian Nuclear Science and Technology Organisation, Lucas Heights, Australia

The impact of inorganic ligands on the sorption behavior of actinide ions is commonly known. However, detailed knowledge of the molecular events occurring during the sorption processes is often lacking. In particular, the presence of inorganic anions forming actinide complexes of low solubility hampers the application of many spectroscopic approaches due to the formation of binary complexes precipitating from the aqueous solutions.

This study sustains our preliminary results on the ternary sorption system U(VI)/phosphate/silica introduced at ATAS 2012 [1]. The advanced results obtained from a combined approach of *in situ* vibrational and luminescence spectroscopy provide a more detailed insight into the surface speciation of this ternary sorption system.

From *in situ* vibrational spectroscopic sorption experiments of the binary system U(VI)/silica, infrared data exhibit the formation of a uranyl inner sphere complex at the silica surface, whereas from the ternary sorption system, spectra showing great homologies to spectra of solid U(VI)phosphate phases are obtained. The results obtained from the *in situ* IR experiments strongly suggest the formation of a solid U(VI) phosphate as a surface precipitate on the silica phase.

Laser fluorescence spectroscopy reveals the presence of U(VI) phosphate species in aqueous solution most probably solid or colloidal $(\text{UO}_2)(\text{PO}_4)_2 \cdot 4\text{H}_2\text{O}$. For the U(VI) sorption samples, two different surface species were derived from luminescence spectra irrespective of the absence or presence of phosphate [2]. However, the spectral differences became more apparent after prolonged equilibration of the solid phase with a stable U(VI) phosphate solution suggesting chemical rearrangements of the sorbed U(VI) ion towards a ternary surface species.

In summary, IR and luminescence data suggest the formation of a ternary surface species where the U(VI) acts as a bridging ion to the SiO_2 surface with subsequent formation of the ternary surface species $\text{SiO}_2\text{-U(VI)-phosphate}$. This ternary species most likely constitutes a precursor of the formation of a surface precipitate showing spectral properties similar to U(VI) phosphate minerals.

[1] Comarmond, M. J. (2012) Report HZDR-027, 59.

[2] Gabriel, U. et al. (2001) J. Colloid Interface Sci. 239, 358-368.

Sorption of (trivalent) actinides and lanthanides

S. Hellebrandt, M. Schmidt, T. Stumpf

Institute of Resource Ecology, Helmholtz-Zentrum Dresden-Rossendorf, Dresden, Germany

The study of trivalent actinides is of particular importance for the safety assessment of nuclear waste disposal sites due to the predominance of this valence in deep geological formations. In particular, studying the solution-solid interface chemistry of these trivalent radioelements in the aqueous phase with a mineral is fundamental for better understanding their interactions at or within the surface of a host phase in a repository. As a relevant near field material (geotechnical barrier) for nuclear waste disposal sites, clay minerals are very important due to their retardation properties. Muscovite, a phyllosilicate material of aluminum and potassium, is very similar to clay minerals but less complex, so we are able to assign results from muscovite to clay minerals. Additionally, investigations concerning trace concentration of actinides appearing in the far field of a nuclear waste disposal are also of interest.

Site-Selective Time-Resolved Laser Fluorescence Spectroscopy (TRLFS) is a characterization technique that can probe the behavior of low concentrated actinides on a molecular level. As a complementary technique Resonant Anomalous X-ray Reflectivity (RAXR) will be used to get a deeper insight and a verification of the TRLFS results.

The aim of this study focuses on understanding the surface interactions of muscovite with aqueous trivalent actinides and lanthanides using Eu(III) and Cm(III), and characterization of the solid and aqueous phase species using TRLFS. Europium (III) is used as a non-radioactive homologue for trivalent actinides due to its similar chemical behavior and its spectroscopic properties as a probe for TRLFS. Direct excitation of the ${}^7F_0 \rightarrow {}^5D_0$ electron transition and consecutive integration of the respective emission generates information pertaining to the chemical coordination and environment of the Eu(III). First investigations in the muscovite-europium system show that there appears one poorly defined species (broad excitation peak) present at one site (Fig. 1). Lifetime measurements of the luminescence are used in accordance with the Horrocks equation (europium) [1] and the number of coordinated waters can be determined. The lifetimes between 208 and 230 μs indicates 4 to 5 coordinated water ligands in the inner sphere. As a consequence of this the europium species is interpreted as inner-sphere sorption on the surface of muscovite.

Tab. 1: Fluorescence lifetimes and coordinated water ligands.

Sample ID	Fluorescence lifetime (μs)	n H ₂ O
Mu1	230.1	4.0
Mu5	208.2	4.5
Mu65	208.8	4.5

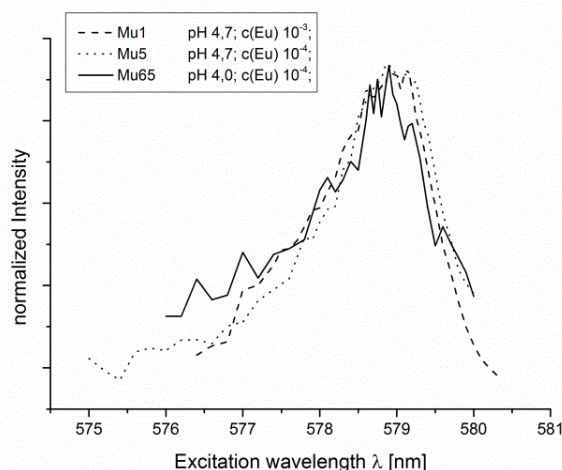


Fig. 1: Excitation spectra of three different muscovite-europium samples with NaCl as background electrolyte (10 mM), different europium concentrations and pH values. Measured with site-selective TRLFS at deep temperature (~ 10 K).

[1] Horrocks, W.D. and Sudnick, D.R. (1979) J. Am. Chem. Soc. 101, 334–340.

A kinetic insight into the formation of neptunium(IV) dioxide NpO_2 nanocrystals

R. Husar,¹ R. Hübner,² S. Weiss,¹ C. Hennig,¹ A. Ikeda-Ohno,¹ H. Zänker,¹
T. Stumpf¹

¹ Institute of Resource Ecology, Helmholtz-Zentrum Dresden-Rossendorf, Dresden, Germany

² Institute of Ion Beam Physics and Materials Research, Helmholtz-Zentrum Dresden-Rossendorf, Dresden, Germany

UV-vis absorption spectroscopy proves itself as a convenient method for *in-situ* monitoring the formation and growth of waterborne An(IV) nanoparticles. Dilution of pure aqueous $\text{Np}(\text{CO}_3)_5^{6-}$ species in ultrapure water leads to the dynamic self-assembling of NpO_2 nanocrystals, monitored among others at absorbance 742 nm.

Nowadays, various state-of-the-art spectroscopic techniques (e. g., X-ray spectroscopies, laser-induced and vibrational spectroscopy, etc.) are available to investigate chemical interactions of actinides (An) on a molecular level. Old-fashioned (or conventional) UV-vis absorption spectroscopy is often underestimated as a powerful tool to investigate the chemistry of An, including An(IV) colloids [1, 2]. The present study spotlights the application of UV-vis absorption spectroscopy to studying the colloid system of An(IV). The chemistry of An(IV) in aqueous solution is typical of a small and highly-charged metal ion with a strong hydrolysis tendency leading low solubility which often results in the underestimation of the migration behavior of An(IV) on the geological disposal of radioactive wastes [3,4,5].

The formation mechanisms of An(IV) colloids, especially under alkaline and near-neutral conditions relevant to the actual environment, are still unexplored even to date. One important issue to be addressed in An(IV) colloid chemistry is the chemical identification of An(IV) colloids. That is, are the colloids formed ill-defined hydroxide precipitate or hydrous oxides, or highly structured clusters/nanoparticles? [6,7]. In order to characterize An(IV) colloids, we investigated *in-situ* the aggregation of neptunium(IV) colloids formed under ambient aqueous alkaline conditions. The kinetics of the ag-

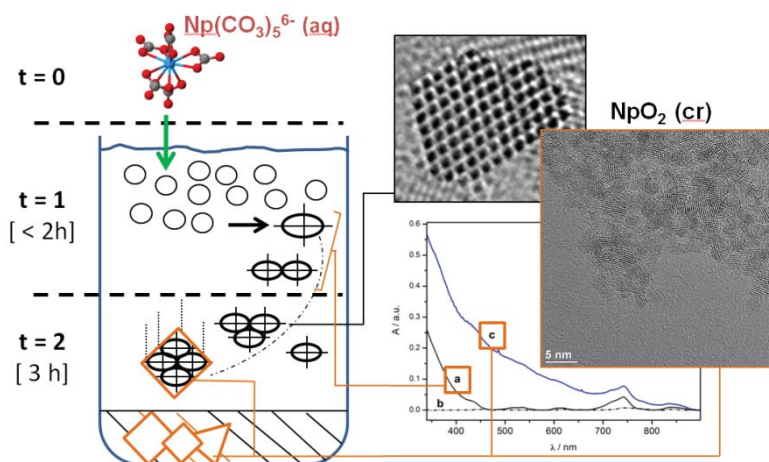


Fig. 1: Proposed formation mechanism of NpO_2 nanocrystals from the initial dissolved species $\text{Np}(\text{CO}_3)_5^{6-}$ (aq) (left), and UV-vis absorption spectra and HRTEM micrographs of Np(IV) species/ NpO_2 nanocrystals formed during hydrolysis (right).

gregation of Np(IV) colloids and the formation of Np(IV) nanoparticles were tracked by UV-vis absorption spectroscopy, and their morphology and internal structures were further investigated by transmission electron microscopy (TEM). In this study, we demonstrate that UV-vis absorption spectroscopy is a unique and powerful tool for *in-situ* monitoring of the hydrolysis reaction of Np(IV) and associated colloid/nanoparticle formation. The obtained results will be further discussed by combining with TEM and X-ray absorption spectroscopy.

- [1] P. Zeh et al., (1999) *Radiochimica Acta* 87, 23.
- [2] V. Neck et al., (2001) *Radiochimica Acta* 89, 439.
- [3] A. B. Kersting et al., (1999) *Nature* 397, 56.
- [4] S. Utsunomiya et al., (2009) *Environ. Sci. Technol.* 43, 1293.
- [5] A. B. Kersting, (2013) *Inorg. Chem.* 52, 3533.
- [6] J. Rothe et al., (2004) *Inorg. Chem.* 43, 4708.
- [7] L. Soderholm, (2008) *Angew. Chem. Int.* 47, 298.

Time resolved luminescence spectroscopy study of Eu(III)-fulvate complexation: influence of pH, ionic strength, and fulvic acid concentration

Y. Kouhail,^{1,2} M. F. Benedetti,¹ P. E. Reiller²

¹ Institut de Physique du Globe de Paris, Sorbonne Paris Cité, Univ Paris Diderot, Paris, France

² CEA/DEN/DANS/DPC/SEARS/LANIE, Gif-sur-Yvette, France

Natural organic matter (NOM) affects the fate of radionuclides in the environment, either by supporting their mobility in water, or by limiting their migration in soils and sediments. Eu(III) was studied as a chemical analogue for actinides(III). Batch experiments were done to build complexation isotherms at different Eu(III) concentrations and pH, using Suwannee River fulvic acid (SRFA) concentrations up to 1 g/L as a proxy for NOM reactivity. Eu(III) speciation was investigated by time-resolved luminescence spectroscopy.

Two different luminescence behaviors of Eu(III) were observed (Fig. 1): (i) the first part of the isotherms at low C(SRFA) is showing the typical luminescence evolution of Eu(III) complexed by humic substances [1]; and (ii) at higher concentration ($C > 100 \text{ mg}_{\text{SRFA}}/\text{L}$ at pH 4, $C > 30 \text{ mg}_{\text{SRFA}}/\text{L}$ at pH 6 and 7), a second luminescence mode is detected and could correspond to a different spatial organization of the complexed europium.

To better understand this second mode, we performed experiments at various ionic strengths. The complexation is typically decreasing with ionic strength in the first part of the isotherm [2,3], whilst the opposite influence was shown in the second part of the isotherm. Luminescence decay times are also showing distinctive evolutions. The fulvic and ionic strength effects evidenced spectroscopically suggest that in addition to intra-particulate complexation mode (first complexation-edge), there might be inter-particulate repulsion between fulvic acid particles that are complexing Eu(III) in the second part of the isotherm, which is not yet accounted within the different complexation models. The account of an interfacial potential for fulvic acid particles, or a Donnan volume depending on the hydrodynamic radius of SRFA was proposed [4,5], and could be considered at high fulvic acid concentration.

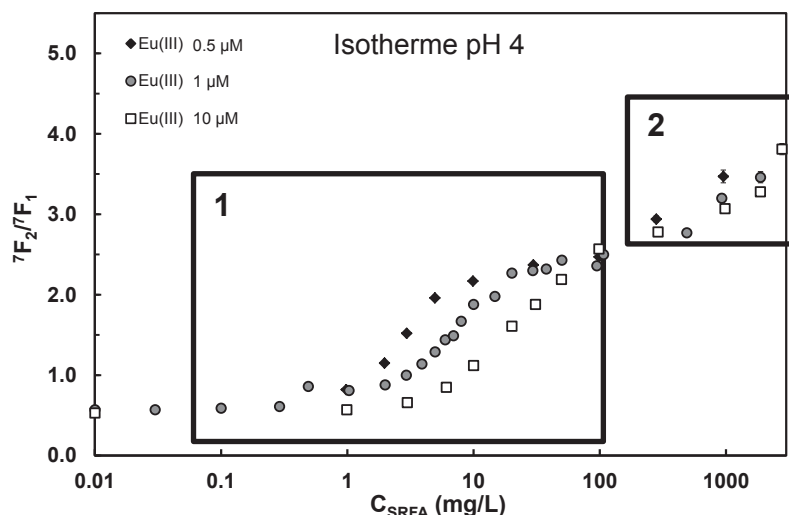


Fig. 1: Evolution of ${}^5\text{D}_0 \rightarrow {}^7\text{F}_2 / {}^5\text{D}_0 \rightarrow {}^7\text{F}_1$ ratio depending on $C(\text{SRFA})$ at $I = 0.1 \text{ M}$, pH 4.

[1] Brevet *et al.* (2009) Spectrochim. Acta A 74, 446–453.

[2] Kinniburgh *et al.* (1999) Colloids Surf A 151, 147–166.

[3] Szabó *et al.* (2010) Radiochim. Acta 98, 13–18.

[4] Saito *et al.* (2005) Colloids Surf. A 265, 104–113.

[5] Saito *et al.* (2009) Colloids Surf. A 347, 27–32.

New Insight into the photochemical reaction mechanism of uranyl citrate by combining NMR experiment and DFT calculation

S. Tsushima, J. Kretzschmar, R. Steudtner

Institute of Resource Ecology, Helmholtz-Zentrum Dresden-Rossendorf, Dresden, Germany

A sound understanding of the major reaction mechanisms is crucial to handle uranium containing waste appropriately. This means both the synthesis of unique compounds and the treatment of uranium occurring in or released into the environment. In an environmental context, uranium occurs in two main redox states: mobile U(VI) and immobile U(IV).

Due to both its model character in U(VI) complexation by chelating polycarboxylates and the citrate being a ubiquitous occurring ligand, particularly being important in the citric acid cycle *in vivo*, the uranyl citrate system itself [1–4] and also its photoreaction [5,6] is already repeatedly investigated, but still not fully understood.

This investigation provides not only further insight into the U(VI)-citrate complexation, but also a better understanding of the (photo-)redox chemistry of uranium in general.

Here we want to present the reaction pathway of the U(VI) citrate complex photooxidation to its degradation products ketoglutaric acid, acetoacetic acid and acetone with concomitant CO₂ formation by several decarboxylation steps and the formation of U(IV). The oxidation state of the latter is indicated by NMR showing ¹H chemical shifts > 50 ppm and proven by UV-vis. Moreover, the yielded U(IV) appears as soluble complexes of citrate and its degradation products. The identity of the formed compounds was experimentally proven by one- and two-dimensional NMR methods and confirmed by DFT calculations.

The photoreaction starts by irradiating the sample with light from a simple light source such as the sun or a commercial mercury lamp. Interestingly, the initial chemical alteration starts by a single electron transfer from a citrate molecule, being hydrogen bonded to the fifth remaining coordination site not occupied by U(VI)-coordinating citrate. Most likely the intermediate, *i.e.* not observable U(V), disproportionates fast to U(VI) and the aforementioned U(IV).

[1] R. Bramley, W. F. Reynolds, I. Feldman (1965) *J. Am. Chem. Soc.* 87, 3329–3332.

[2] E. Ohyoshi, J. Oda, A. Ohyoshi (1975) *Bull. Chem. Soc. Jap.* 48, 227–229.

[3] S. P. Pasilis and J. E. Pemberton (2003) *Inorg. Chem.* 42, 6793–6800.

[4] A. Günther, R. Steudtner, K. Schmeide, G. Bernhard (2011) *Radiochim. Acta* 99, 535–541.

[5] H. D. Burrows and T. J. Kemp (1974) *Chem. Soc. Rev.* 3, 139–165.

[6] A. J. Francis and C. J. Dodge (2008) DAE-BRNS Biennial Symposium on Emerging Trends in Separation Science and Technology (SESTEC)(BNL-80322-2008-CP).

Quantum chemical modeling of actinide borate complexes in aqueous solution

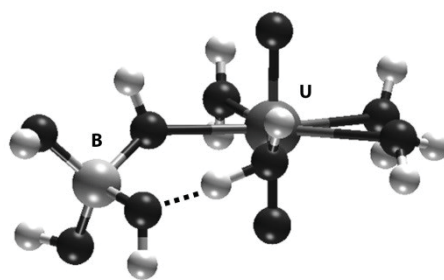
S. Krüger

Theoretische Chemie, Department Chemie, Technische Universität München, Garching, Germany

Borate as a component of geological salt formations and of borosilicate glass, used in the vitrification of highly radioactive waste, only recently was considered in the environmental chemistry of actinides as a possible ligand in complexes and solids. While solid actinide borates are known, thus far no complexes have been unequivocally determined.

We carried out scalar relativistic density functional calculations with the parallel code ParaGauss [1,2] to explore structures and thermodynamic properties of monoborate complexes of actinides in aqueous solution. The complexes modelled explicitly include the first solvation shell of the highly charged actinide ions. Long-range solvation effects were accounted for by embedding these model complexes in a polarizable continuum.

Referring to low concentrations of borate in solution, boric acid and the Lewis borate anion $B(OH)_4^-$ are considered as most relevant species to interact with solvated actinide ions. We explored complexes with uranyl(VI) and americium(III). Gibbs free energies show that boric acid does not form complexes with boric acid. On the other hand, stable complexes of borate with U(VI) and Am(III) are obtained with borate coordinating in mono- or bidentate fashion. For Am(III) we confirmed the complexing ability of borate by comparison with acetate and perchlorate. As the Brønsted anion of boric acid, $B(OH)_2O^-$, is energetically close to the Lewis anion in aqueous solution, it also has been considered as a ligand. Monodentate complexes of comparable stability as for the Lewis anion have been calculated for uranyl(VI). In addition to these binary complexes, also ternary hydroxoborate species have been computationally characterized. Our results suggest that actinide borate complexes may be present in pertinent solutions. Their concentration may be low due to more stable solid phases, hampering an experimental identification.



Uranyl(VI) borate complex $UO_2B(OH)_4(H_2O)_4^-$.

-
- [1] T. Belling, T. Grauschopf, S. Krüger, M. Mayer, F. Nörtemann, M. Staufer, C. Zenger, N. Rösch (1999) Quantum chemistry on parallel computers: Concepts and results of a density functional method, in: High performance scientific and engineering computing; H.-J. Bungartz, F. Durst, Chr. Zenger (Eds.), *Lecture Notes in Computational Science and Engineering*, Vol. 8, p. 439, Springer, Heidelberg.
- [2] T. Belling, T. Grauschopf, S. Krüger, F. Nörtemann, M. Staufer, M. Mayer, V. A. Nasluzov, U. Birkenheuer, A. Hu, A. V. Matveev, A. M. Shor, M. S. K. Fuchs-Rohr, K. M. Neyman, D. I. Ganyushin, T. Kerdcharoen, A. Woiterski, A. B. Gordienko, S. Majumder, M. Huix i Rotllant, R. Ramakrishnan, G. Dixit, A. Nikodem, T. M. Soini, M. Roderus, N. Rösch (2012) PARAGAUSS 3.1, Technische Universität München, München.

Probing the electronic structures of uranyl halides using anion photoelectron spectroscopy

H.-T. Liu,^{1,2} P. D. Dau,² J. Su,^{3,4} J. Li,⁴ L.-S. Wang²

¹ Division of Radiochemistry Engineering and Technology, Shanghai Institute of Applied Physics, Chinese Academy of Sciences, Shanghai, China

² Department of Chemistry, Brown University, Providence, U.S.A.

³ Division of Nuclear Materials Science and Engineering, Shanghai Institute of Applied Physics, Chinese Academy of Sciences, Shanghai, China

⁴ Department of Chemistry, Tsinghua University, Beijing, China

The uranyl dication (UO_2^{2+}) is the most stable form of uranium in nature and is usually coordinated by ligands or solvent molecules. Investigations of uranyl complexes and their stabilities are important in understanding the chemical transformation and migration of nuclear waste, as well as the coordination

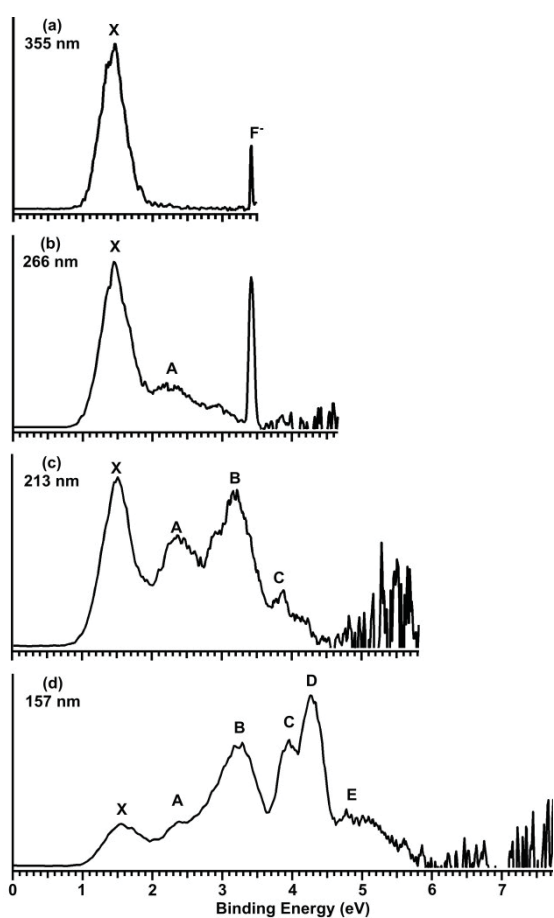


Fig. 1: Photoelectron spectra of $\text{UO}_2\text{F}_4^{2-}$ at (a) 355 nm (3.496 eV), (b) 266 nm (4.661 eV), (c) 213 nm (5.821 eV), and (d) 157 nm.

chemistry in recycling spent nuclear fuel. Uranyl halides in the form of $\text{UO}_2\text{X}_m^{(m-2)-}$ commonly exist in aqueous solution. However, the solvation effect and exact coordination number (including solvents) of uranyl varied depending on the given environment. By using electron spray ionization (ESI) and anion photoelectron spectroscopy, variety of uranyl-halide complexes including solvent molecule were able to be probed in the gas phase. It was the first time that the multiply charged uranyl halide anions such as $\text{UO}_2\text{F}_4^{2-}$ and $\text{UO}_2\text{Cl}_4^{2-}$ were observed in the gas phase and probed by anion photoelectron spectroscopy together with theoretical calculations [1,2]. A brief description of experimental method will be presented, and especially the recent development of cold ion trap will be addressed. Besides the dianions, we report a series of mono-charged anions, UO_2X_3^- ($\text{X} = \text{F}, \text{Cl}, \text{Br}, \text{and I}$), which were steadily formed in the gas phase at certain ESI condition [3]. Interestingly, no isolated uranyl halides with fewer than four equatorial ligands have been observed in the condensed phases. Uranyl species tend to retain low equatorial coordination numbers in the gas phase, due to increased Coulomb repulsion between the ligands. We have observed stable $\text{UO}_2\text{F}_4^{2-}$ and $\text{UO}_2\text{Cl}_4^{2-}$ dianions and their solvation complexes with water and acetonitrile molecules [1,2], but we did not observe $\text{UO}_2\text{Br}_4^{2-}$ and $\text{UO}_2\text{I}_4^{2-}$ in these experiments. The thermodynamic and kinetic stabilities of the $\text{UO}_2\text{X}_4^{2-}$ ($\text{X} = \text{F}, \text{Cl}, \text{Br}$ and I) dianions are also explored in relation to the UO_2X_3^- monoanions.

[1] P. D. Dau, J. Su, H. T. Liu, J. B. Liu, D. L. Huang, J. Li and L. S. Wang, (2012) Chem. Sci. 3, 1137–1146.

[2] P. D. Dau, J. Su, H. T. Liu, D. L. Huang, J. Li and L. S. Wang, (2012) J. Chem. Phys. 137, 064315.

[3] J. Su, P. D. Dau, Y. H. Qiu, H. T. Liu, C. F. Xu, D. L. Huang, J. Li and L. S. Wang, (2013) Inorg. Chem. 52, 6617–6626.

Kinetic study of the oxidation of neptunium by hypobromite

A. Martínez-Torrents,¹ J. F. Lucchini,² D. T. Reed,² J. de Pablo,^{1,3} I. Casas³

¹ Environmental Technology Area, CTM-Centre Tecnològic, Manresa, Spain

² Los Alamos National Laboratory, Repository Science & Operations, Carlsbad, NM, U.S.A.

³ Chemical Engineering Dept. Universitat Politècnica de Catalunya (UPC), Barcelona, Spain

Transuranium elements are a major concern in the safety assessment of a deep geologic repository [1]. The study of the redox processes affecting these elements is very important in order to know the solubility and thus the mobility of them. In a salt repository the brines could contain NaCl and NaBr. Due to alpha radiolysis, hypobromite could be formed through a series of chained reactions [2]. The oxidation of Np by BrO⁻ is not well known. Due to that, in this work the kinetics of the oxidation of Np by BrO⁻ is studied.

Np solutions were prepared and purified evaporating and redissolving in HCl 0.1 mol·dm⁻³. BrO⁻ solutions were prepared from ClO⁻ and NaBr solutions. The kinetics of the oxidation of Np were followed using a UV-VIS-NIR spectrophotometer (Varian CARY 5000).

Measurements were made at different ionic strengths and different initial concentrations of Np(IV) and BrO⁻ (Tab. 1). The pH of the different solutions corrected for the ionic strength was 1.3 ± 0.1. For each spectrum taken, the maximum peak values were used to calculate the Np concentration (Fig. 1). Np(IV) has a peak at 960 nm and Np(V) has a peak at 980 nm. Their extinction coefficients are known [3]. The concentration of Np(IV) and Np(V) was represented against time obtaining two different straight lines. From the slope of these lines the oxidation rates were obtained. It was observed that the oxidation rate of Np(IV) is proportional to the initial concentration of Np(IV) and the initial concentration of BrO⁻.

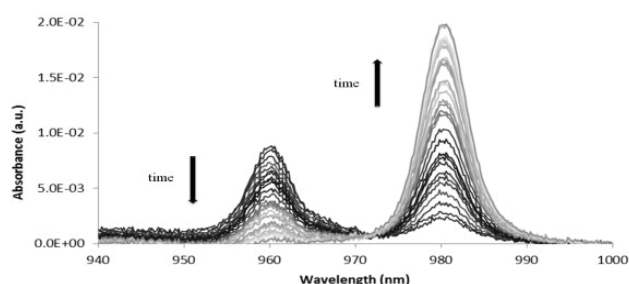


Fig. 1: Spectra of Np(IV) at 960 nm and Np(V) at 980 nm at different times.

$$\frac{dNp(IV)}{dt} = k'[Np(IV)][BrO] \quad [\text{eq. 1}]$$

The concentration of hypobromite in excess can be considered as constant and therefore a new constant $k = k'[BrO]$ was considered. The ionic strength affects the oxidation rate. At high ionic strengths the oxidation is slower than for low ionic strengths.

Tab. 1: Experiments carried out at different initial concentrations of Np(IV) and BrO⁻ and different ionic strength.

[Np(IV)] (mol dm ⁻³)	[BrO ⁻] ₀ (mol dm ⁻³)	I.S.	Rate (mol dm ⁻³ s ⁻¹)	k' (s ⁻¹)	K (dm ³ mol ⁻¹ s ⁻¹)
(5.2 ± 0.0) × 10 ⁻⁵	(1.0 ± 0.0) × 10 ⁻³	5	(1.0 ± 0.1) × 10 ⁻¹⁰	(2.0 ± 0.3) × 10 ⁻⁶	(2.0 ± 0.3) × 10 ⁻³
(1.0 ± 0.0) × 10 ⁻⁴	(1.0 ± 0.0) × 10 ⁻³	5	(2.1 ± 0.3) × 10 ⁻¹⁰	(2.0 ± 0.3) × 10 ⁻⁶	(2.0 ± 0.3) × 10 ⁻³
(4.0 ± 2.0) × 10 ⁻⁵	(1.1 ± 0.0) × 10 ⁻³	0.1	(5.3 ± 0.2) × 10 ⁻⁹	(1.3 ± 0.7) × 10 ⁻⁴	(1.2 ± 0.6) × 10 ⁻¹
(6.2 ± 0.4) × 10 ⁻⁶	(1.1 ± 0.0) × 10 ⁻³	0.1	(4.7 ± 1.3) × 10 ⁻¹⁰	(7.5 ± 2.1) × 10 ⁻⁵	(7.1 ± 2.0) × 10 ⁻²
(4.5 ± 0.1) × 10 ⁻⁵	(1.0 ± 0.0) × 10 ⁻³	1	(1.3 ± 0.1) × 10 ⁻⁹	(2.8 ± 0.3) × 10 ⁻⁵	(2.8 ± 0.3) × 10 ⁻²

The authors would like to acknowledge all the staff of LANL-ACRSP and NMSU/CEMRC, for all the experimental support and collaboration.

[1] Borkowski, M. et al. (2009) Trans. Am. Nucl. Soc. 100, 121.

[2] Bousher, A. et al. (1986) Water Res. 20, 7, 865–870.

[3] Yoshida, Z. (2006) in: The Chemistry of the Actinide and Transactinide elements, Springer Netherlands, 699–812.

Biogeochemical processes at the interface mineral-bacteria-radionuclides: multidisciplinary approach characterization

M. L. Merroun,¹ M. López Fernandez,¹ I. Sánchez Castro,¹ A. Günther,² P. L. Solari,³ H. Moll²

¹ Department of Microbiology, University of Granada, Campus Fuentenueva, Granada, Spain

² Institute of Resource Ecology, Helmholtz-Zentrum Dresden-Rossendorf, Dresden, Germany

³ Synchrotron SOLEIL, MARS Beamline, Gif-sur-Yvette, France

Cabo de Gata's bentonites, located in the southeast of Spain, were considered as artificial barriers and host rock reference for deep geological disposal of radioactive wastes. Culture dependent and independent techniques indicated the high microbial diversity of these clay formations [1]. The aerobic and facultative anaerobic microbial strains identified in these clays were described for their ability to affect the biogeochemical cycle of structural Fe(III) in bentonite [1]. The present work describes the interaction of actinides (U, Cm) and lanthanides (Eu) with the bentonite yeast strain *Rhodotorula mucilaginosa* R8, and the bacterial strain *Stenotrophomonas maltophilia* R7 using a multidisciplinary approach combining flow cytometry, spectroscopy (EXAFS, TRLFS), imaging (STEM/HAADF, HRTEM/EDX, FESEM, etc.). In the case of uranium, XAS and TRLFS analysis indicated that the speciation of this radionuclide depends on the microbial strain. In contrast, the cells of yeast R8 coordinated uranium through organic phosphate groups with a structure similar to that of meta-autunite. A uranium phosphate mineral phase is precipitated by the cells of *Stenotrophomonas maltophilia* R7. STEM/HAADF analysis indicated, in both cases, cell wall and intracellular U accumulates. Moreover, and in order to simulate natural conditions of the radioactive waste repositories, ternary systems including bentonite, microbe and uranium were constructed and preliminary results will be presented. These studies revealed the efficiency of microbes to interact with uranium in the presence of bentonite. The interaction between Cm(III) and the two microbial strains was studied at trace Cm(III) concentrations (0.3 μM) using TRLFS. Two Cm³⁺-*S. maltophilia* R7 species were identified having emission maxima at 599.7 (hydrogen phosphoryl bond Cm) and 602.7 nm (carboxyl bond Cm). In the case of yeast strain R8, two Cm³⁺ species were identified having emission maxima at 600.1 and 603.2 nm. A preliminary data fitting showed that the first species could be described by a coordination of Cm(III) onto carboxyl sites, whereas the second species could be interpreted by a mixed species containing phosphoryl and amine moieties.

[1] Lopez-Fernandez, M., et al. (2014) Appl. Geochem. (in press).

Uniform micro-particles as reference material for mass spectrometry

R. Middendorp,¹ A. Knott,¹ M. Dürr¹

¹ Forschungszentrum Jülich GmbH, IEK-6, Jülich, Germany

For the determination of isotope ratios, mass spectrometry represents the predominant measurement method capable of reaching a high sensitivity at the same time providing results with high accuracy and precision. The application of analytical procedures involves calibration and tests to assure high quality measurements. To this end, test objects with known properties are used as a standard, e.g. reference materials provided by national institutions or commercial providers. Some reference materials are customized for specific analytical procedures, e.g. with properties matched to typical measurement samples.

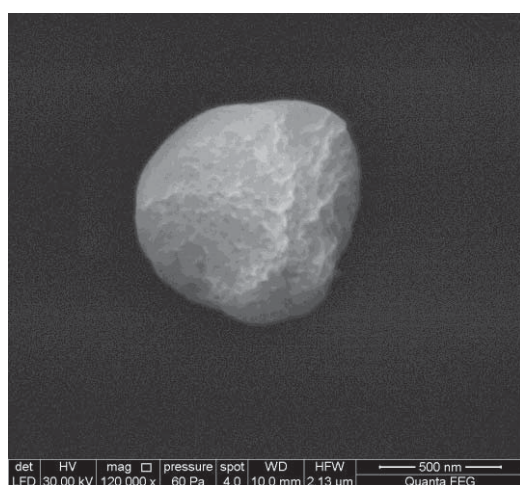


Fig. 1: Scanning electron microscope image of a synthetic uranium particle.

Isotopic ratio determination of micrometer-sized particles is a tool used for nuclear safeguards by the International Atomic Energy Agency (IAEA) in order to verify the non-proliferation obligations of states signatory to the Non-Proliferation Treaty. For example, uranium particles are recovered from swipe samples and analyzed for the isotopic ratios of uranium isotopes in each individual particle [1]. Hereby signatures from processing of nuclear materials are revealed which provides a tool to detect possible clandestine activities. At the Forschungszentrum Jülich uniform (monodisperse) micro-particles consisting of uranium oxide are synthetically produced using a vibrating orifice aerosol generator (VOAG). The VOAG creates a stream of droplets identical in size from a liquid feed consisting of a dilute uranyl-nitrate solution that has been prepared from a material with certified uranium isotope ratios [2]. The droplets are dried and calcinated yielding solid micro-particles with a specific uranium elemental content per particle in the range of a few picograms and uranium isotope ratios as present in the liquid feed.

The goal is to provide reference material for micro-analytical techniques, mainly for particle analysis with Large-Geometry Secondary Ion Mass Spectrometry and the so-called Fission Track Thermal Ionization Mass Spectrometry. These mass spectrometric techniques represent the state-of-the-art in the particle analysis for IAEA safeguards purposes.

First uranium particles of approximately one micrometer diameter have been produced at Forschungszentrum Jülich (Fig. 1) and are currently being analyzed with respect to size, morphology and homogeneity of these properties across the produced batch of particles. The production process based on an aerosol with uniform droplets should yield particles with specific elemental content and isotope ratio for each individual particle, which can be verified for a subsample of particles using isotope dilution mass spectrometry [3]. Further future work will study methods to produced micro-particles into a solid matrix for simplified handling, storage, transport and measurement. The production principle has the potential to provide particles that are suitable as certified reference material for micro-analytical methods on actinides in general.

[1] Kraiem, M. et al. (2011) *Anal. Chem.*, 3011–3016.

[2] Ranebo, Y. et al. (2010) *Anal. Chem.*, 4055–4062.

[3] Kraiem, M. et al. (2012) *Anal. Chimica Acta*, 37–44.

In situ spectroscopic characterization of Np(V) sorption complexes at manganese and iron oxide surfaces

K. Müller,¹ A. Rossberg,¹ B. Simon,^{1,2} J. Berger^{1,3}

¹ Institute of Resource Ecology, Helmholtz-Zentrum Dresden-Rossendorf, Dresden, Germany

² Chimie ParisTech, Paris, France

³ Dresden University of Applied Sciences, Dresden, Germany

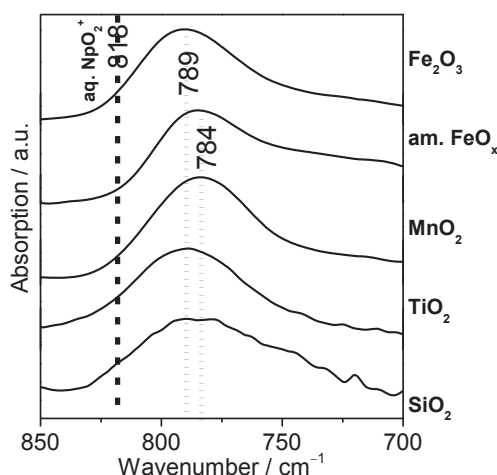


Fig. 1: ATR FT-IR spectra of the sorption complexes formed onto several mineral oxides (50 μ M Np(V), 0.1 M NaCl, pH 7, 60 min sorption, 0.1 mg mineral oxide/cm², N₂).

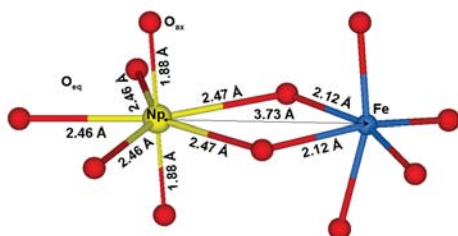


Fig. 2: Hypothetical edge-sharing Np(V)-hematite surface complex used for EXAFS structural determination. FeO₆ octahedron taken from [4].

conditions in an aqueous solution shows the absorption of $\nu_3(\text{Np}^{\text{V}}\text{O}_2)$ at 818 cm⁻¹ [3]. The red shift of ν_3 to 789 cm⁻¹ upon sorption can be assigned to an inner-sphere sorption complex. Kinetic experiments have shown that only one sorption complex was formed independent from Np(V) loading. Furthermore, no impact of ionic strength (1–10⁻⁴ M NaCl) and pH (≤ 10) on the sorbed species was found. By EXAFS structural analysis of batch samples the surface complex was further characterized being a binary edge-sharing Np(V) sorption species (Fig. 2). From a comparison of Np(V) surface complexation on different mineral oxides of iron, manganese, silicon, and titanium a very similar sorption behavior was elucidated.

Neptunium (Np) is one of the most important components of nuclear waste to consider for the long-term safety assessment of nuclear waste repositories, due to the increasing enrichment, the long half-life and the high toxicity of Np-237. Hence, great attention is attracted to its geochemistry [1]. Components of geological materials, such as manganese and iron oxides and hydroxides play an important role in regulating the mobility of actinides in aquifers, due to their widespread environmental presence, high sorption capacity and tendency to form coatings on mineral surfaces. In recent years, the sorption behavior of Np(V), the most relevant oxidation state under ambient conditions, onto iron oxides was mainly studied by macroscopic experiments [2]. Manganese oxides were rarely investigated. For a better understanding of the molecular events occurring at the mineral's surfaces, ATR FT-IR spectroscopy is a useful tool for the in situ identification of surface species [3]. In addition, time-resolved measurements provide kinetic information on the surface reactions. Complementary information on molecular structure and atomic environment can be elucidated from EXAFS spectroscopy.

In this work, Np(V) sorption on the oxyhydroxides of Fe and Mn is investigated comprehensively by combining in-situ ATR FT-IR and EXAFS spectroscopy under a variety of environmentally relevant sorption conditions. As an example, upon sorption of micromolar Np(V) on Fe₂O₃, a band observed at 789 cm⁻¹ is assigned to the antisymmetric stretching vibrational mode (ν_3) of the neptunyl ion (Fig. 1). The IR spectrum obtained at equal

Financial support from DFG (MU 3207/1-1) is highly appreciated.

[1] Kaszuba, J.P. et al. (1999) Environ. Sci. Technol. 33, 4427–4433.

[2] Li, D. et al. (2012) J. Hazard. Mater. 243, 1–18.

[3] Müller, K. et al. (2009) Environ. Sci. Technol. 43, 7665–7670.

[4] Blake, R. L. et al. (1966) Am. Mineral. 51, 123–129.

New reactivity of the uranyl ion: Ring opening catalysis of oxygen and sulfur containing monomers

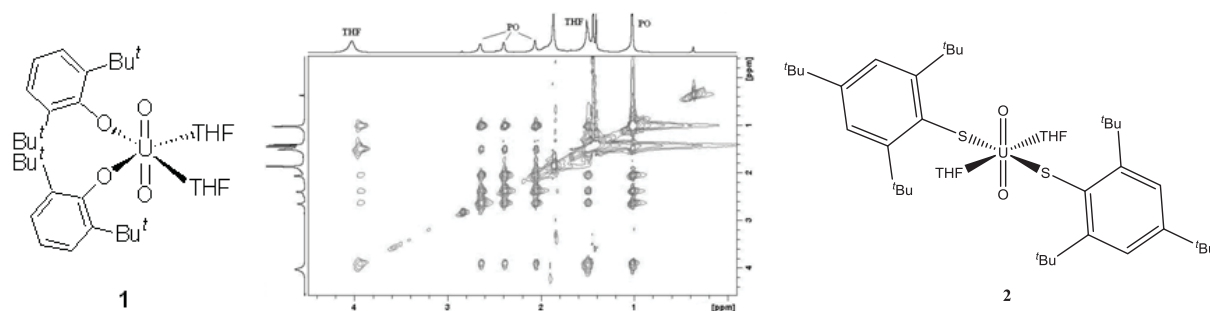
S. Nuzzo, A. Walshe, R. J. Baker

School of Chemistry, Trinity College, Dublin, Ireland

Recent research has shown that thorium and uranium compounds in their +4 oxidation state are active catalysts for a number of C–C bond forming reactions [1]. However, as the high oxophilicity of the actinide ion would predict that low activities would be observed for oxygen containing substrates, these have not been explored to a great extent. The ring opening polymerization of ϵ -caprolactone and *rac*-lactide by $[\text{Cp}^*_2\text{MMe}_2]$ (M = Th, U) suggest that this may not be the case [2,3]. The reactivity can be traced to the energy released in the ring opening as when a U–O bond in the initiating species is exchanged for a U–O bond during propagation then the change in ΔH is small.

Herein, we report on the use of uranyl aryloxyde **1** in the ring opening polymerization of epoxides, lactides and caprolactones [4,5]. This is the first example of a high oxidation state actinide complex that acts as a catalyst for this reaction. A comprehensive NMR spectroscopic study has allowed for the mechanism to be determined and theoretical calculations have also been performed and will be discussed.

In order to extend this unusual reactivity we have expanded the scope to the softer sulfur containing epoxides which have not been explored for any actinide complex in any oxidation state. Accordingly, we have prepared and fully characterized **2**, which does ring open polymerize propylene sulfide.



[1] A.R. Fox, S.C. Bart, K. Meyer, C.C. Cummins (2008) *Nature* 455, 341.

[2] E. Rabinovich, S. Aharonovich, M. Botoshansky, M.S. Eisen, (2010) *Dalton Trans.* 39, 6667.

[3] E. Barnea, D. Moradove, J.-C. Berthet, M. Ephritikhine, M.S. Eisen, (2006) *Organometallics* 25, 320.

[4] R.J. Baker, A. Walshe, *Chem. Commun.* 2012, 48, 985; J. Fang, A. Walshe, L. Maron and R.J. Baker (2012) *Inorg. Chem.* 51, 9132.

[5] A. Walshe, J. Fang, L. Maron and R.J. Baker (2013) *Inorg. Chem.* 52, 9077.

Europium(III)-calcite study with site-selective TRLFS

S. Peschel, M. Schmidt, T. Stumpf

Institute of Resource Ecology, Helmholtz-Zentrum Dresden-Rossendorf, Dresden, Germany

Calcite is an important mineral that plays a significant role in nuclear waste disposal concerning the safety and performance in geological formations. At these sites it can be found in the near field as a secondary phase (weathering of the geochemical barrier) and as a rock-forming mineral in the surrounding rocks. Geochemically, calcite has the potential to adsorb as well as incorporate guest ions with a similar ionic radius, such as europium and curium, for calcium in the host lattice. Because of the long half-lives of actinides like curium and americium, they and their lanthanide homologues (i.e., europium) are the subject of recent research.

Calcite samples were doped with Eu^{3+} in batch experiments. Calcium carbonate powder was contacted with a Eu(III) solution (5×10^{-7} M) in a calcium carbonate saturated solution with a NaCl (10 mM) background electrolyte solution. Batch samples were analyzed at varying contact times to understand the step-by-step kinetic and mechanistic behavior of incorporation of Eu(III) into the solid phase. After the contact period, the supernatant was investigated with ICP-MS. The Eu^{3+} concentration in solution varies from 0.1 to 3.2% of the initial concentration, which indicates that almost all Eu^{3+} is adsorbed.

The calcite powder was examined with site-selective TRLFS at temperatures below 20 K. The direct excitation of the ${}^7F_0 \rightarrow {}^5D_0$ transition in the range of 576–581 nm and the integration of the respective emission spectra yields a characteristic excitation spectrum. These excitation spectra show only one broad peak with a maximum at ~ 579.2 nm (Fig. 1), independent of the sorption time (up to 31 days). This behavior is dissimilar to that determined by Stumpf and Fanghänel [1] who investigated Cm^{3+} sorption on calcite with NaClO_4 as background electrolyte and found 2 peaks, which change over time. Lifetime measurements of our samples exhibit biexponential decay indicative of two species. The first specie has a lifetime of 460 to 985 μs (see Tab. 1) and the second 2155 to 4577 μs . Using Horrock's equation [2] the number of coordinating water molecules in the first sphere surrounding the Eu(III) can be determined. This value corresponds to its location (surface sorbed vs incorporated) on or within the calcite lattice. Therefore, calculated values of 0.5 to 1.7 indicate the formation of an inner sphere sorption species whereas a value of 0 is indicative of incorporation of the Eu^{3+} within the calcite. The emission spectrum shows a threefold splitting of the 7F_1 band (see Fig. 2). This indicates a ligand field with low symmetry. To better understand these surface species, future measurements with CTR and RAXR will be performed.

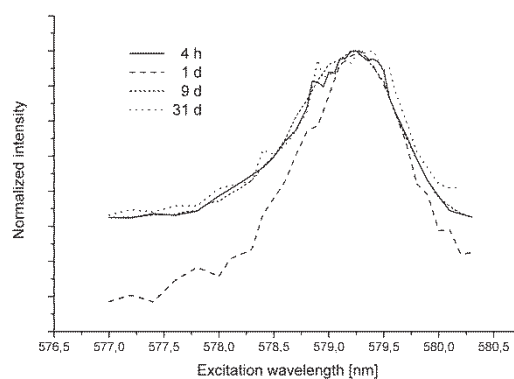


Fig. 1: TRLFS excitation spectra of Eu(III) doped calcite sample with various contact time.

Tab. 1: Fluorescence lifetimes and number of water molecules with different sorption times.

Contact time	Fluorescence lifetime (μs)	$n(\text{H}_2\text{O})$
4 h	460	1,7
	2233	0
1 d	985	0,5
	4577	0
31 d	514	1,5
	2155	0

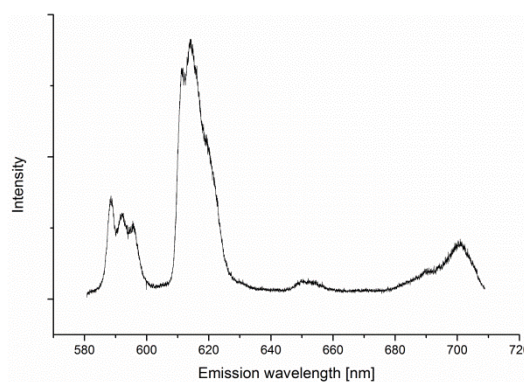


Fig. 2: Site selective TRLFS emission of Eu(III) doped calcite sample with 9 d contact time.

[1] Stumpf, T. and T. Fanghänel (2002). J. Colloid Interf. Sci. 249, 119–122.

[2] Horrocks (1979) J. Am. Chem. Soc. 101, 334.

A quantum chemical study on Tc(IV) hydrolysis species and ternary Ca-Tc^{IV}-OH complexes in alkaline CaCl₂ solutions

R. Polly, B. Schimmelpfennig, E. Yalcintas, X. Gaona, M. Altmaier

Institute for Nuclear Waste Disposal, Karlsruhe Institute of Technology, Eggenstein-Leopoldshafen, Germany

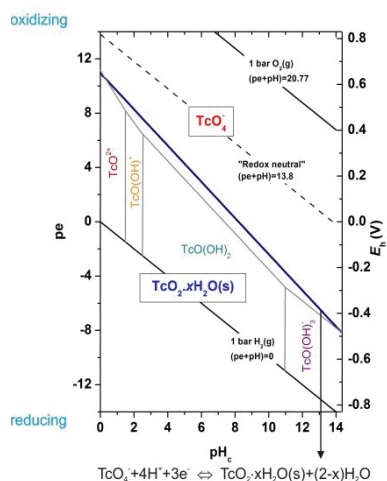


Fig. 1: Pourbaix diagram of Tc.

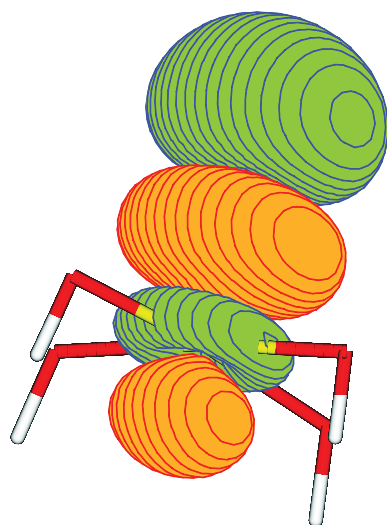


Fig. 3: Bonding σ orbital in $[\text{TcO}(\text{OH})_4]^{2-}$.

Our calculations using advanced quantum chemical tools show for the first time that the ground states of the species, $[\text{TcO}]^{2+}$, $[\text{TcO}(\text{OH})_y]^{2-y}$ and $\text{Ca}_x[\text{TcO}(\text{OH})_y]^{2+2x-y}$ are single reference states and therefore the application of large-scale DFT calculations is permitted in this case. This will enable us to further apply large DFT calculations and determine the structure of relevant Tc(IV) species in alkaline solutions involving a large number of water molecules and solvated ions in more detail.

Tc-99 is a redox-sensitive β -emitting fission product with very long half-life ($t_{1/2} \sim 211.000$ a). Tetravalent Tc(IV) exists under very reducing conditions like expected for operative deep geological nuclear waste repositories. Tc(IV) hydrolyzes very strongly. The anionic species $\text{TcO}(\text{OH})_3^-$ is known to dominate the aqueous chemistry of Tc(IV) at high pH conditions. In concentrated alkaline CaCl_2 solutions, comprehensive solubility studies performed by E. Yalcintas of KIT-INE recently established the hitherto unknown formation of higher hydrolysis species of the type $\text{Ca}_x[\text{TcO}(\text{OH})_y]^{2+2x-y}$.

Quantum chemical calculations are well suited to analyze Tc(IV) solvation processes in aqueous solution. However, so far there are no ab initio calculations on $[\text{TcO}]^{2+}$ or Tc(IV) hydrolysis species, but only on TcO [1] and Density functional theory (DFT) calculations on $[\text{TcO}]^{2+}$ [2]. In the present work we performed pilot studies on these species with high level Complete Active Space Self Consistent Field (CASSCF) and Multi Reference Configuration Interaction (MRCI) calculations to determine the character of the ground states of these species. The calculations were carried out with MOLPRO and TURBOMOLE.

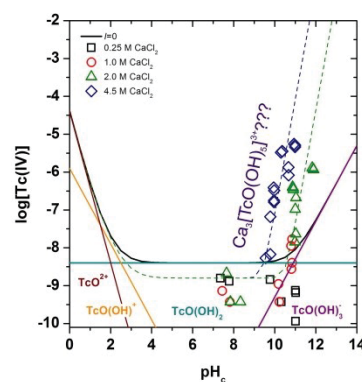


Fig. 2: Solubility curve of Tc(IV) in CaCl_2 .

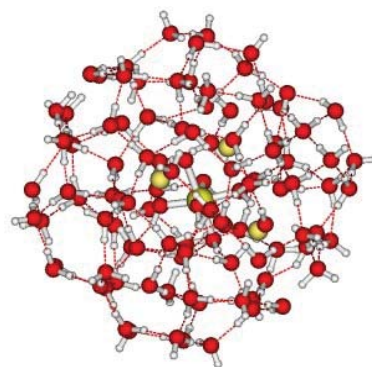


Fig. 4: $\text{Ca}_3[\text{TcO}(\text{OH})_5]^{3+}$ complex embedded in 100 water molecules.

- [1] S. R. Langhoff, C. W. Bauschlicher Jr., L. G.M. Pettersson (1989) Chemical Physics 132, 49.
 [2] E. Breynaert, C. E. A. Kirschhock, A. Maes (2009) Dalton Trans. 43, 9398.

Influence of aromatics and substituents on the time-resolved luminescence spectroscopy of Eu(III)-complexes

P. E. Reiller

CEA/DEN/DANS/DPC/SEARS/LANIE, Gif-sur-Yvette, France

Simple organic carboxylic ligands have since long been proposed as analogues of the metallic cations complexation processes of complex organic mixtures, *e. g.* natural organic matter (NOM). There are quite substantial amounts of spectroscopic evidence that are showing that this approximation is not totally verified experimentally. The main evidence is the widespread occurrence of the luminescence bi-exponential decay of the NOM-complexed lanthanides (Ln) and actinides (An) at their +III redox state [1–3].

Even if numerous complexation constants of Ln(III)- and An(III)-carboxylate complexes were determined spectroscopically in time-resolved luminescence spectroscopy [4], a global view on the influence of the different types of organic acids is still lacking, especially for aromatic acids. Some data are available [5–7], but no clear evolution of both the luminescence spectra and decay times have been proposed.

I here propose to compare the luminescence compartment of Eu(III) complexed by a series of organic carboxylic acids, namely acetic, benzoic, phthalic, *para*-hydroxybenzoic, and 3,4-dihydroxybenzoic acid. The luminescence spectrum will be compared as well as their relative luminescence decay (Fig. 1). The influence of the different substituents will be evidenced.

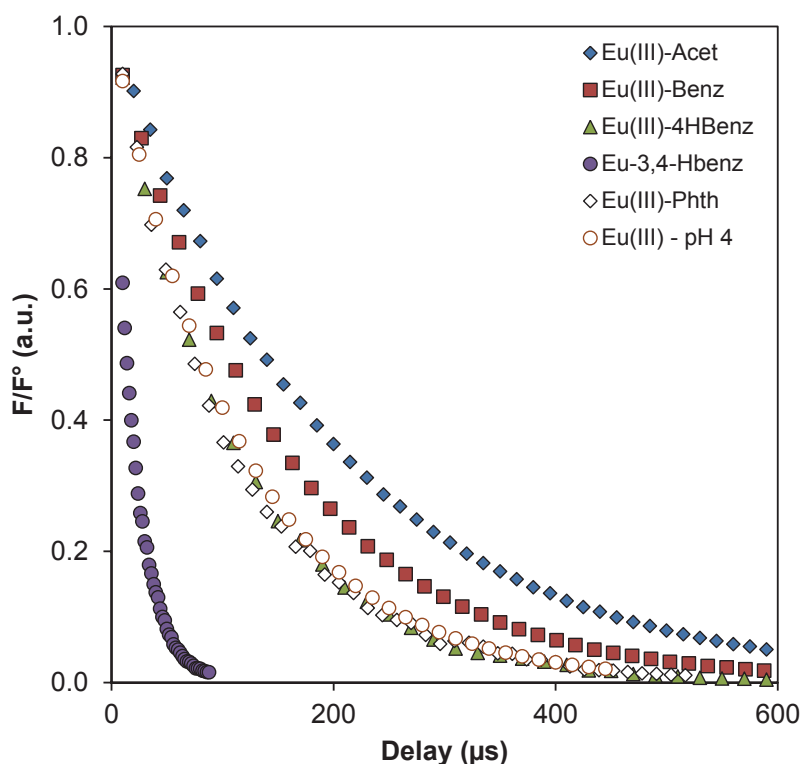


Fig. 1: Evolution of the relative luminescence decays for carboxylic acids bearing different substituents.

- [1] Brevet *et al.* (2009) *Spectrochim. Acta A* 74, 446–453.
- [2] Janot *et al.* (2013) *Geochim. Cosmochim. Acta* 123, 35–54.
- [3] Freyer *et al.* (2009) *Radiochim. Acta* 97, 547–558.
- [4] Wang *et al.* (1999) *Inorg. Chim. Acta* 293, 167–177.
- [5] Plancque *et al.* (2005) *Appl. Spectrosc.* 59, 432–441.
- [6] Kuke *et al.* (2010) *Spectrochim. Acta A* 75, 1333–1340.
- [7] Barkleit *et al.* (2013) *Inorg. Chim. Acta* 394, 535–541.

New insights into actinides interactions with calmodulin

F. Brulfert,¹ C. Berthomieu,² A. Jeanson,¹ J. Roques,¹ S. Sauge-Merle,² S. Safi,¹
E. Simoni¹

¹ IPN d'Orsay, Paris Sud University, Orsay, France

² Laboratoire des interactions protéine métal (LIPM), DSV/CEA Cadarache St Paul lez Durance, France

In recent years coordination of actinides by proteins has garnered a considerable interest not only due to their inherent toxicity [1] and their metabolic impact but also to the possibility of engineering highly specific proteins for actinide sequestration [2] or chemical sensing [3]. To further develop such specific biomolecules structural and thermodynamic data has to be critically acquired since affinity was shown to be dependent on the coordinating environment. In this framework, our interest focused on the structural analysis of the U(VI) and Np(V) calmodulin (CaM) complexes and evaluating the impact of structural distortion on the protein biological functionality.

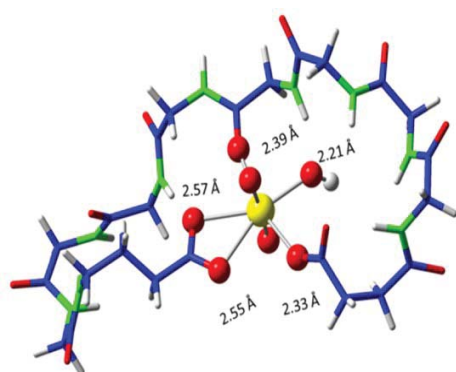


Fig. 1: Density functional theory U(VI) model with corresponding first coordination sphere distances.

CaM is an EF-Hand protein containing four specific calcium sites. This protein was selected since it was reported to bind U(VI) at the nM affinity range within the calcium binding sites [3]. Furthermore toxicological data suggested CaM to bind Np(V) in liver cells [4]. The structural similarities between both dioxo-cation structures (neptunyl and uranyl) suggest that both ions should present a similar coordination environment. In order to isolate one calcium binding site (out of four), a single site recombinant CaM was synthesized and eliminated the possibility of multisite complexes. The structural characterization was successfully achieved by combining X-ray Absorption Spectroscopy

(XAS) and Density Functional Theory (DFT). To evaluate the consequences of actinide complexation, a calorimetric method is being developed using the heat generated by CaM modulated enzymatic reaction and gave encouraging results with calcium prior to uranyl and neptunyl runs.

[1] Safi, S. et al. (2013) Chem. Eur. J. 19, 11261–11269.

[2] Zhou, L. et al. (2014) Nature Chem. 6, 236–241.

[3] Pardoux, R. et al (2012) PLoS ONE 7(8): e41922.

[4] Taylor, D. M. et al. (1987) Inorg. Chim. Acta 140, 361–363.

Sorption of Eu^{3+} on montmorillonite studied by time-resolved laser fluorescence spectroscopy and surface complexation modeling

T. Sasaki,¹ K. Ueda,¹ T. Saito,² N. Aoyagi,³ T. Kobayashi,¹ I. Takagi,¹ T. Kimura,³ Y. Tachi⁴

¹ Department of Nuclear Engineering, Kyoto University, Kyoto, Japan

² Nuclear Professional School, School of Engineering, The University of Tokyo, Tokai, Ibaraki, Japan

³ Nuclear Science and Engineering Directorate, Japan Atomic Energy Agency (JAEA), Tokai, Ibaraki, Japan

⁴ Sector of Decommissioning and Radioactive Waste Management, Japan Atomic Energy Agency (JAEA), Tokai, Ibaraki, Japan

The influence of pH, ionic strength, and the concentrations of Eu^{3+} and nitrate salts on the sorption of Eu^{3+} onto Na-montmorillonite, in the form of commercially available Kunipia F, was investigated through batch sorption measurements. The proton concentration had little effect on the distribution coefficient (K_d) values in the range of pH 4–7 at 0.1 M NaClO_4 or NaNO_3 , which indicated that the cation exchange reaction was significant. Meanwhile, the pH dependence of K_d presented apparent correlation with the formation of inner-sphere surface complexes at 1 M NaClO_4 or NaNO_3 .

The surface species of Eu^{3+} on Na-montmorillonite were also investigated using time-resolved laser fluorescence spectroscopy (TRLFS [1]) with parallel factor analysis (PARAFAC [2]). The PARAFAC modeling provided the fluorescence spectra, decay lifetimes, and relative intensity profiles of two kinds of Eu^{3+} sorption species on Na-montmorillonite, the outer-sphere (factor A) and inner-sphere (factor B) Eu^{3+} complexes. Factor B became dominant at relatively high pH and ionic strength. After comparing the spectra and lifetimes of sorbed and aqueous species, factor B was determined to be a Eu colloidal species formed at relatively high Eu^{3+} concentrations. As the K_d values in the presence of 1 M NaNO_3 were similar to those in the NaClO_4 system, the TRLFS analysis suggested NO_3^- ions have no effects on the types of Eu^{3+} surface complexes with Na-montmorillonite at least at this concentration.

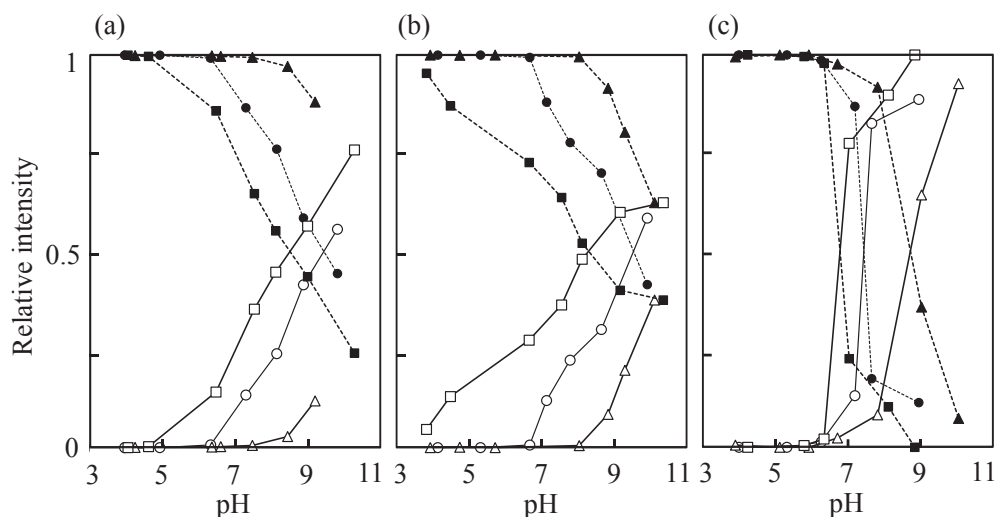


Fig. 1: Dependence of the ionic strength on the relative intensity profiles of the two factors from the PARAFAC decomposition with $M = 2$, for the Na-montmorillonite in the presence of NaClO_4 (a), and of NaNO_3 (b), and for the solution in the NaClO_4 system (c). Broken line and solid line are factor A and factor B, and triangular, circle, and square plots show $I = 0.01, 0.1$, and 1 M NaClO_4 or NaNO_3 , respectively.

A cation exchange model combined with a one-site non-electrostatic surface complexation model was applied to the measured K_d data, using the results of the TRLFS-PARAFAC analyses. In the determination of the model parameters, linear free energy relationship was used to estimate the formation constants of the surface species from those of the corresponding aqueous hydrolyzed species $\text{Eu}(\text{OH})_n$, which was then used to calculate a K_d value. This model could describe the measured K_d values with a given set of chemical conditions, and could reproduce some data previously reported in the literature.

[1] K. Ishida, et al. (2012) *J. Colloid and Interface Science* 374, 258–266.

[2] T. Saito, et al. (2010) *Environ Sci Technol.* 44, 5055–5060.

Complexation of Eu(III) with ⁿPr-BTP studied by XPS

D. Schild,¹ B. B. Beele,^{1,3} B. Schimmelfennig,¹ S. Trumm,² P. J. Panak^{1,3}

¹ Institute for Nuclear Waste Disposal, Karlsruhe Institute of Technology, Karlsruhe, Germany

² Center for Advanced Technological and Environmental Training (FTU), Karlsruhe Institute of Technology, Karlsruhe, Germany

³ Institut für Physikalische Chemie, Ruprecht-Karls-Universität Heidelberg, Heidelberg, Germany

Partitioning and transmutation is a strategy to reduce the long-term radiotoxicity of spent nuclear fuel by separating long-lived actinides from fission products. Separation of An(III) from Ln(III) is a key step in the partitioning process. BTPs extract An(III) from up to 1 M nitric acid with high selectivity; however, the reason of selectivity is still under consideration.

In this study, the complexation of Eu(III) with 2,6-bis(5,6-dipropyl-1,2,4-triazin-3-yl)pyridine (ⁿPr-BTP) in 2-propanol containing nitrate anions is studied using X-ray photoelectron spectroscopy (XPS). As a first step, C1s and N1s XP spectra of ⁿPr-BTP are recorded and compared to results of single-point Hartree-Fock (HF) calculations on DFT-optimized molecular structures. Comparison of HF energies and binding energies (BE) measured by XPS is not straightforward since intra-atomic and extra-atomic relaxation energies [1] shift the BE to lower values, i. e. the photoelectron's energy is enhanced. The XP spectra are charge referenced to aliphatic C1s at 284.8 eV (propyl chains of ⁿPr-BTP). The shape of the N1s spectrum coincides with the sum curve of Gaussian functions with intensities according to the respective number of nitrogen atoms and fixed relative distances as calculated (Fig. 1).

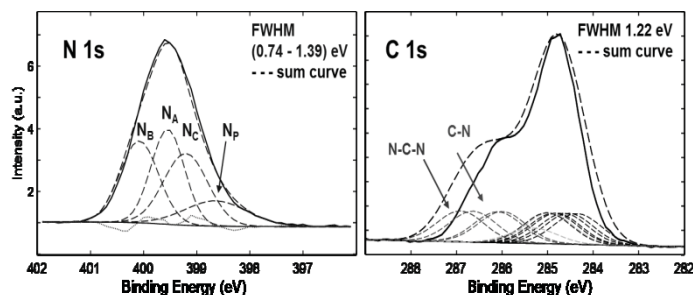


Fig. 1: Narrow scans of N 1s and C 1s spectra (solid lines) and Gaussians at fixed relative binding energies corresponding to HF orbital energies.

The N1s spectrum of the 1:3 complex Eu(III)-(ⁿPr-BTP)₃(NO₃)₃ shows NO₃ species at 406.7 eV and 405.6 eV with intensities corresponding to one and two nitrogen atoms, respectively (Fig. 2). The peaks assigned to NO₃ confirm the calculations that one nitrate to be coordinated to the metal center and two nitrate anions to be weakly coordinated to the BTP ligands. Since the metal is coordinated by 3 nitrogen atoms from each ⁿPr-BTP molecule, a 10-fold coordination of the metal results. The N1s main peak is shifted 0.2 eV to higher BE in relation to the C1s main peak (C_xH_y), like C1s (N-C-N), indicating a decrease of electron density at these atoms due to complexation. Addition of 0.05 M nitric acid intensifies solely the peak at 406.7 eV similar to the peak at 406.8 eV if nitric acid is added to ⁿPr-BTP. The remaining parts of N1s and C1s spectra are unaffected by nitric acid addition indicating no detectable modification of the complex.

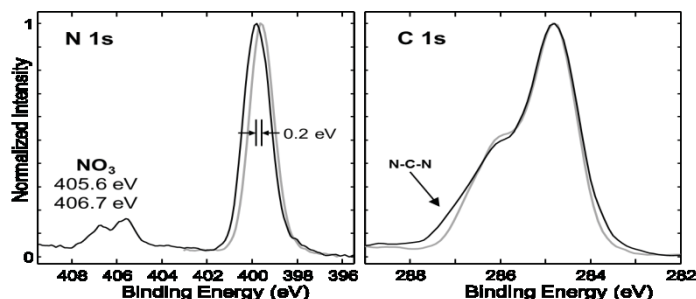


Fig. 2: Comparison of N 1s and C 1s spectra of ⁿPr-BTP (grey) and Eu(III)-(ⁿPr-BTP)₃(NO₃)₃ (black).

[1] Gelius, U. (1974) J. Electron Spectrosc. 5, 985.

Insight into the An/Ln(III)-borate-organic system – Combination of different spectroscopic techniques and theory is the key

J. Schott,¹ J. Kretzschmar,² M. Acker,¹ S. Tsushima,² B. Drobot,² S. Eidner,³
M. U. Kumke,³ A. Barkleit,² V. Brendler,² S. Taut,¹ T. Stumpf²

¹ Central Radionuclide Laboratory, Technische Universität Dresden, Dresden, Germany

² Institute of Resource Ecology, Helmholtz-Zentrum Dresden-Rossendorf, Dresden, Germany

³ University of Potsdam, Institute of Chemistry (Physical Chemistry), Potsdam-Golm, Germany

The storage of nuclear waste in deep geological formations (salt, argillaceous rock, granite) is an option handling this waste form over thousands of years. Water ingress in such a nuclear waste repository is a possible worst-case scenario in which radionuclides (RN) could be mobilized. The safety and risk assessment of a nuclear waste repository requires the understanding of physicochemical reactions of RN (complexation, sorption, diffusion, formation of solid phases, etc.) in such a case.

Borates are compounds occurring in a nuclear waste repository (minerals, glass coquilles) and, thus, interactions with RN are conceivable. In the present work the interaction of borates with Europium(III) was investigated as an analog for trivalent actinides, e.g. Am(III), Pu(III). Because of several difficulties a direct study of Eu(III)-B(OH)₄⁻ (monoborate as simplest form of a borate compound) was not possible. Thus, different approaches have to be devised to get an insight into the An/Ln(III)-borate system. In the used approaches it is hypothesized that in all investigated borate structures (inorganic as well as organic) the responsible binding site to An/Ln(III) is a B(OR)₄⁻ unit showing a similar complexation behavior with the metal ion.

The first (inorganic) approach uses the formation of polyborates [1]. The polyborate formation was studied by means of ¹¹B-NMR spectroscopy (see abstract and talk of J. Kretzschmar et al.) at pH 5 and pH 6 in the range [B]_{total} = 0.1–0.7 M. The boron species B(OH)₃, tetraborate and pentaborate were determined. The two latter species are able to complex Eu(III). The data for the complexation studies were obtained from TRLFS (time-resolved laser-induced fluorescence spectroscopy) measurements. The PARAFAC (parallel factor analysis [2]) allows the conclusion of the existence of one Eu(III)-B(OR)₄⁻ complex under the investigated conditions ([Eu]_{total} = 3 × 10⁻⁵ M; pH 6; [B]_{total} = 0.1–0.7 M). The complexation constant of the Eu(III)-B(OR)₄⁻ complex was determined with lg β = 2.0 ± 0.33 (2σ). After a while (depending on [B]_{total}) a precipitation of a Eu(III) borate solid is observed, characterized by solution and solid-state TRLFS, PARAFAC and IR spectroscopy.

The second (organic) approach uses the formation of organoborates [3]. The formation of the studied organoborates was confirmed by ¹¹B-NMR spectroscopy. Furthermore, using ¹¹B-NMR spectroscopy (see abstract and talk of J. Kretzschmar et al.) and TRLFS a complexation constant for the Eu(III)-organoborate complex was determined with lg β ~ 2.0.

DFT calculations of polyborate and organoborate structures predicted a similar complexation behavior of these borate compounds (inorganic as well as organic) concerning Eu(III) (similar geometry of the B(OR)₄⁻ unit occurring in all investigated borate compounds). This was confirmed by spectroscopic experiments. Furthermore, from DFT calculations a chelate coordination of Eu(III) by the B(OR)₄⁻ unit can be postulated.

Interpreting the strength of complexation in the Eu(III) borate system (lg β ~ 2) it can be concluded that the relevance of borates to mobilize An/Ln(III) in a nuclear waste repository should play a minor role. Rather borate species have a potential to immobilize An/Ln(III) due to precipitation.

[1] Schott, J. et al. (2014) Dalton Trans. 43, 11516-11528.

[2] Andersson, C. A. et al. (2000) Chemom. Intell. Lab. Syst. 52, 1-4.

[3] Schott, J. et al. Dalton Trans., submitted.

Characterisation of irradiated graphite: combined study by X-ray diffraction and scattering, digital autoradiography and Raman microspectroscopy

A. A. Shiryaev,¹ E. A. Dolgoplova,² A. G. Volkova,¹ A. A. Averin,¹ E. V. Zakharova¹

¹ Institute of Physical Chemistry and Electrochemistry RAS, Moscow, Russia

² Chemistry Department, Moscow State University, Moscow, Russia

Decommissioning of certain types of nuclear reactors raised an important problem of isolation of huge amounts of irradiated graphite. The principal share of total radioactivity is due to ³⁶Cl and ¹⁴C. Despite intense research numerous unsolved questions of fundamental and of applied interest persist. One of the most important questions is location (graphite lattice or amorphised pockets) and speciation of the radionuclides. We report results of investigation of graphite samples from a Russian reactor. The samples span a range of fluence/temperature conditions. The averaged structure of the samples was assessed using X-ray diffraction (XRD) and small-angle scattering (SAXS). Spatial distribution of radionuclides was investigated by autoradiography using Imaging plates; these maps were compared with data of Raman microspectroscopic mapping of graphite perfection. In this work individual Raman spectra were decomposed taking into account not only most prominent D and G peaks, but also broad underlying Gaussian peak, which is likely due to G-band of amorphous carbon. Leaching experiments were performed to investigate kinetics of radionuclides release.

The sample with the largest degree of lattice damage as seen by the X-ray methods and Raman microspectroscopy is the one which was subjected to the highest integral neutron fluence. The diffraction peaks of this sample indicate noticeable swelling and modification of the 2D peak shape and intensity, which shown that neutron irradiation increases interlayer spacing and induces numerous defects in grapheme sheets. SAXS curve of this sample shows presence of defects clusters. However, its radionuclide content is not very high.

Digital autoradiography reveals that whereas in samples from some reactors the activity is homogeneously distributed in the pellets, for other reactors highly heterogeneous spatial distribution of radionuclides with numerous hot spots separated by clean regions is observed (Fig. 1). Raman mapping shows highly non-uniform distribution of graphite lattice damage (Fig. 2), thus questioning conclusions derived from investigation of individual randomly taken spectra. Whereas for some samples reasonable correlation is observed between the radiographic images and the Raman maps, this is not a universal dependence. The simplest explanation lies in the fact that the total radionuclides concentration is low and the nuclides are not necessarily accumulated in the most damages lattice regions as probed by Raman spectroscopy.

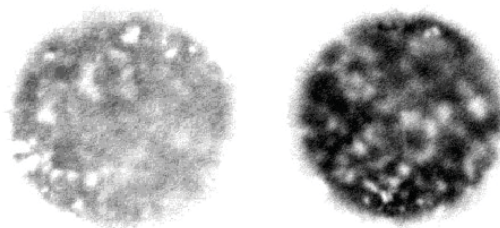


Fig. 1: Digital autoradiographs of two graphite pellets with markedly different activities. Heterogeneity of activity distribution is obvious.

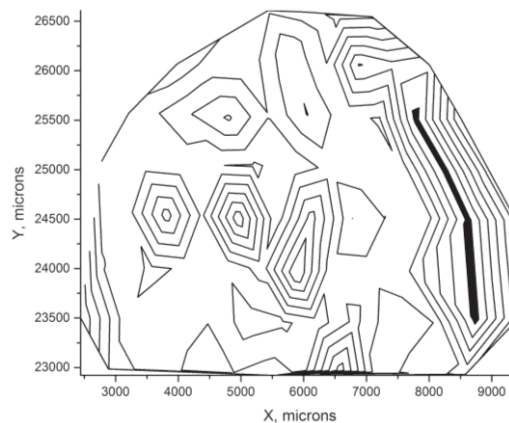


Fig. 2: A map of graphite G-peak FWHM.

Characterization of mixed Mo(VI)-Eu(III) species in strongly acidic media by a combination of Electrospray Ionization Mass Spectrometry and Time Resolved Laser Fluorescence Spectroscopy

M. Steppert,¹ M. Cheng,^{1,2} C. Walther¹

¹ Institut für Radioökologie und Strahlenschutz, Leibniz Universität Hannover, Hannover, Germany

² Institute for Nuclear Waste Disposal, Karlsruhe Institute of Technology, Eggenstein-Leopoldshafen, Germany

Molybdenum metal is one possible candidate as an inert fuel matrix to embed the fissile material for new proposed reactor types. Besides uranium and plutonium as fissile material, the Minor Actinide Am should be embedded in the matrix and burned during the operation. The European ASGAR-Project [1] focuses on the reprocessing of the new reactor fuels. Here the separation processes of the fissile material from the matrix in order to recycle it for new reactor fuel is in focus.

Our present studies focus on the interaction of Eu(III) as an analogue for Am(III) with the molybdenum species formed during reprocessing steps. These take place in 3 M nitric acid medium. The question, whether Eu(III) forms mixed solution species with molybdenum is addressed in this study.

To this end, we investigated solutions of isotopically pure ⁹⁸Mo-metal with [⁹⁸Mo] = 10 mM and europium (with [Eu] = 10 mM and 1 mM respectively) in three different acidic strengths ([HNO₃] = 3 M, 1 M and 0.5 M) by means of nano-electrospray ionization mass spectrometry [2,3] (nano-ESI TOF MS) and time resolved laser fluorescence spectroscopy (TRLFS) [4].

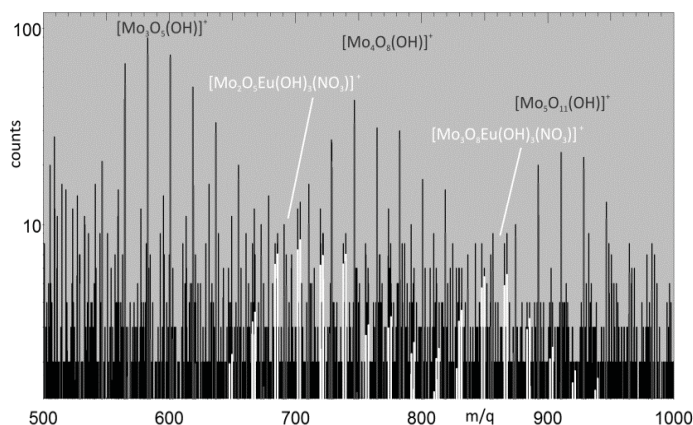


Fig. 1: ESI-MS spectrum in the region of m/q 500 – 1000 of a solution containing [Mo] = 10 mM, [Eu] = 1 mM in 1 M HNO₃. The grey peaks are due to the pure Molybdenum species. The white peaks show the presence of mixed Mo-Eu-species.

By nano-ESI TOF MS the ionic species present in solution can be characterized and quantified by transferring them into the gas phase under soft conditions and determining their mass-to-charge ratio [5]. Figure 1 shows an example of an ESI TOF spectrum measured by the ALBATROS MS [6]. Besides the expected pure Mo (shown in grey) and Eu species, the spectra hint on a possible formation of mixed Mo-Eu species of the sum formulas $[\text{Mo}_2\text{O}_5\text{Eu}(\text{OH})_3(\text{NO}_3)]^+$ and $[\text{Mo}_3\text{O}_8\text{Eu}(\text{OH})_3(\text{NO}_3)]^+$ (white peaks) with relative abundances of 5–17% with respect to the total Eu-content. Unfortunately, the method does not give any structural information on the formed species. In order to confirm the mixed Mo-Eu-species Eu(III) TRLFS measurements are performed. By these, the direct chemical environment of the Eu ions can be probed and further insights in the characteristics of the mixed species can be obtained.

[1] www.asgardproject.eu.

[2] Wilm, M. and M. Mann (1996) *Analytical properties of the nanoelectrospray ion source*. Anal. Chem. 68(1), 1–8.

[3] Cole, R.B. (1997) *Electrospray ionization mass spectrometry*. John Wiley and Sons, New York..

[4] Schmidt, M.; Stumpf, T.; Fernandes, M. M.; Walther, C.; Fanghänel, T (2008) *Charge compensation in solid solutions*, Angew. Chem., Int. Ed. 47, 5846–5850.

[5] Walther, C., et al. (2007) Investigation of polynuclear Zr-hydroxide complexes by nano-electrospray mass-spectrometry combined with XAFS. Anal. Bioanal. Chem. 388, 409–431.

[6] T. Bergmann, T. P. Martin, H. Schaber, (1989) *High-resolution time-of-flight mass spectrometer*, Rev. Sci. Instrum. 60, 792.

Uranium(VI) sorption on mineral phases studied by in situ laser fluorescence spectroscopy

R. Steudtner,¹ M. Berger,^{1,2} K. Müller,¹ V. Brendler¹

¹ Institute of Resource Ecology, Helmholtz-Zentrum Dresden-Rossendorf, Dresden, Germany

² Dresden University of Applied Sciences, Dresden, Germany

The determination and verification of thermodynamic and kinetic parameters of complexation, redox and sorption processes will improve the safety assessment of nuclear waste disposal sites. Sorption processes of U(VI) on mineral surface were traditionally investigated as a function of different reaction parameters (pH, I, T, Eh, c, atm., gs) by employing batch sorption experiments and surface complexation modeling (SCM). In the last decades, the batch sorption experiments were additionally investigated by the application of different spectroscopic techniques (TRLFS, EXAFS, ATR FT-IR). Especially the in situ ATR FT-IR experiments provide an online monitoring of the absorption changes of the sorption processes by the formation of the U(VI) surface complexes. The main objective of this study is to demonstrate the possibility of laser fluorescence spectroscopy for in situ monitoring and characterization of U(VI) sorption reactions. Therefore we investigated the sorption of an aqueous solution of U(VI) onto SiO₂.

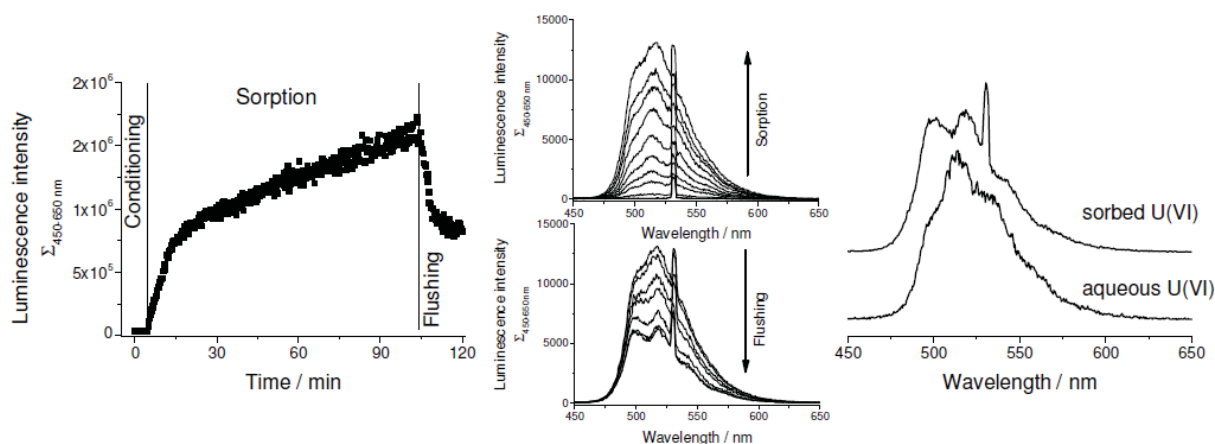


Fig. 1: In situ laser luminescence spectra of U(VI) sorption on SiO₂

In analogy to the in situ ATR FT-IR measurements, three subprocesses (conditioning, sorption, flushing) are performed in in situ laser fluorescence experiments, as shown in Fig. 1. The resulting fluorescence spectra showed significantly different fluorescence characteristics between the aqueous U(VI) and the sorbed U(VI) species. These preliminary results show that the application of the in situ laser fluorescence spectroscopy is a new alternative technique for identification and characterization of U(VI) complexes at mineral-water interfaces on a molecular level. Furthermore, the time resolution in the sub-minute range allows kinetic studies of the surface reactions.

How does uranium(VI) photochemically trigger the DNA cleavage? A density functional theory study

S. Tsushima

Institute of Resource Ecology, Helmholtz-Zentrum Dresden-Rossendorf, Dresden, Germany

Photocleavage of DNA in the presence of uranium is well-known phenomenon yet its reaction mechanism is not fully elucidated. Generally, the reaction is believed to occur through hydrogen atom abstraction by photoexcited uranyl(VI). The “yl”-oxygen in the excited uranyl(VI) is indeed a strong hydrogen acceptor and it can reduce small organic molecules such as methanol [1] and oxalic acid [2]. In the highest occupied molecular orbitals (HOMOs) of methanol and oxalic acid there is large contribution from hydrogen 1s atomic orbitals (AOs) that leads to HOMO–LUMO transition involving hydrogen atom. On the other hand, the HOMOs of the ground state DNA is mainly localized on phosphate groups and on the aromatic rings of the base pairs and there is little contribution from hydrogen AOs. It is unlikely that photoexcited uranyl(VI) can abstract hydrogen from DNA.

Therefore I focus here on charge transfer scenario; that is direct charge transfer from DNA to uranyl(VI) in the uranyl(VI)–DNA adduct. Three sets of base pairs (GC and two ATs) assisted by phosphate–deoxyribose backbones was used as a model of DNA (hereafter called “GC/AT/AT”). Structure of the uranyl(VI)–GC/AT/AT adduct where uranyl(VI) is bound through the phosphate group has been calculated at the B3LYP level. To be consistent with previous findings uranyl–to–phosphate coordination was assumed to be unidentate. In Fig. 1 Mulliken spin density α – β the lowest-lying triplet state of the U–GC/AT/AT adduct is given. In the lowest triplet state of the U–GC/AT/AT, the electron deficiency is centered mainly on guanine (G) and adenine (A) but partly on two phosphate groups sitting opposite to uranyl binding phosphate. Upon photoexcitation there is electron transfer from DNA to uranyl. It is known that oxidative DNA damage can occur through long-range electron transfer (up to 37 Å, [3]) hence the present result in which long transfer of electron is observed is not surprising. Half of the two unpaired electron is localized on uranyl and the rest is distributed on guanine, adenine, and free phosphate. Spin density of UO_2 moiety is close to 1.00 and the unpaired electron on uranium is localized on non-bonding U $5f_5$ or $5f_0$ orbitals constituting $5f^1$ electronic configuration. One can reasonably assume that the oxidation state of uranium is U(V). The GC/AT/AT part is oxidized with a loss of one electron. The electron deficiency gets mainly centered on guanine because of low oxidation potential of this residue compared to cytosine, thymine, and adenine [4]. The model having only two AT pairs (AT/AT) has been also tested. Similar to the GC/AT/AT case, photoinduced electron transfer from AT/AT to uranyl is observed in the lowest-lying triplet state of the U–AT/AT adduct. Roughly half of the spin density is localized on the uranyl unit and the rest is distributed on adenine and thymine and on free phosphate group. Therefore also in the U–AT/AT adduct upon photoexcitation there is a DNA-to-uranyl charge transfer and U(VI) gets reduced to U(V). However, in the lowest triplet state of the U–AT/AT adduct, when compared to U–GC/AT/AT, there is larger electron deficiency in free phosphate group. Apparently guanine is the best electron donor and upon its absence its role is substituted by phosphate and/or other nucleobases. From this result it appears that feasibility of phosphate oxidation (thereby the cleavage of DNA) gets higher if guanine is absent in the vicinity of uranium.

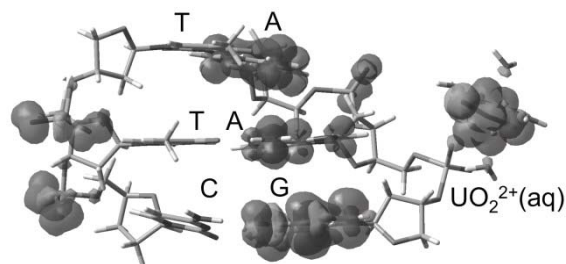


Fig. 1: Structures and Mulliken spin density α – β of the lowest-lying triplet states of U–GC/AT/AT adduct. Isovalue of the surface is 0.0004 a.u.

- [1] Tsushima, S. (2009) *Inorg. Chem.* 48, 4856–4862.
[2] Tsushima, S. et al. (2010) *Dalton Trans.* 39, 10953–10958.
[3] Hall, D. B. et al. (1996) *Nature* 382, 731–735.
[4] Steenken, S. et al. (1997) *J. Am. Chem. Soc.* 119, 617–618.

Spectroscopy characterization of uranyl(VI) species bound to minerals using luminescence spectroscopy

M. A. Williams,¹ A. N. Swinburne,¹ L. S. Natrajan,¹ S. Shaw²

¹ Centre for Radiochemistry Research, University of Manchester, Manchester, U.K.

² School of Earth, Atmospheric and Environmental Science, University of Manchester, Manchester, U.K.

The assessment of long term nuclear waste repositories requires an absolute knowledge of radionuclide mobility, reactivity and bioavailability. This project will draw together a multitude of techniques such as luminescence spectroscopy, X-ray adsorption spectroscopy and scintillation counting/atomic emission spectroscopy to characterize and define molecular species. Speciation of the 5f elements is unique within the periodic table; their elucidation has contributed heavily to the fundamental understanding of heavy element behavior in the environment. The speciation of uranium has relevance to the remediation of nuclear sites and reactive transport modelling, and thus has both fundamental relevance and directly practical application.

The properties of uranium in an aqueous environment are dominated by the hexavalent triatomic uranyl (UO_2^{2+}) species. Although stable and consistently linear in single crystal determination, uranyl containing species differ considerably with changes to pH, E_H and concentration. Luminescence spectroscopy provides the sensitivity to study such systems and to probe any differences in electronic structure in detail.

The sorption of uranyl(VI) onto the clay minerals, montmorillonite, kaolinite and the simpler 'building-block minerals' silica and alumina, has been studied successfully. Sorption has been investigated by scintillation counting and luminescence spectroscopy. Batch experiments were performed to determine the kinetics of uranyl(VI)-clay sorption in salt solution (0.1 M) within natural groundwater pH ranges (4.0 to 10.0), spectra and lifetime information have been obtained of the uranyl-minerals. PHREEQC analysis has been used to aid in identification, as well as highlighting the effect of carbonate, pH and ionic strength. Both low temperature luminescence and room temperature luminescence will be presented, with the aim of substantiating a luminescent fingerprinting database.

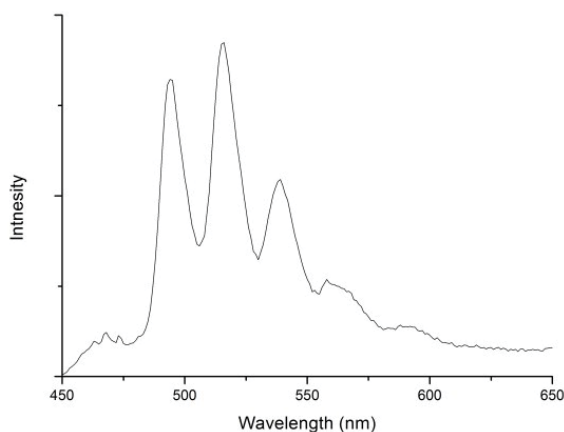


Fig. 1: Emission spectra of uranyl loaded montmorillonite: pH 5; P_{CO_2} atm; 77 K; $\lambda_{\text{ex}} = 250$ nm.

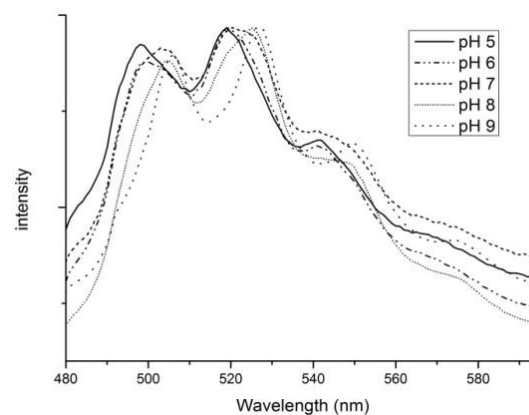


Fig. 2: A comparison of emission across pH for uranyl loaded montmorillonite. P_{CO_2} atm; 300 K; $\lambda_{\text{ex}} = 410$ nm.

C. Chisholm-Brause, J. Berg, R. Matzner and D. Morris (2001) *J. Colloid Interface Sci.* 233, 38–49.

L. S. Natrajan (2012) *Coord. Chem. Rev.* 256, 1583–1603.

C. Chisholm-Baruse, J. Berg, K. Little, R. Matzner and D. Morris (2004) *J. Colloid Interface Sci.* 277, 366–82.

A. Kowal-Fouchard, D. Drot, E. Simoni and J. Ehrhardt (2004) *Environ. Sci. Technol.* 38, 1399–1407.

Vibrational spectroscopic signature of ice at mineral surfaces

M. Yeşilbaş, J.-F. Boily

Department of Chemistry, Umeå University, Sweden

Mineral-ice interactions are of paramount importance in atmospheric and terrestrial environments of the cryosphere, and wherever freeze-thaw cycles are of common occurrence. Ice can not only lock chemical species (*e.g.* actinides, organics) but also participate in (photo)catalytic transformation reactions. As mineral surface structure often templates interfacial water layers under ambient temperatures, the same could occur for the case of ice, likely resulting in mineral-specific properties. In this study, the vibration spectroscopic signatures of thin ice layers associated to mineral surfaces were monitored by Fourier-transform infrared (FT-IR) spectroscopy, a technique with a particularly strong sensitivity for subtle changes in the hydrogen bonding environments of compounds. Minerals of varied structure, composition, particle size, shape and surface roughness were used to identify mineral-specific and generalities in thin interfacial films of ice. These minerals include goethite, akaganéite, lepidocrocite, hematite, ferrihydrite, kaolinite, quartz, gibbsite, illite, microcline, as well as mixtures in Arizona test dust and Icelandic volcanic ash. This work shows that interfacial ice has a weaker hydrogen bonding network than hexagonal ice ($\nu_{\text{OH}} = 3250 \text{ cm}^{-1}$), with values shifted to $\nu_{\text{OH}} \approx 3408\text{--}3425 \text{ cm}^{-1}$. These latter values are comparable to O–H stretching frequencies of room temperature liquid water as well as those condensed water vapor at these mineral surfaces [1,2]. This work underscores distinct attributes of ice associated to mineral surfaces, and represents a sound platform for further studies in our group that are dedicated to gas-phase interfacial reactions involving mineral-ice admixtures.

[1] Song, X. and Boily, J.-F. (2013) *Environ. Sci. Technol.* 47, 7171–7177.

[2] Song, X. and Boily, J.-F. (2013) *Chem. Phys. Lett.* 560, 1–9.

ROUND-ROBIN TEST
IN ACTINIDE SPECTROSCOPY

Round-Robin test in actinide spectroscopy

R. Steudtner, K. Müller, S. Tsushima, H. Foerstendorf

Institute of Resource Ecology, Helmholtz-Zentrum Dresden-Rossendorf, Dresden, Germany

The main goal of the inter-laboratory round robin test (RRT) is the comprehensive molecular analysis of the actinide complex system U(VI)/acetate in aqueous solution independently investigated by different spectroscopic and quantum chemical methods applied by leading laboratories in geochemical research. Conformities as well as sources of discrepancies between the results of the different methods are to be evaluated, illuminating the potentials and limitations of coupling different spectroscopic and theoretical approaches as tools for the comprehensive study of actinide molecule complexes. The test is understood to stimulate scientific discussions, but not as a competitive exercise between the labs of the community.

CLUSTERS & PARTICIPATING INSTITUTIONS. The RRT was initiated in late 2013 at HZDR. After the acceptance of the participating institutions, six clusters were formed according to the respective approach, namely Time-resolved Fluorescence Spectroscopy (TRLFS), vibrational spectroscopy (IR/Raman spectroscopy), Nuclear Magnetic Resonance spectroscopy (NMR), Electron Spray Ionization-Mass Spectrometry (ESI-MS), X-ray Absorption spectroscopy (XAS), and Quantum-Chemical

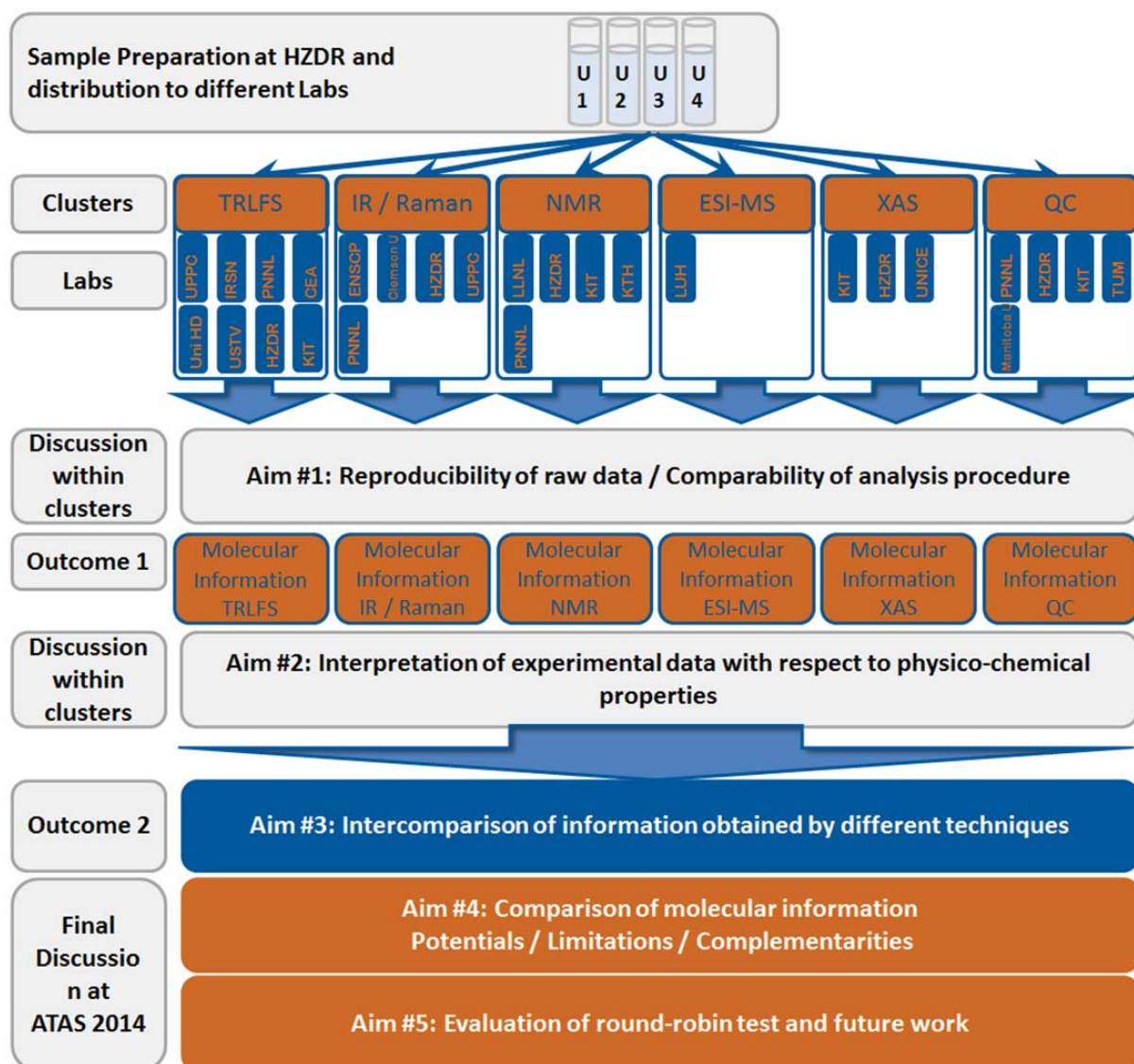


Fig. 1: Overall organization chart of the RRT.

calculations (QC). For each cluster a representative speaker was nominated. The overall organization chart of the RRT and the list of participating institutions are given in Fig. 1 and Tab. 1, respectively.

SYSTEM SELECTION. The actinide system to be investigated during the RRT was discussed among all participants. The joint system was thought to be acceptably simple, homogenous, easily accessible, and measureable by the different techniques. Eventually, the organizers conclude that the acetate complexes of U(VI) are most suitable for this inter-laboratory test. Different sample compositions were tested concerning their spectroscopic response and long-term stability. To keep the test as simple as possible, the focus was set on four U(VI) acetate samples at a distinct metal and ligand concentration and as a function of different pH values ranging from 1.0 to 3.5. The U(VI) concentration was set to 0.025 M to ensure detection by each spectroscopic method. Ligand concentration and ionic strength was 1 M. As the comparison of molecular information obtained from the different spectroscopic and theoretical methods are already very ambitious, the impact of metal and ligand concentration, ionic strength and temperature on U(VI) complexation was not considered this time. The preparation of the samples was performed at HZDR and subsequently shipped to each participating institution in appropriate sample compartments.

ACQUISITION & TREATMENT OF DATA. The measurement of the samples should be performed according to the settings of routine experiments selected by each operator. The originally obtained raw data including a detailed description of these settings should be transferred to the respective

Tab. 1: Cluster and participating institution of the RRT.

CLUSTER	CONTRIBUTING INSTITUTION	COUNTRY
TRLFS (Speaker: M.U. Kumke, University of Potsdam, Germany)	French Alternative Energies and Atomic Energy Commission	France
	French Institute for Radioprotection and Nuclear Safety	France
	Helmholtz-Zentrum Dresden-Rossendorf	Germany
	Karlsruhe Institute of Technology	Germany
	Pacific Northwest National Laboratory	U.S.A.
	Trinity College Dublin	Ireland
	University of Heidelberg	Germany
	University of Potsdam	Germany
	Université de Toulon	France
IR / Raman (Speaker: G. Lefèvre, École nationale supérieure de chimie de Paris, France)	École Nationale Supérieure de Chimie de Paris	France
	Clemson University	U.S.A.
	Helmholtz-Zentrum Dresden-Rossendorf	Germany
	Pacific Northwest National Laboratory	U.S.A.
	University of Potsdam	Germany
NMR (Speaker: Z. Szabò, Royal Institute of Technology, Stockholm, Sweden)	Helmholtz-Zentrum Dresden-Rossendorf	Germany
	Karlsruhe Institute of Technology	Germany
	Lawrence Livermore National Laboratory	U.S.A.
	Pacific Northwest National Laboratory	U.S.A.
	Royal Institute of Technology	Sweden
ESI-MS (Speaker: C. Walther, University of Hannover, Germany)	University of Hannover	Germany
XAS (Speaker: J. Rothe, Institute for Nuclear Waste Disposal, Karlsruhe, Germany)	Helmholtz-Zentrum Dresden-Rossendorf	Germany
	Karlsruhe Institute of Technology	Germany
	Université de Nice Sophia Antipolis	France
QC (Speaker: P. Yang, Pacific Northwest National Laboratory, Richland, U.S.A.)	Cardiff University	U.K.
	Helmholtz-Zentrum Dresden-Rossendorf	Germany
	Karlsruhe Institute of Technology	Germany
	Pacific Northwest National Laboratory	U.S.A.
	University Manitoba	Canada

cluster speaker. The analysis of the raw data (e.g. data transformations, background subtraction, smoothing, deconvolution,...) was done according to the expert knowledge and mostly applied procedure by each operator. The report of this analysis, including a detailed description of all working steps, was submitted to the cluster speaker. Finally, the interpretation of the refined data was transmitted containing all molecular information extracted from the data obtained so far. All results were documented in a brief report and transferred to the cluster speaker for preparation of a final summary.

PRESENTATION & DISCUSSION AT ATAS 2014. The results of the RRT will be presented and discussed during three sessions on Wednesday, 05th at ATAS. During the first two sessions the summarized results of each technique will be presented by a short talk given by the respective cluster speaker followed by a plenum discussion. The overall outcome of the RRT will be evaluated in a third session in the afternoon particularly focusing on the interplay of theoretical and experimental approaches in actinide sciences and on the strategy of a common publication of the RRT's results.

All attendees of ATAS 2014 are cordially invited to contribute to these sessions providing a golden opportunity for gaining insights into analytical techniques which might appear unfamiliar until then and for a deeper understanding of complementarities or intrinsic incompatibilities of information obtained from different methodological approaches.

HUMAN HEALTH

ENVIRONMENTAL HEALTH

ONE RUN
LETS YOU
SEE IT ALL

© 2014 PerkinElmer, Inc. 400298_12. All trademarks or registered trademarks are the property of PerkinElmer, Inc. and/or its subsidiaries.



Nanoparticle concentration, composition, size and distribution, dissolution and agglomeration tracking – all in under a minute.

Nanoparticles' unique characteristics and increasing usage in consumer products will inevitably lead to their release into the environment. Characterizing them required hours of analysis time and manual calculations – until now. The NexION® 350 ICP-MS single-particle analyzer combines best-in-class data acquisition rates with proprietary software to deliver full characterization in one run – *that's 60 seconds or less*. Want to understand more from your nanoparticle research? Just give us a minute.

www.perkinelmer.com/NexIONnano


PerkinElmer
For the Better

Index of Authors

Acker, M.	56, 78	Eidner, S.	50, 78
Adam, C.	20	Elo, O.	59
Alessi, D. S.	15	Eloirdi, R.	41, 44
Altmaier, M.	73	Fellhauer, D.	28
Andersson, D. A.	18	Foerstendorf, H.	60, 87
Aoyagi, N.	51, 76	Forster, R. A.	32
Arinicheva, Y.	38, 55	Gaona, X.	73
Autillo, M.	27	Geckeis, H.	37, 39
Averin, A. A.	36, 79	Geipel, G.	24
Bader, M.	23	Geist, A.	20, 52
Bahl, S.	39	Gibson, J.	29
Baker, R. J.	32, 71	Gilbertson, S. M.	18
Banik, N.	20	Golser, R.	37
Bargar, J. R.	15	Gong, Y.	29
Barkleit, A.	30, 56, 78	Gouder, T.	41, 44
Battesti, C.	26	Großmann, K.	47
Beccia, M. R.	26	Guilbaud, P.	26
Beele, B. B.	20, 77	Günther, A.	68
Benedetti, M. F.	63	Ha, Y.-K.	49
Berger, J.	70	Heim, K.	59, 60
Berger, M.	81	Hellebrandt, S.	61
Bernier-Latmani, R.	15	Hennig, C.	40, 62
Berthomieu, C.	26, 75	Hess, N.	42
Berthon, C.	27	Holthausen, J.	38
Bohnert, E.	28	Hölttä, P.	59
Boily, J.-F.	19, 33, 84	Huber, F.	41, 44
Bosbach, D.	55	Hübner, R.	62
Boyanov, M. I.	17	Huitinen, N.	38, 59
Bremond, N.	26	Husar, R.	62
Brendler, V.	30, 78, 81	Ikeda-Ohno, A.	40, 62
Brennenstuhl, K.	50	Ito, C.	35
Britz, S.	47	Jeanson, A.	75
Brulfert, F.	75	Jung, E. C.	49
Brunner, E.	30	Kaden, P.	20
Burakov, B. E.	36	Kehl, J.	18
Burek, K.	50	Kemner, K. M.	17
Çakir, P.	41, 44	Kerridge, A.	20
Campbell, A.	42	Keys, T. A.	32
Casas, I.	67	Kimura, T.	51, 76
Cha, W.	49	Kirishima, A.	51
Cheng, M.	57, 80	Knott, A.	69
Cherkouk, A.	23	Kobayashi, T.	76
Cho, H.-R.	49	Koldeisz, V.	39
Clavier, N.	55	Konings, R. J. M.	41, 44
Comarmond, M. J.	60	Kouhail, Y.	63
Conradson, S. D.	18	Kremleva, A.	45
Creff, G.	25	Kretzschmar, J.	30, 56, 64, 78
Daifuku, S.	18	Krüger, S.	45, 65
Dardenne, K.	28	Kumke, M. U.	50, 78
Dau, P. D.	48, 66	Kvashnina, K.	39
de Pablo, J.	67	Kwon, K. D.	43
Delangle, P.	26	Lagos, M.	37
Den Auwer, C.	25	Latta, D. E.	17
Dolgoplova, E. A.	79	Lehto, J.	59
Drobot, B.	23, 58, 78	Lemaire, D.	26
Durakiewicz, T.	18		
Dürr, M.	69		

Li, J.	31, 48, 66
Liu, C.	33
Liu, H.-T.	48, 66
López Fernandez, M.	68
Lorenzo Solari, P.	25
Lozano-Rodriguez, M. J.	55
Lucchini, J. F.	67
Martínez-Torrents, A.	67
Merroun, M. L.	26, 68
Middendorp, R.	69
Mishra, B.	17
Moisy, P.	27
Moll, H.	68
Müller, K.	59, 60, 70, 81, 87
Nankawa, T.	22
Natrajan, L. S.	20, 83
Neidig, M. L.	18
Neubert, N.	15
Neumeier, S.	38, 55
Nuzzo, S.	71
O’Loughlin, E. J.	17
Ogorodnikov, B. I.	36
Ohba, H.	35
Ohnuki, T.	22
Paasch, S.	30
Pakhnevich, A.	36
Pan, D.	29, 33
Panak, P. J.	20, 52, 77
Pardoux, R.	26
Park, Y.-S.	49
Peschel, S.	72
Pidchenko, I.	28, 39
Plaschke, M.	37
Polly, R.	73
Prüßmann, T.	28, 32
Quinto, F.	37
Raff, J.	58
Randall, S.	20
Reed, D. T.	67
Reiller, P. E.	63, 74
Resch, C. T.	33
Rodriguez, G.	18
Roques, J.	75
Rossberg, A.	46, 70
Rothe, J.	28
Saeki, M.	35
Safi, S.	25, 75
Saito, T.	34, 76
Sakka, T.	35
Sánchez Castro, I.	68
Sasaki, T.	76
Sato, N.	51
Sauge-Merle, S.	26, 75
Schäfer, T.	37
Scheinost, A. C.	46, 55
Schild, D.	77
Schimmelpfennig, B.	28, 52, 73, 77
Schmidt, M.	61, 72
Scholz, G.	30
Schott, J.	30, 78
Schreckenbach, G.	16
Schulze, A.	47
Schwarz, W. H. E.	31
Senin, R. A.	36
Shao, P. S.	15
Shaw, S.	83
Shiryayev, A. A.	36, 79
Simon, B.	70
Simoni, E.	75
Solari, P. L.	26, 68
Spain, E. D.	32
Steier, P.	37
Steppert, M.	57, 80
Steutner, R.	47, 58, 60, 64, 81, 87
Stumpf, T.	23, 38, 61, 62, 72, 78
Stylo, M.	15
Su, J.	31, 48, 66
Suzuki, Y.	22
Swinburne, A. N.	20, 83
Tachi, Y.	76
Takagi, I.	76
Tanaka, K.	22
Taut, S.	78
Thornton, B.	35
Trumm, M.	52
Trumm, S.	77
Tsushima, S.	30, 40, 56, 58, 64, 78, 82, 87
Ueda, K.	76
Vidaud, C.	25
Viehweger, K.	24
Vitova, T.	28, 32, 39
Vlasova, I. E.	36
Volkova, A. G.	79
Wakaida, I.	35
Walshe, A.	32, 71
Walther, C.	57, 80
Wang, L.-S.	48, 66
Wang, Z.	29, 33
Watanabe, M.	51
Wei, F.	31
Weiss, S.	40, 62
Weyer, S.	15
Williams, M. A.	83
Woodall, S. D.	20
Wu, W.	33
Yalcintas, E.	73
Yang, P.	29
Yeşilbaş, M.	84
Yokosawa, T.	39
Zachara, J. M.	33
Zakharova, E. V.	79
Zänker, H.	62
Zubavichus, Y. V.	36

Time-resolved spectroscopy with iStar ICCD from Andor Technology

Observe your actinides with spectral and temporal information



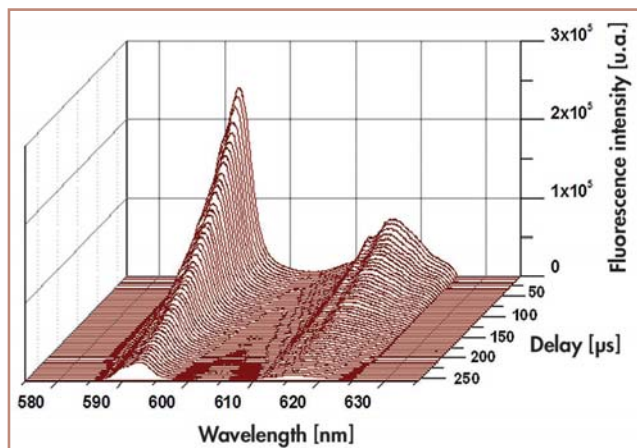
ANDOR
an Oxford Instruments company

Key features

- Pre-aligned and pre-calibrated
- Czerny-Turner system
- Rugged and compact
- Image astigmatism correction
- USB 2.0 interface
- Motorized, indexed triple grating turret
- Dual detector outputs

Key applications

- Laser Induced Breakdown Spectroscopy (LIBS)
- Time-resolved Raman and Resonance Raman Spectroscopy (TR3)
- Time-resolved fluorescence/luminescence
- Time-resolved actinides spectroscopy
- Plasma studies
- Laser flash photolysis
- Single molecule spectroscopy

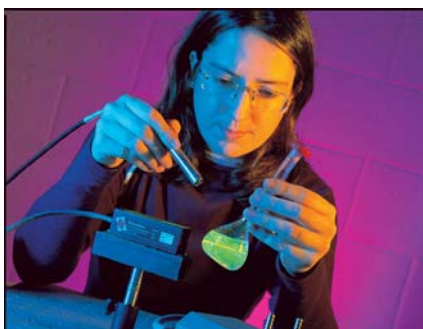
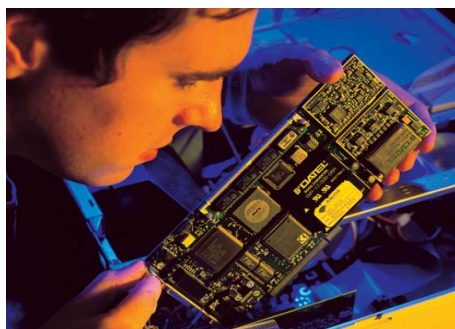


Development of the solvated Eu(III) emission band as function of the delay time, $[Eu(III)] = 1.8 \cdot 10^{-5} \text{ mol L}^{-1}$ in $0.01 \text{ mol L}^{-1} \text{ HClO}_4$.

Graph is used with kind permission of Prof. Dr. Panak Group, Karlsruhe Institute of Technology, Institute for Nuclear waste Disposal (INE), Germany

// The new ICCD camera time-resolved spectroscopy set-up allows very easy change between different gratings and much lower detection limit, allowing a significant saving of the applied Eu(III) and Cm(III) material. //

Björn B. Beele, Prof. Dr. Panak Group, Karlsruhe Institute of Technology, Institute for Nuclear Waste Disposal (INE), Germany



www.lot-qd.com/de



LOT-QD Gruppe Europa. Im Tiefen See 58. 64293 Darmstadt.
Telefon: 06151-8806-0. Fax: 06151-896667. eMail: info@lot-qd.de

LOT
Quantum Design

HZDR

 HELMHOLTZ
ZENTRUM DRESDEN
ROSSENDORF

Institute of Resource Ecology
P.O. Box 51 01 19 · 01314 Dresden/Germany
Phone +49 351 260-3210
Fax +49 351 260-3553
Email contact.resourceecology@hzdr.de
<http://www.hzdr.de>

Member of the Helmholtz Association